
Alma Mater Studiorum – Università di Bologna

PhD in Geoengineering, Georesources and Geotechnical Engineering

Settore concorsuale 08/A2 - S.S.D. ING-IND/28

XXIV cycle

***Characterization of geothermal reservoirs'
parameters by inverse problem resolution and
geostatistical simulations***

Candidate

Sara Focaccia

Coordinator of Doctoral School

Prof. Eng. Paolo Berry

Thesis director UniBo

Prof. Eng. Roberto Bruno

Thesis director IST

Prof. Eng. Amilcar Soares

Summary

In recent years, there has been an increase in the market of air conditioning heat pump systems coupled to shallow geothermal reservoirs. By installing appropriate "geo-exchangers", the underground is used as a seasonal storage of thermal energy, from which it is possible to extract heat in winter and to stock heat in the summer. In fact, UTES (underground thermal energy storage) systems not only permit to save a lot of energy and money, but also they exploit a renewable energy and have no pollutants emissions in the atmosphere: they are the ideal systems for contributing to environmental policies as the 20-20-20 of EU (Fig. 1).

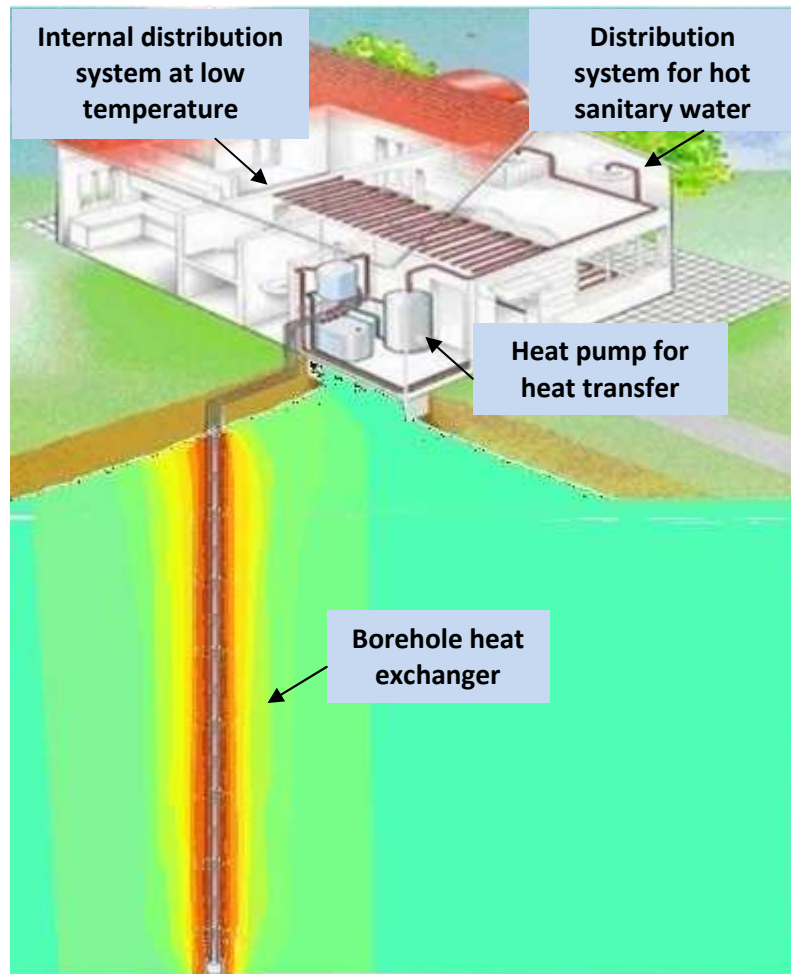


Figure a *Scheme of a shallow geothermal system based on a vertical borehole heat exchanger.*

The heat exchangers, of different type and size, are mostly closed loop, generally called BHE (borehole heat exchangers) or BTES (borehole thermal energy storage) systems that consist of a series of boreholes, inside which a tube, called collector, is grouted. A fluid flows in the collector and transfers heat by convection; BTES systems exchange thermal energy by conduction with the surrounding ground through borehole materials (Sanner, et al., 2003). The presence of an aquifer could call for an advection term.

The spatial variability of the geological properties and the space-time variability of hydrogeological conditions, specific to each installation, affect the real power rate of heat exchangers, and consequently the amount of energy extracted from / injected into the ground.

For this reason, it is not an easy task to identify the underground thermal properties to be considered when designing (Witte, et al., 2006).

At the current state of technology, the Thermal Response Test (TRT) is the in situ test for the characterization of ground thermal properties with the higher degree of accuracy (Fig. 2). This consists of simulating the BTES operation of heat injection/extraction for a limited time.

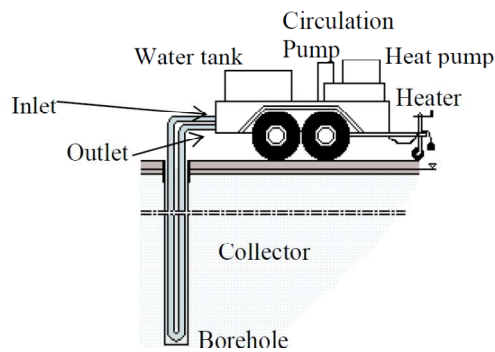


Figure b Thermal Response Test rig

By analyzing the temperature variation of the circulating fluid, it is possible to estimate the equivalent thermal properties of the quasi-cylindrical ring affected by the heat exchanger. The cylindrical ring is composed by several materials; some of them are artificial and have constant thermal properties, while others, the natural ones, have variable ones. The perfect cylindrical geometry of the borehole depends on drilling procedure. The impossibility to have a perfect vertical borehole adds another source of variability.

The TRT doesn't fully solve the problem of characterizing the thermal properties of a shallow geothermal reservoir, simply because it characterizes just the neighborhood of the heat exchanger at hand and just for the test duration. In fact, the 3D/2D variability of thermal properties through the whole reservoir cannot be studied if just one test is available, which is the normal practice. Such variability can be an important concern if a multi-borehole geothermal field has to be implemented. Moreover, the temporal variability of groundwater level could change the equivalent thermal properties of each heat exchanger. Nevertheless TRT is the most adequate, popular and efficient tool for identifying the parameters to be considered when designing the BTES system. Different analytical and numerical models exist for the characterization of the shallow geothermal reservoir, but they are still inadequate and not exhaustive, as instead it is for other types of reservoir (water, oil, gas, deep geothermal): more sophisticated models must be taken into account and a geostatistical approach is needed to tackle the natural variability and the estimates uncertainty.

The approach adopted for reservoir characterization is the "inverse problem", typical of oil&gas field analysis, given the existing similarities.

In fact, normally, inverse method consists on the perturbation of a set fine grid values of hydraulic conductivity and porosity numerical model, in order to feed a process simulator and to match the production real response. Similarly, we create different realizations of thermal properties by direct sequential simulation and we find the best one fitting real production data (fluid temperature along time).

The software used to develop heat production simulation is FEFLOW 5.4 (Finite Element subsurface FLOW system). In this first study, a geostatistical reservoir model has been set up based on literature thermal properties data and spatial variability hypotheses, and a real TRT has been tested. To compare simulation results with classical results obtained by ILS (Infinite Line Source) theory, we set up an upscaling procedure of vector properties (thermal and hydraulic conductivity). The whole procedure adopted is presented and commented. The main conclusion is the positive evaluation of this first attempt of shallow geothermal reservoir characterization by inverse problem solution. Then we performed other simulations by using two other codes (SA-Geotherm and FV-Geotherm), that use the same numerical model developed by Al-Khoury and implemented in FEFLOW. Some inversion results are shown and a sensitivity analysis as well.

Nomenclature

Symbols

ρ = ground density [kg/m³]

C = ground heat capacity [J/(kg·K)]

c_g = ground volumetric heat capacity [J/(m³·K)]

c_b = borehole volumetric heat capacity [J/(m³·K)]

λ_g = ground thermal conductivity [W/(m·K)]

γ = Euler's constant (0,5772)

R_b = borehole thermal resistance [K/(W/m)]

R_g = ground thermal resistance [K/(W/m)]

r_b = borehole radius [m]

Q = thermal power [W]

q = thermal power per meter [W/m]

H = borehole length [m]

t = time [s]

τ = log – time space [s]

t_0 = initial time of fluid temperature data analysis [s]

t_f = final time of fluid temperature data analysis [s]

a_g = ground thermal diffusivity [m²/s]

a_b = borehole thermal diffusivity [m²/s]

a = intercept of the regression line in the fluid temperature data analysis

b = slope of the regression line in the fluid temperature data analysis

T_g = undisturbed ground temperature [°C]

T_f = circulating fluid temperature [°C]

T_b = temperature at the borehole wall [°C]

V = volume [m³]

p = index

α = index

w = index

n = number of data

n_c = number of increments

$m(t)$ = mean temperature function of heat carrier / circulating fluid

$Y(t)$ = fluctuation of fluid temperature around the mean function

$\gamma(h)$ = variogram function of fluctuations

h = time lag

σ_ε^2 = estimation error variance

v = weight

Acronyms

UTES = underground thermal energy storage

BTES = borehole thermal energy storage

ILS = infinite line source

ReV = regionalized variables

RF = random function

StRF = stationary random function

MW = moving windows

Index

Alma Mater Studiorum – Università di Bologna	1
Summary	2
Nomenclature	5
Table of figures.....	10
Table of tables.....	12
Introduction	13
The classic inverse problem: the oil case	14
The geothermal case	14
Outline of this study	15
PART I Geothermal Energy:	17
an overview.....	17
1. RENEWABLE ENERGIES: THE PLACE OF GEOTHERMAL	18
2. THE EXPLOITATION OF GEOTHERMAL ENERGY.....	20
2.1 High enthalpy geothermal.....	22
2.2 Medium enthalpy geothermal energy	24
2.3 Low enthalpy geothermal energy	25
PART II Vertical borehole heat exchangers and thermal conductivity.....	30
1. INTRODUCTION ON VERTICAL BOREHOLES HEAT EXCHANGERS AND THEIR FUNCTIONING	31
1.1 Physical background.....	36
1.1.1 Hydraulics.....	36
2. THERMAL CONDUCTIVITY: STATE OF THE ART	42
2.1 Theoretical studies on thermal conductivity.....	44
2.2 Thermal conductivity laboratory measurement	47
2.3. Thermal conductivity in situ measurement	56
2.4 Comments on the actual ways of measuring thermal conductivity	68
2.5 Which are the values used for designing a BHE in common practice?	69
3. OVERVIEW ON THE BOREHOLE HEAT EXCHANGERS' MODELS.....	71
3.1 Analytical models	71
3. 2 Numerical methods.....	77
PART III Inverse Modeling of a Geothermal Reservoir.....	80
1. INTRODUCTION TO INVERSE MODELING TECHNIQUE.....	81
2. GEOSTATISTICAL SIMULATION OF THERMAL PARAMETERS.....	84

2.1 Sequential Gaussian Simulation (SGS)	84
2.2 Direct Sequential Simulation (DSS) and Co-Simulation (Co-DSS).....	84
2.3 Building up the synthetic data	86
3. DYNAMIC SIMULATION OF A GEOTHERMAL SYSTEM.....	88
3.1 State of the art	88
3.2 Choice of the simulator	90
4. FEM: FINITE ELEMENT METHOD	92
4.1 Galerkin Method	93
5. FEFLOW MODEL OF THE BOREHOLE	95
5.1 Analytical solution of BHE	95
5.2 Numerical solution of BHE	99
5.3 Upscaling of underground properties	101
6. BOREHOLE HEAT EXCHANGER SYNTHETIC COMPUTATIONAL MODEL.....	103
6.1 Results from few synthetic models	104
7. RECONSTRUCTION OF A REAL TRT WITH THE NUMERICAL MODEL OF FEFLOW	106
7.1 Reconstruction of a TRT by using FEFLOW model for BHE	106
7.2 Is it possible to have a consistent reproduction of reality by using the numerical model implemented on FEFLOW?.....	108
7.3 Comparisons with other solutions	114
8. RECONSTRUCTION OF A REAL TRT WITH OTHER NUMERICAL MODELS.....	117
8.1 Spectral model	117
8.1.1 Reconstruction of a thermal response test.....	118
8.2 Finite volume model.....	122
8.2.1 Reconstruction of a thermal response test.....	123
CONCLUSION	125
WHAT'S NEXT?	127
The medium term conditions and the geothermal system monitoring (GSM).....	127
Bibliography	132
Annexes – Published articles and conferences' act	141
a)“Recent developments of thermal response test”	141
b) “La caractérisation d’un réservoir géothermique superficiel ”	142
c) “Geostatistical modeling of shallow geothermal reservoir ”	143
e) “Analysis of Thermal Response Test data“	145
f) Annex 21 Thermal Response Test Final Report.....	146

g) Test di Risposta Termica per la geotermia superficiale: un approccio geostatistico....	147
h) Geostatistical modeling of a shallow geothermal reservoir for air conditioning of buildings	148
i) “Inverse modeling applied to shallow geothermal reservoirs”	149
l) Thermal Response Test for shallow geothermal applications: a geostatistical approach & the DCE Analysis Method. Part I and II.....	150

Table of figures

Figure 1 Map of geothermal areas in Italy. Legend refers to the temperature in °C that we can encounter while increasing the depth from the surface (modified by Della Vedova et al. 2001).	21
Figure 2 Evolution of ground temperature with depth. The first 10-15 meters are influenced by external temperature, but after 20 m of depth we reach the omothermal area (until 100-150 meters of depth). This is relative to Switzerland's temperatures: in Italy it will be centered on 15°C, instead of 10°C. (http://www.casainnovativa.com/fonti-rinnovabili/geotermia-note-storiche-e-scientifiche).....	22
Figure 3 General scheme of a geothermal field: on the left, geological section and on the right temperature values on a vertical profile (Facca & Tonani, 1964).....	23
Figure 4 Average ground temperature of the first 100-150 meters (www.geotrainer.net)	26
Figure 5 Scheme of a shallow geothermal system based on a vertical borehole heat exchanger with open loop (www.energysavers.org).....	27
Figure 6 Scheme of a shallow geothermal system based on a vertical borehole heat exchanger	27
Figure 7 Schematic diagram of spiral coils	28
Figure 8 Scheme of a shallow geothermal system based on a horizontal borehole heat exchanger (www.energysavers.gov)	29
Figure 9 Scheme of a shallow geothermal system based on pond/lake heat exchanger (www.energysavers.gov).....	29
Figure 10 Heat pump circuit and its state curve (from a seminary of Padova university).....	34
Figure 11 Types of thermal exchange existing between the heat exchanger and the ground. A) is the summer condition while B) is the winter condition.	38
Figure 12 Permeability and conductivity radial averages	44
Figure 13 a) Thermal conductivity of frozen base-course materials as a function of water content; b) Thermal conductivity of unfrozen base-course materials as a function of water content and thermal conductivity of solid particles	46
Figure 14 Comparative cut bar (ASTM E1225 Test Method) (ANTER)	47
Figure 15 Guarded heat flow meter (Netzsch).....	48
Figure 16 Guarded hot plate method: the main heater is sandwiched in the middle of the specimens.....	49
Figure 17 Schematic diagram of thermal conductivity needle probe (Daw, et al., 2010).	50
Figure 18 Typical experimental probe method test results (this an idealized curve) (Manohar, et al., 2000)	50
Figure 19 Munoz laboratory heating test to measure thermal and hydraulic conductivity in saturated condition of argillaceous rocks by means of a heater pulse.	51
Figure 20 Schematic view of the thermo-time domain reflectometry	51
Figure 21 Principal components of the plates of the PEDB: each brass plate is fitted with a separate thermocouple. ΔT is the ratio of the temperature of the plates of the PEDB: $\Delta T = (T_2 - T_3) / ((T_1 - T_2) + (T_3 - T_4))$. The heat source is above the top pair of brass plates, and the cold source is below the bottom pair; the consequence is that heat flows across the rock sample (Antriasian, 2010).....	52

Figure 22 Summary of thermal conductivity data from six meta-sedimentary rock specimens; the six differently shaped symbols indicating the different specimens studied. Each specimen was measured for thermal conductivity at several angles with respect to the specimen's foliation. The vertical axis is thermal conductivity in W/m·K; the horizontal axis is the angle between the foliation of the rock sample, and the direction of heat flow across the rock sample while within the PEDB, measured in degrees (°). A relationship exists between the magnitude of thermal conductivity and the direction of heat flow with respect to the specimen's foliation (Antriasian, 2010).....	52
Figure 23 Device for measuring the thermal conductivity coefficient of a rock specimen	53
Figure 24 Modified hot wire method.....	54
Figure 25 Experimental setup used by Coté and Konrad.....	55
Figure 26 TRT apparatus.....	56
Figure 27 Scheme with the different radius used, boreholes' and concentric surfaces used for the calculation.....	57
Figure 28 Penalty temperature in the 4 cases for the 3 different values of thermal conductivity	59
Figure 29 Evolution of penalty temperature by changing the ground thermal conductivity.	60
Figure 30 Evolution of the investigated distance, with constant power injected equal to 5400 W – 6200 W , constant ground thermal capacity equal to 2,2 – 2,5 MJ/m ³ K and variable thermal conductivity.....	62
Figure 31 This is the system diagram of this kind of measurement: the main components are the thermal properties sensor (1), the measurement control unit (4) and a computer (2). (3) is the sample of soil on which we are performing the measure. This tool gives an estimation of thermal conductivity and an associated standard deviation.....	63
Figure 32 Block diagram of the probe: all the components are inserted in a probe with a length of 235 mm, a diameter of 23 mm and weighs only 99.8 g.	64
Figure 33 Appearance of miniature data logger "Nimo-T"	64
Figure 34 Fiber optic sensor is inserted in the U-tube or coaxial pipe.....	65
Figure 35 Energy flow through a control volume during drilling. W1 is injected energy, W2 is energy leaving the borehole, and W3 is energy transferred to the formation. Q _{cv} represents the internal energy of the control volume (Gustafsson, 2006).....	66
Figure 36 Isothermal curves showing the position where the formation's temperature has increased by 1°C (to 11°C) at t=320 min (drilling at 160 meters depth). The different curves represent formations with thermal conductivity λ=1, λ=3 and λ=5 W/(m·K).....	66
Figure 37 Fluid temperature evolution during the sequential pulses of heat flux	67
Figure 38 Resistances arranged in series representing the borehole and the ground	73
Figure 39 Evolution of temperature distance from the borehole center.	73
Figure 40 Linear regression of fluid temperature T _f on time_log scale, ln(t).....	74
Figure 41 Example of a histogram of frequency of sandstone thermal conductivity.....	86
Figure 42 Image of a simulation 60x60x100 m ³ of sandstone thermal conductivity obtained by using borehole data.	87
Figure 43 Simulation of thermal conductivity with a spherical model and with a gaussian one.	87
Figure 44 Dominium of our problem.	92
Figure 45 Discretized 2U exchanger borehole.....	99

Figure 46 a) Fictitious borehole b) n boreholes extracted from the simulation.....	103
Figure 47 Mesh used in the synthetic case: refined mesh near the six boreholes.....	104
Figure 48 Evolution of outlet temperature of one of the six boreholes, subjected to the constant rate of injection of $4.2 \cdot 10^8$ J/d for 3 days.....	105
Figure 49 Real thermal response test results compared with the simulated ones.	107
Figure 50 Evolution of the difference of temperature between simulated and real thermal response test results.	108
Figure 51 Coarse mesh used for the model.	109
Figure 52 Temperature on the investigated volume.	109
Figure 53 Comparison between the real outlet temperature and the simulated ones.....	110
Figure 54 Comparison between the real outlet temperature and the simulated ones through BHE loop module.....	112
Figure 55 a) this is the evolution of inlet and outlet temperature simulated with the power as input. B) this is the evolution of outlet temperature real and simulated in the case of inlet temperature as input.	114
Figure 56 Mesh used in the new numerical model run in FEFLOW. The number of layers is 20.	115
Figure 57 Simulation of thermal response test curve with the new input file as suggested by Alexander Renz, there are still problems in reconstructing the curve.	116

Table of tables

Table 1 Characteristics of soils considered in this study.....	36
Table 2 Thermal properties for different soils (Ingenieure, 2004)	69
Table 3 Résumé of all the minimization function	83
Table 4 Most relevant features for defining a model	89
Table 5 Boundary and initial conditions used in different models.	89
Table 6 Grout characteristics	106
Table 7 Simulation characteristics	107
Table 8 Parameters set per each different simulations run.....	110
Table 9 Parameters set per each different simulations run.....	112

Introduction

Geostatistical techniques, based on the spatial correlation between the values of variables within the reservoir, are popularly used for reservoir characterization, mostly in oil and gas field. In this work they have been applied in the area of shallow geothermal energy and its related reservoir characterization.

Geostatistics is, in fact, a reliable tool for reservoir modeling because it permits us to recreate the variability of natural properties (permeability and porosity in the oil field, thermal conductivity and thermal capacity in the geothermal one). There are also other variability that we need to take into account while modeling a geothermal system.

In the shallow geothermal system there are many components influencing the extraction power rate. Some of them depend on the characteristics of geothermal reservoir (equivalent thermal conductivity of each specific volume considered, equivalent hydraulic conductivity, etc), while others depend on the operation and management of end-user (buildings thermal loads, heat pump efficiency, etc.).

All of them are time varying:

- Natural properties of the underground vary along time because of the saturation, presence, level and velocity of groundwater flow, etc.
- Building thermal loads vary along time because of the seasonal variations and management of the heat pump system.

Therefore, the different components (borehole heat exchangers, heat pump and internal thermal distribution) are strictly linked so that a variation in one circuit generates the variation into the other one.

For all these reasons, extraction power rate from the shallow geothermal reservoir is never constant during the working time of the heat pump; consequently, equivalent thermal conductivity is not constant at all. Moreover the equivalent value measured by thermal response test is limited to a very narrow cylindrical volume and is not reliable for all system duration and life time (influencing an area of radius 5-15 cm). Here follows the importance of improving the knowledge of this parameter all over the reservoir and the correct evaluation for its equivalent value. The approach proposed is directly taken from the oil & gas experience: we will apply the so called “inverse problem” to the geothermal problem.

In reservoir engineering, the studied reservoir is physically inaccessible, so its properties have to be determined through indirect methods (Mata-Lima, 2006). In this context one of the most used processes is inverse modeling, which is useful for characterizing petrophysical properties through the integration of static and dynamic data (Mata-Lima, 2006).

There is an evident parallelism between the oil & gas case and the geothermal one: in both case we have a sort of production test, which is, for the former, a well test, while, for the latter, a thermal response test. Through these tests we want to obtain the most important parameters for our cases: hydraulic conductivity and porosity, saturations for the oil & gas case, ground thermal conductivity and ground volumetric heat capacity for the geothermal problem.

Our aim then is to apply the inverse modeling to our research in order to get a better model of the involved ground and therefore a better dimensioning of the geothermal system coupled to the heat pump.

It is useful, in order to understand better the topic, to deepen both the cases, oil and geothermal ones.

The classic inverse problem: the oil case

Modelization of an oil reservoir requires the characterization of both the formation field (lithology, permeability, porosity, saturation distribution, etc.) and fluid mobility properties (Mata-Lima, 2008). Moreover it requires the knowledge of production data for modeling the internal properties of the reservoir. Normally, in a simple problem of porous flow, it is used a progressive mathematical modeling (*forward modeling*) in which it is assumed that underground properties, initial and boundary conditions are known.

But in reality information doesn't exist characterizing the entire spatial domain in the considered case; on the other hand indirect methods, used to obtain data, give us secondary information (*soft data*) that needs a joint validation with primary information (*hard data*). This information furnishes the spatial distribution of reservoir properties.

These data, so called static, aren't sufficient for characterizing reservoirs' performances: for doing that we have to integrate dynamic data (production ones). Landa (Landa, 1997) distinguishes three groups of methods for reservoir study:

- a. Probabilistic or stochastic (with static data)
- b. Deterministic (with dynamic data)
- c. Emergent (combining previous methods).

Considered that in reservoir engineering the system is physically inaccessible, emergent methods are used, coupled with inverse modeling to characterize its petrophysical properties.

In its general form, an inverse problem refers therefore to the determination of the plausible physical properties of the system, or information about these properties, given the observed response of the system to some stimulus (Oliver, et al., 2008).

In a geostatistical approach to the inverse problem, a set fine grid values of permeability and porosity is perturbed in order to match the synthetic response of the model with real production data. The biggest advantage of this method is that, by perturbing the images (previously created through a geostatistical process as different realizations of the same variable), we preserve the spatial distribution of data as revealed by variograms and distributions of original variables (Hu, 2002; Hu, et al., 2001).

The geothermal case

By applying the inverse problem to the geothermal case, we will create different realizations of thermal conductivity (through a direct sequential simulation) (Soares, 2001) and we will find which one is the best one to fit the real production data (temperature evolution along time).

The software that has been used to develop this procedure is FEFLOW 5.4 (Finite Element subsurface FLOW system).

So far, there are still problems in a direct measuring of real thermal conductivity of the different geology of the geothermal reservoir; usually the values for thermal conductivity are taken from the VDI norms. This first study is a synthetic one, based on literature data and spatial variability hypotheses.

After testing this procedure, we will try to reconstruct a real thermal response test. In this case, we have some information about the thermal conductivities involved, we create our realizations and we run the model with the same initial and boundary condition as in the real test. The procedure is the same as before, but in this case we will work with real data and not fictitious.

In order to perform a comparison between the result of a normal TRT analysis (through ILS model) and the result of the inverse problem, we need to perform an upscaling of our best thermal conductivity realization for obtaining a single value of thermal conductivity comparable with ILS result.

The whole process of the inverse problem applied to shallow geothermal exploitation suffers the problem of lack of thermal conductivity measures. In fact, up to now, there are not well developed and cheap technologies for direct measuring, in laboratory and on site, thermal properties of soils, while for rocks' ones the technology is much more developed. Moreover thermal conductivity's maps are in progress just in some regions of Italy (see work in process of Emilia Romagna region on it) (Martelli, et al., 2011) .

Outline of this study

This study aims to model a geothermal reservoir used for air conditioning purposes. Reservoir characterization requires modeling of spatial distribution of thermal parameters, linked to petro-physical properties as well as to water content and water flow. Direct small scale data are actually scarce and the main tool to characterize the reservoir is Thermal Response Test (TRT), a sort of production test which allows estimating underground equivalent values of thermal properties. There are also many space-time components that are never constant during system working time and that influence the equivalent thermal conductivity. Therefore we need a numerical model to simulate the reservoir performance in a complex dynamic framework.

The approach adopted for reservoir characterization is the "inverse problem", typical of oil&gas field analysis, given the existing similarities.

In fact, normally, inverse method consists on the perturbation of a set fine grid values of hydraulic conductivity and porosity numerical model, in order to feed a process simulator and to match the production real response. Similarly, we create different realizations of thermal properties by direct sequential simulation and we find the best one fitting real production data (fluid temperature along time).

A geostatistical reservoir model has been set up based on literature thermal properties data and spatial variability hypotheses and some cases have been created. First, some synthetic cases have been simulated and compared with the synthetic real case. Then some real TRTs have been tested.

Part I will be an overview on geothermal energy, both on the general science and, then, more specifically on low enthalpy geothermal energy (how to exploit it, how the system functions). Part II deepens into the low enthalpy theme, explaining borehole heat exchanger modeling, with analytical and numerical model (some of them are explained more in details, because they are more important for our aims). Part III is about the inverse model, its results and the follow up of this work.

PART I Geothermal Energy: an overview

1. RENEWABLE ENERGIES: THE PLACE OF GEOTHERMAL

In the last decade one of the most important world's topics had been how to reach the limits imposed by *Kyoto Protocol* (the target agreed was an average reduction of 5.2% from 1990 levels by the year 2012).

The application of this protocol in the European Union legislation led to the so-called 20-20-20 objective: every country of European Union has to reach this objective before 2020, which means it has to reduce greenhouse gas emissions of 20% compared to 1990 levels, to increase of 20% the percentage of renewable energy and to reduce energy consumption of 20% improving energy efficiency.

As it is written in the "Communication from the Commission to the European Council and the European Parliament - an energy policy for Europe" of 10th of January 2007 "the point of departure for an European energy policy is threefold: combating climate change, limiting the EU's external vulnerability to imported hydrocarbons, and promoting growth and jobs, thereby providing secure and affordable energy to consumers".

A technology coming to our minds thinking about how to reach these objectives is renewable energy (also called alternative energy), which encompasses a variety of power generation sources. The name renewable comes directly from the fact that resources used to create electrical power are naturally replenished. The most common forms of alternative energy are solar power, wind power and small hydro power, but other forms can also be mentioned: tides, waves, ground heat and biomass.

In the way of reaching Kyoto objectives, these energies are very useful because they are characterized by:

- 1) Non-emissions (solar, wind, water and geothermal)
- 2) No production of harmful exhaust (geothermal, water, solar and wind)
- 3) No production of toxic or radioactive waste products (geothermal, water)
- 4) No noise (mostly solar and water)
- 5) No "use up" of resources (solar, wind)
- 6) Possibility of power energy storing as a backup (solar, water).

Considering all the advantages that these energies are able to give, it's strange to think they are still relatively rare. The major problem is that in many cases and in many countries there are still significant drawbacks to relying on them as a sole home power source (<http://www.absak.com/library/alternative-renewable-energy>).

In order to achieve the legislated target to reduce emissions in 2050 by 80% relative to 1990 levels, it is normal to guess that heat from buildings has to be almost fully decarbonized (Change, 2011). The principal heat options to work on are air-source or ground-source heat pumps and district heating.

As it was presented in the last World Geothermal Congress (Lund, et al., 2010), held in Bali in April 2010, geothermal direct-use in Italy has increased by a factor of 1.2 in the last five years, to 867 MWt and 9,941 TJ/year. This big development is basically due to the birth of new geothermal district heating cases and to the increasing number of single house installation, mostly in the northern part of Italy. Single house installations are of both types, closed and open loop (see next chapter) systems (installation of geothermal heat pumps has increased

15% in 2009 with about 12.000 units installed); concerning the district heating, some are operating in the country (Ferrara is the most important one).

The installed capacity and annual energy use for the various applications (Lund, et al., 2010) are:

- 92 MWt and 1,769 TJ/yr for individual space heating;
- 118 MWt and 963 TJ/yr for district heating;
- 111 MWt and 1,329 TJ/yr for greenhouse heating;
- 100 MWt and 1,632 TJ/yr for fish farming;
- 28 MWt and 130 TJ/yr for industrial applications;
- 187 MWt and 3,157 TJ/yr for swimming and bathing;
- 231 MWt and 961 TJ/yr for geothermal heat pumps for heating and cooling.

Concerning European legislation, we have to refer to the *Directive 2006/118/EC*, called Groundwater Directive, and the *Directive 2009/28/CE*. Italian legislation refers principally to *D.Lgs. 152/2006*, *Legge 99/2009*, *D.Lgs. 22/2010* and *D.Lgs. 28/2011* as the application of the European Directive 2009/28.

Considering the application of this system in Italy, some are the incentives applied in case of installation of renewable supplies. This matter is defined into "*Legge Finanziaria 2011*": in fact, after a great debate, lasted the last few months, it was re-approved a 55% bonus (for 2011) for energetic requalification of buildings (fiscal deduction diluted in 10 years). In particular deduction concerns these expenses:

- ✓ Those leading to a limit value of energy demand per year for winter acclimatization less than 20% respect to values written in annex C, n°1, table 1 of *D.Lgs. 192/2005*
- ✓ Regarding the installation of solar panels for hot water production (domestic, sportive or industrial use) till a maximum value of deduction of 60 thousands euro
- ✓ Regarding the installation of condensing boilers till a maximum value of deduction of 30 thousands euro
- ✓ Regarding the installation of windows, pavements, etc. till a maximum value of deduction of 60 thousands euro (see table 3, *Legge 296/2006*).

Concerning houses' renovation, public can ask for a 36% deduction also on the works for energetic savings (see *Legge 9 January 1991 n. 10* and *D.P.R. 26 august 1993 n. 412*).

Moreover *Delibera 348/2007* of Electric Energy and Gas Authority, titled "Economic condition for the connection service supply" establish that there is an electric tariff which incentives heat pump (0,14 €/kWh_e).

As far as these incentives (see first one) exist, it can be foreseen an increase in the use of this technology; therefore it is important to have a consistent and reliable method for dimensioning a geothermal field. In fact, two are the problems linked to the errors in dimensioning (over/under estimation of the amount of boreholes):

- Over-estimating can lead us to an increase of the price of all the system
- Over/Under-estimating can lead us to the collapse of the system and/or of the reservoir or not to reaching the temperature in the building.

That's why it is such an important issue the proper dimensioning: we want our system to be reliable for a long time and fulfilling the objectives for whose it was built up. After all these considerations it's therefore clear that a good project behind our system is the best way to sell it and to make people trust the technology and use it.

First of all it has to be understood what a good project is: a primary approach is to define it in the final balance, examining the best practices to promote in economic terms. But we cannot do a good project without a correct prior analysis. That's why it is important to have all the prior data and to try to simulate an operational condition of the system to be designed. More the project is correct, with fewer mistakes, the longer it will last and the higher the return will be.

Moreover ground coupled heat pumps are recognized as being among the most efficient and comfortable heating and cooling systems available, by the US Environmental Protection Agency (Magraner, et al., 2010). The typical advantages of these pumps are the reduced noise, lower greenhouse gas emissions and reasonable environment safety, lower annual operating cost (compared to the cost of a conventional system (Lund, et al., 2010).

After this introduction I can underline which is my objective and how the study will be developed.

2. THE EXPLOITATION OF GEOTHERMAL ENERGY

Geothermal is the science which studies the thermal phenomena occurring in the internal part of earth Geothermal flux is the amount of heat coming to the surface from inside the earth (nucleus and mantle), that irradiate then towards the crust and therefore to the atmosphere. The average flux is $Q = 0,065 \text{ W/m}$.

Geothermal gradient determines the increase of temperature with depth; depends directly from the thermal characteristics of the ground and it is the measurable effect of the nucleus heat. The average value is $3^{\circ}\text{C}/100 \text{ m}$.

Geothermal anomalies, linked to geo-structural context, are instable areas with uprising magma and volcanism. These "hot" critical areas are characterized by a gradient that can easily be 10-15 times higher than the average one (one of these areas can be located in the central southern Tyrrhenian band, in between Toscana, Lazio and Campania: the well-known area of Larderello-Travale).

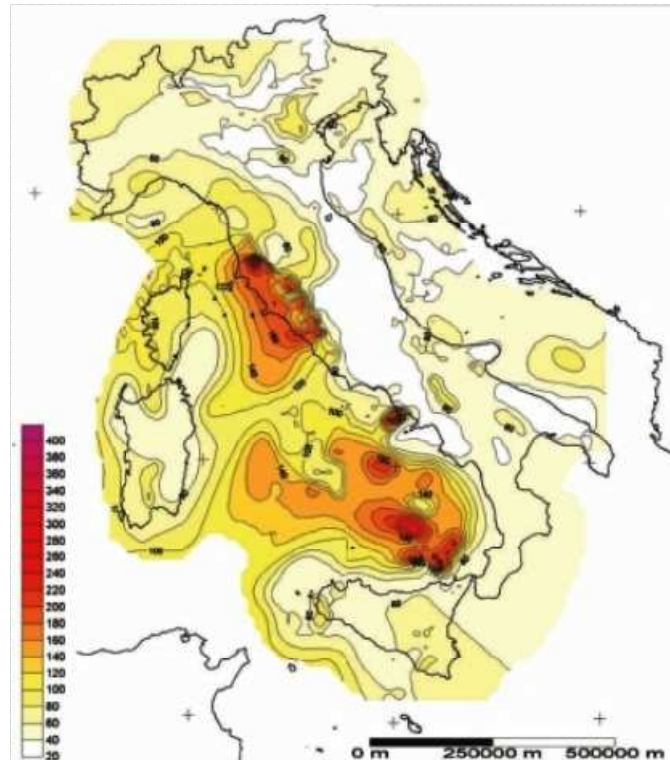


Figure 1 Map of geothermal areas in Italy. Legend refers to the temperature in °C that we can encounter while increasing the depth from the surface (modified by Della Vedova et al. 2001).

In most part of earth, rocks have a temperature around 25-30 °C at 500 m of depth, and of 35-45°C at 1000 m. In other areas, where geological conditions are more favorable (less thick crust, volcanism or tectonical fractures), temperature can reach and overcome 200°C. Thermal energy stored in these places is made available at accessible depths through thermal vector existent in earth crust and called geothermal fluids.

Thermal energy stored in these areas is made available at accessible depth through thermal vector existents in earth crust and called geothermal fluids.

Going back to the surface, above 15-20 m of depth we find the *omothermal area*, in which the heat is given exclusively from the thermal flux coming from the earth itself, with an average increase of temperature of 1°C every 33 meters of depth. In most of the Italian regions, independently from the rocks, from the geological-structural asset and from stratigraphy, temperature in the omothermal area is comprised between 12 and 17°C (Fig. 4).

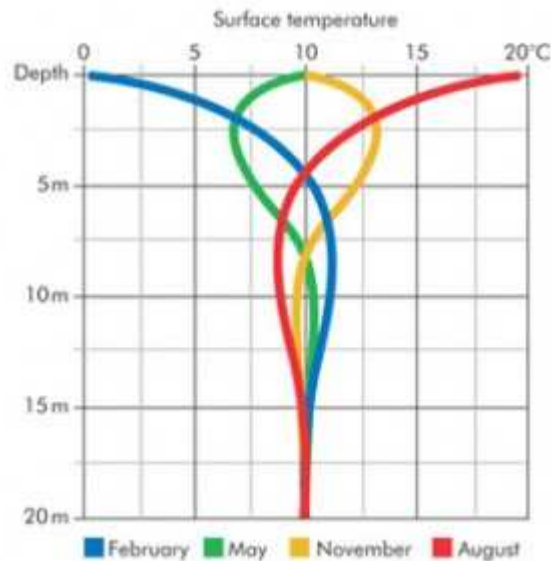


Figure 2 Evolution of ground temperature with depth. The first 10-15 meters are influenced by external temperature, but after 20 m of depth we reach the omothermal area (until 100-150 meters of depth). This is relative to Switzerland's temperatures: in Italy it will be centered on 15°C, instead of 10°C. (<http://www.casainnovativa.com/fonti-rinnovabili/geotermia-note-storiche-e-scientifiche>)

Fundamental for defining how to exploit ground temperatures is the concept of enthalpy, that is the measure of the total energy of a thermodynamic system: it includes the internal energy (energy required to create a system) and the amount of energy required to make room for it by displacing its environment and establishing its volume and pressure. The relation between enthalpy and heat is really important, because an increase in enthalpy of a system is exactly equal to the energy added through heat (if the system is under constant pressure). Concerning geothermal energies, we can define different types of energy by considering the enthalpy content of the involved fluids: high enthalpy energies are those in which fluids have more than 1000 kJ/kg of enthalpy content; medium-low enthalpy energies are those in which fluids have less than 1000 kJ/kg of enthalpy content. These are the uses of geothermal energies, relating them to their enthalpy degree:

- 1) *High enthalpy energy* for production of electricity through high temperature steam which activates turbines and transforms its energetic content into mechanical energy;
- 2) *Medium enthalpy energy* directly used for district heating or used (even with temperature lower than 100°C) with ORC (Organic Rankine Cycle) turbines;
- 3) *Low enthalpy energy* based on the thermal exchange with the underground through systems made by probes included in the ground and by geothermal heat pumps (GHP) for the air conditioning of buildings (heating and cooling).

In this work we will focus on low enthalpy energy and the modeling necessary to create a good operative project.

2.1 High enthalpy geothermal

As said before, high enthalpy geothermal energy is used for production of electricity through high temperature steam coming from the underground. In particular some are the necessary conditions for its existence:

- We need to have an exceptional heat source not too deep (in this case the only source with these characteristics is a magmatic mass)
- In the underground has to be present a high permeability layer, with permeability and porosity values useful for establishing stationary conditions in the convective water circulation. This layer is therefore called reservoir.
- In the underground has to be present an impermeable layer (cap rock) that covers our reservoir and it has to be on top of the other layers. Permeability of this layer has to be low in order to avoid the leak of hot fluids from the reservoir.

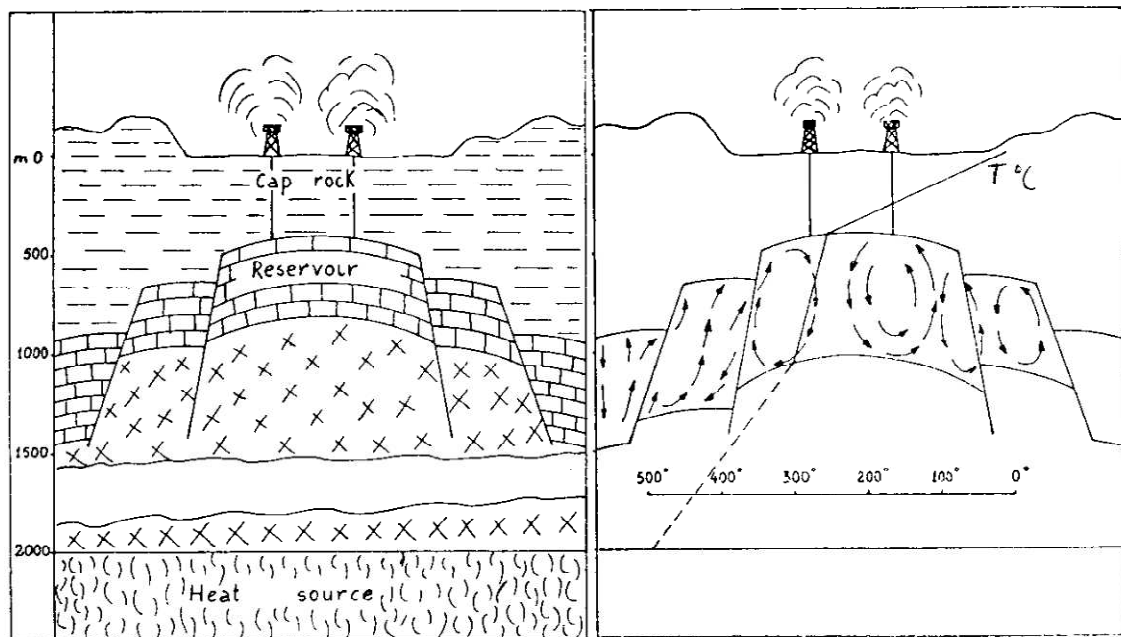


Figure 3 General scheme of a geothermal field: on the left, geological section and on the right temperature values on a vertical profile (Facca & Tonani, 1964)

Normally the depth investigated and exploited with these systems are below 1000 meters. The energy of the fluid used for producing mechanical energy depends on the difference of temperature existing in the turbines (difference between superheated steam temperature and room temperature); in fact the efficiency of the engine depends on the difference of temperature.

Heat transmitted from the heat source can be used in an advantageous way only if it is contained in a fluid that reaches the surface with temperature and fluxes necessary for producing energy in economic terms.

The classification of geothermal systems is the following (presentation about geothermal energy, N. Graniglia):

1. Hydrothermal systems
2. Geo- pressured systems
3. Hot dry rocks
4. Magmatic systems

1. Hydrothermal systems are the most diffused ones and they can be divided into two types, depending on the temperature and chemical characteristics of the fluid:

-
- *Water dominant reservoirs*: they produce fluids constituted by water in liquid phase or water and steam mixtures. The reservoir is filled up by water at high temperature and high pressure. They can be divided as well in two types: hot water systems (lower temperature, water reaches the surface with a temperature between 30 and 100°C) and wet steam systems (cap rock is impermeable and obstacles the flux towards the surface, increasing the pressure of the reservoir).
 - *Steam dominant reservoir*: water and steam coexist, but steam is the dominant phase. Wet saturated steam, while flowing up to the surface, becomes super-heated steam and blows out with high pressure (up to 5-10 bar) and high temperatures (more than 250°C). These systems are the most important for electricity production.

2. Geo- pressured systems are located in sedimentary basin where sedimentation had been rapid and without expelling interstitial fluids. Systems' pressure could reach values up to 100MPa. The element limiting the exploitation of these systems is the low capacity of maintaining high constant fluid flow rate.

3. Hot dry rocks can be encountered in low permeability systems, where a magmatic body had intruded during an advanced cooling phase. These rocks can be cultivated by pumping water at high pressure that fractures the rocks.

Concerning the geothermal power plants, three are the most important ones (<http://www.renewableenergyworld.com/rea/tech/geoelectricity>):

- *Dry steam power plants* use steam piped directly from underground wells to the power plant, where it is directed into a turbine/generator unit (examples of this application are The Geysers in northern California and Yellowstone National Park in Wyoming).
- *Flash steam power plants* are the most common; they use geothermal reservoirs of water with temperatures greater than 180°C. This very hot water flows up through wells in the ground under its own pressure: as it flows upward, the pressure decreases and some of the hot water boils into steam. The steam is then separated from the water and used to power a turbine/generator. Any leftover water and condensed steam are injected back into the reservoir, making this a sustainable resource (obviously depending on the amount of water re-injected and on the auto-recharge of the reservoir).
- *Binary cycle power plants* operate on water at lower temperatures of about 105°-180°C. These plants use the heat from the hot water to boil a working fluid, usually an organic compound with a low boiling point. The working fluid is vaporized in a heat exchanger and used to turn a turbine. The water is then injected back into the ground to be reheated. The water and the working fluid are kept separated during the whole process, so there are little or no air emissions.

2.2 Medium enthalpy geothermal energy

In case we are using temperature average between the high and the low enthalpy we can talk about medium enthalpy energy, that can be exploited in two main important ways: directly for district heating or indirectly with Organic Rankine Cycle turbines.

District heating is a system for distributing heat generated in a centralized location for residential and commercial heating requirements such as space heating and water heating. In

case of geothermal heating, we are using the water heated underground (temperatures up to 100°C) which is brought to the surface and pumped through large pipes directly into businesses and homes for space heating. Some are the examples existing in Italy, using district heating and cooling, as Ferrara, Torino and Milano. The heat is distributed to the customer via a network of insulated pipes: district heating systems consists of feed and return lines. It has to be noted that this system can also be realized in case of high enthalpy geothermal systems: in this case, in fact, we will use the steam coming out from the boreholes.

Another way of using medium enthalpy geothermal systems is to use their heat in an indirect way through the Organic Rankine Cycle turbines. These cycles RE based on the Rankine Cycle which is a thermodynamic cycle converting heat into work and that uses water as working fluid (www.turboden.eu/en/rankine/rankine-history.php). The Organic Rankine Cycle is a thermodynamic process where heat is transferred to a fluid at a constant pressure. The fluid is vaporized and then expanded in a vapor turbine that drives a generator, producing electricity. The spent vapor is condensed to liquid and recycled back. The main difference between the Rankine Cycle and the Organic one is the type of fluid used: ORC makes use of an organic fluid with a boiling point lower than water. This characteristic enables the recovery of heat from lower temperature sources such as medium enthalpy geothermal heat. The low temperature heat is used to drive a turbine and create electricity.

2.3 Low enthalpy geothermal energy

This kind of energy exploits the constant temperature that we have in the ground above 15-20 m depth (for lower depth there is still a seasonal influence) and that is equal to the average value of external temperature during all year (10-15 °C) in Italy. Obviously this temperature depends not only on the external temperature but also from the heat flux coming from inside the earth, but in the first 100 meters it is still much more influenced by the external temperature.

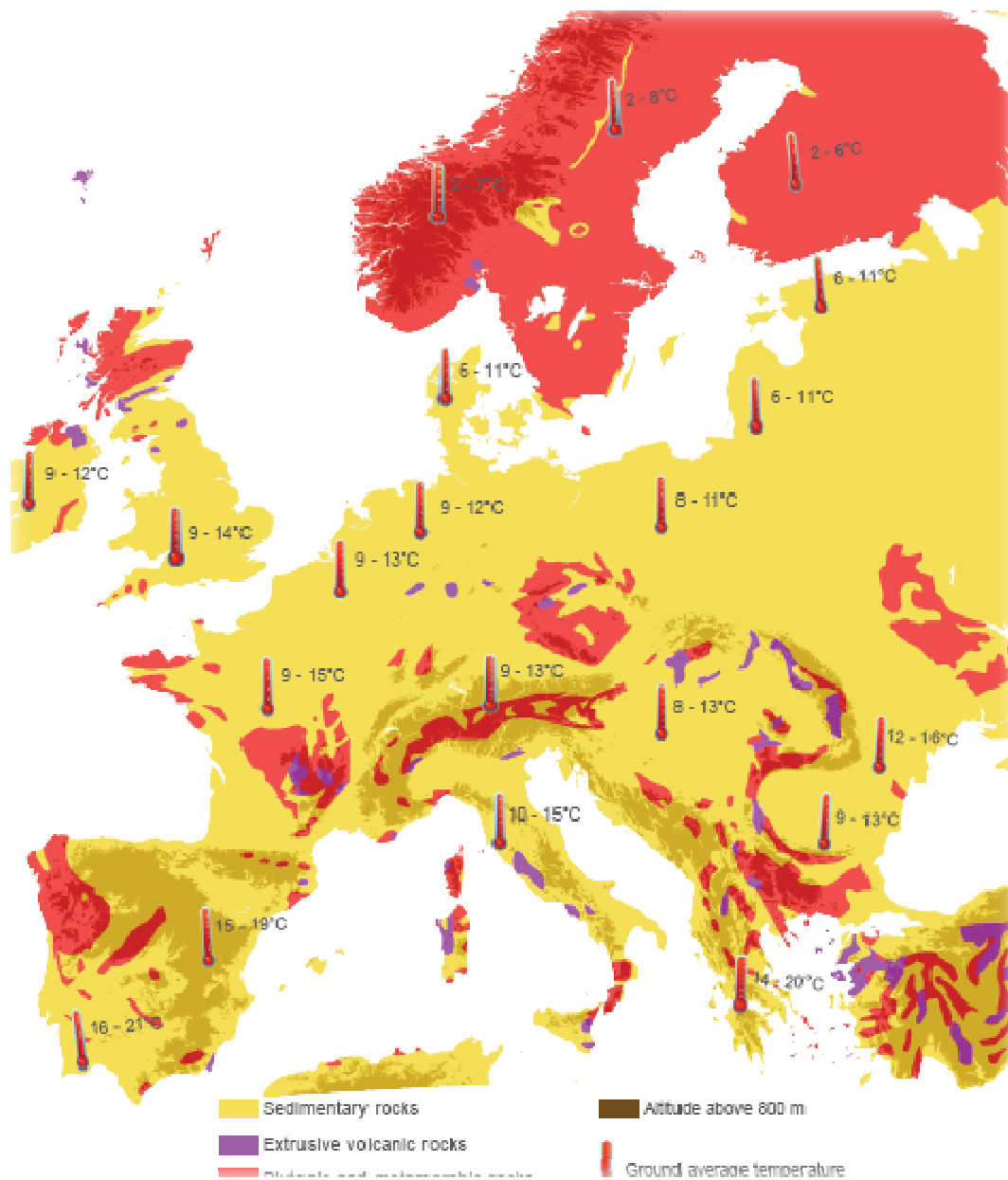


Figure 4 Average ground temperature of the first 100-150 meters (www.geotrainer.net)

In the case of exploitation of shallow geothermal energy, different are the systems feasible. In fact we can have vertical (open or closed loop) or horizontal tubes; there are also some new options, like the spiral tube, energy piles, etc.

In Italy, *open loops* are more common than closed loops, moreover in the northern part of Italy (Lombardia region). Some are the problems related to this kind of technology (Maritan, et al., 2008) that we need to take into account:

- Eventual pollution of the aquifer and respect of legislation limits
- The use of the submerged pump implies a considerable energy consumption that has to be considered in performances' evaluations
- Lower reliability than a closed loop system
- Need of an aquifer always available and with a constant condition

- Complex authorization iter
- Max ΔT usable: 3-4°

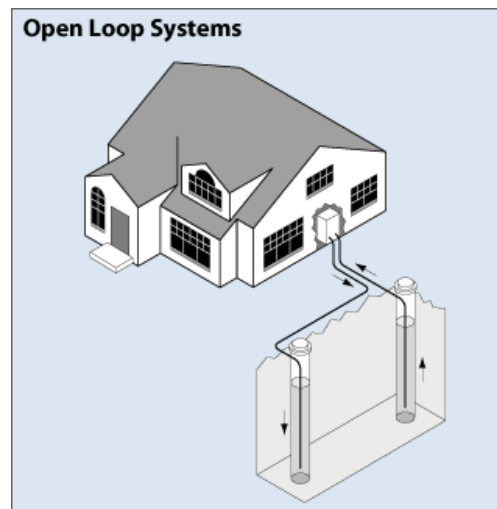


Figure 5 Scheme of a shallow geothermal system based on a vertical borehole heat exchanger with open loop (www.energysavers.org)

In case of *vertical closed loop*, polyethylene pipes are installed in small diameter boreholes (20 to 40 mm) and a closed circuit exchanges energy with the ground; in an open loop, water from an aquifer is pumped to the heat pump or to a heat exchanger and then to the same or to another aquifer with a second borehole or the waste water line (Maritan, et al., 2008).

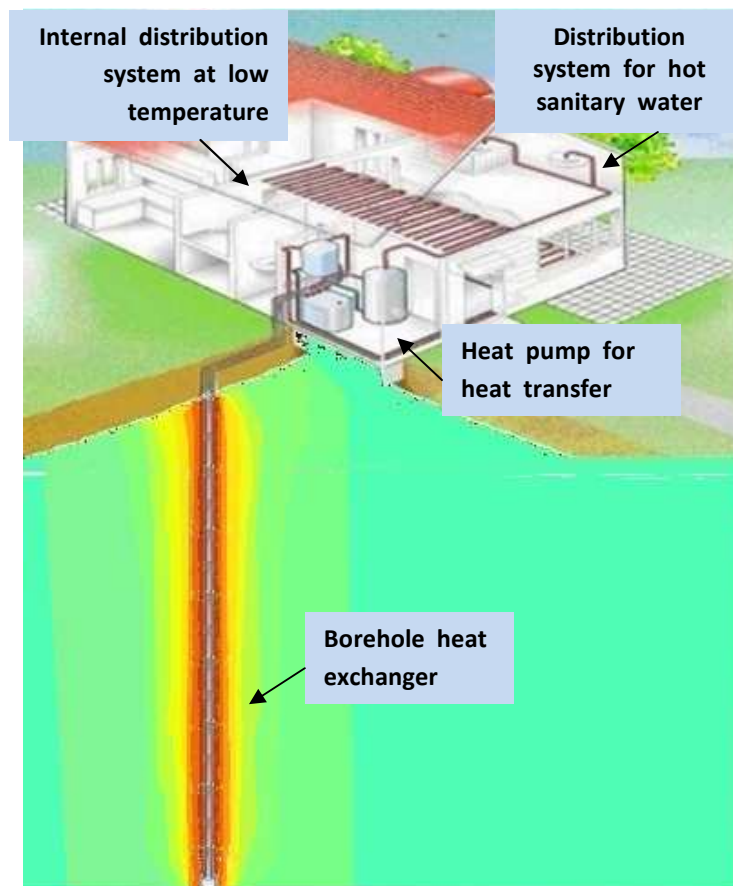


Figure 6 Scheme of a shallow geothermal system based on a vertical borehole heat exchanger

Another possible option in the vertical case is the *spiral tube*: the system is the same as the one of a vertical borehole heat exchanger, but the difference consists in the tubes. Normally in the vertical systems tubes are in a U position, while in the spiral case they are rounded into a spiral that reaches the end of the borehole and it comes up straight to the surface. They do not take up much space and this means you can use less of the ground area. They are easy to use as the capture is made at a shallow (4 m) depth. Depending on the nature of the ground, the captors allow heat extraction of between 0.7 and 1.2 kW (<http://www.archiexpo.com/prod/amzair/ground-collector-kits-62590-293822.html>). Of course we have to consider the seasonal influence of the external temperature on the first meters below the surface.

Cui et al. (Cui, et al., 2011) have studied this system and they affirm that the spiral coil configuration has the advantages of more heat transfer area in a certain pile (BHE or energetic pile) and better flow pattern without air chocking in the pipes compared with the serial or parallel U-tubes in the pile. In addition, the spiral coil system can reduce the complexity of the pipe connections and decrease to a certain extent the thermal “short-circuit” between supply and return pipes. Their study considers the application of the spiral coil to the energy piles.

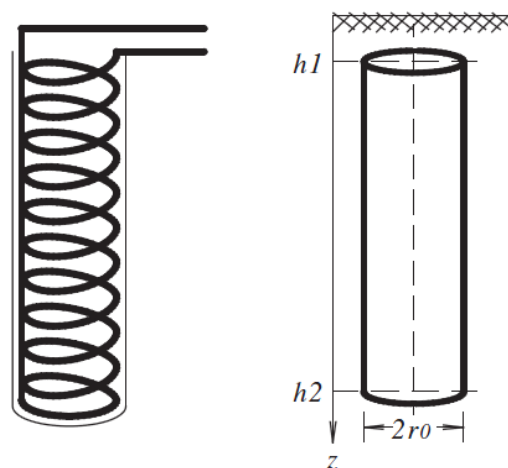


Figure 7 Schematic diagram of spiral coils

So far, not many are the applications done of this new system as not many are the studies developed on the subject: therefore the reliability of these systems has still to be confirmed. It has to be pointed out, in any case, that the creation of new solution implies that low enthalpy geothermal energy is a developing research area.

In case of *horizontal collectors*, the solution is less expensive, because it won't need borehole's drilling; the inconvenient is, then, that it is more influenced by the fluctuations of surface temperature (tubes are inserted at 2-3 meters of depth and spaced 0.6-1.5 meters one from the other). Moreover the surface used is much more than in the vertical case, in fact it can be even twice the surface to acclimatize.

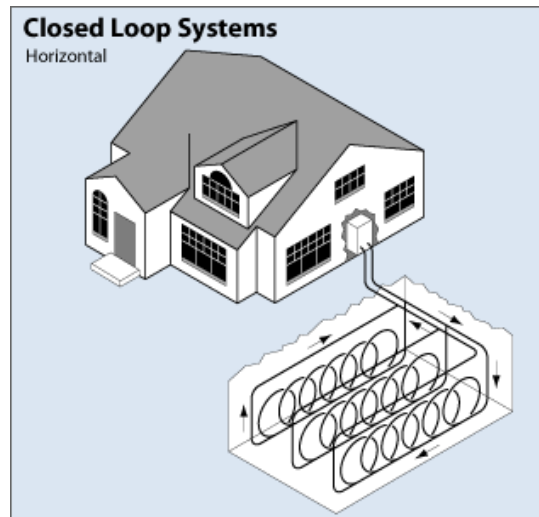


Figure 8 Scheme of a shallow geothermal system based on a horizontal borehole heat exchanger (www.energysavers.gov)

Energy piles are another solution: they consist in inserting the geothermal probes inside foundation piles while constructing the building. In case foundation piles are used for this purpose, their diameter is dimensioned also in order to optimize heat exchange between the ground and the circulating fluid. The project of these systems is more complicated than the one of a normal vertical borehole field, because while dimensioning the piles it has to consider both the thermal solicitations and the mechanical properties.

There is also another way, which is not really related to the ground: in fact it uses a pond or a lake exploiting it as a normal system exploits the ground. The fluid circulates through polyethylene pipes in a closed system. Pipes are usually run to the water with longer sections submerged in the water itself. Pond loops with closed systems do not affect water bodies in any adverse way.

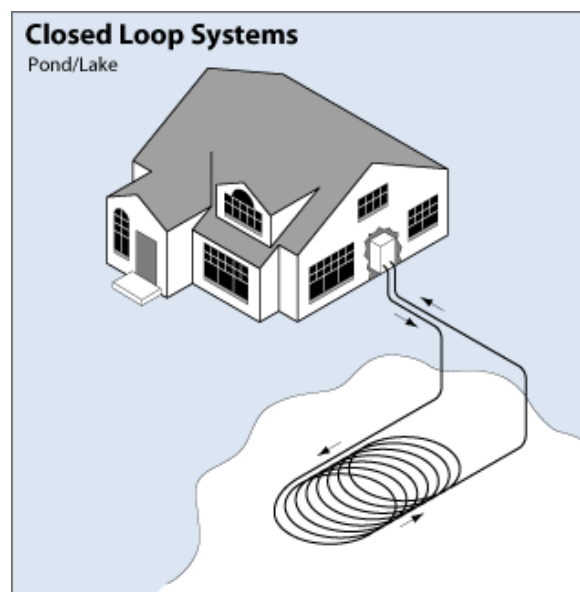


Figure 9 Scheme of a shallow geothermal system based on pond/lake heat exchanger (www.energysavers.gov)

PART II Vertical borehole heat exchangers and thermal conductivity

1. INTRODUCTION ON VERTICAL BOREHOLES HEAT EXCHANGERS AND THEIR FUNCTIONING

In this work we will focus on the vertical collectors, which are the type mostly used in Emilia Romagna region (where Bologna is) and also in northern part of Europe.

The choice of the heat pump and the dimensioning of geothermal probes require the knowledge of:

1. Geological characteristics of the underground
2. Thermal power extracted from the ground expressed in kW_t
3. Length of the geothermal probe
4. Technical documentation of the heat pump given by the constructor.

The geo-exchanger most used for house conditioning is the one with vertical collectors; for its dimensioning we need these values: ground thermal conductivity λ , ground thermal capacity ρC , difference of inlet and outlet temperatures ΔT , borehole thermal resistance R_b . For obtaining these values we should follow this procedure:

- 1) Geological and hydrogeological framework
- 2) Thermal properties of the soils of the first 100-150 m and around the probe with particular reference to the stratigraphy
- 3) Estimation of the average thermal return of the ground, measure of the ground temperature (geothermal gradient, seasonal influence)
- 4) Estimation of borehole thermal resistance (depending on the filling material and on the collectors' distribution)
- 5) Environmental impacts' evaluation .

Concerning thermal characteristics (2), we should take into consideration the fact that thermal conductivity depends on different factors:

- Soil type (granulometry, density and stratigraphic succession)
- Aquifer characteristics (temperature, flux velocity and depth).

Presence of water favors contact between the system and the underground (which increases the potential efficiency) and restoration of the underground thermal condition modified by the geothermal probes.

Concerning the estimation of the thermal return (3), practice relies on Thermal Response Test (TRT) which consists of an injection of heat with constant power in the geothermal probe for 3 days normally (time for reaching a steady state, see Chap.3).

The system is composed by a closed circuit which is made of:

- a. *Geothermal borehole* ($d = 127\text{-}152$ mm, depth 100-150 m) containing a U tube (single or double) with a diameter of 32-40 mm, made of polyethylene. This borehole is filled by a mixture of cement, bentonite and silica sand (thermal resistance of the mixture is in the range $0.8\text{-}2$ $\text{W/m}\cdot\text{K}$).
- b. *Heat pump* that allows transferring heat from a system with a certain temperature to a system with a higher temperature, furnishing work from the outside. Inside this circuit an inverse Carnot cycle occurs.

-
- c. *Fluid* (water with refrigerants, normally propylenic glycol) which circulates inside the U tube and then in the heat pump.

The general way of functioning is inverted considering the season:

1) **Winter – Heating**

- T_m inlet probe $<$ T_r outlet
 - $(T_r - T_m)$ variable; average $\Delta T = 4^\circ\text{C}$
 - *Cause*: thermal exchange in the ground
 - Two passages of phase in the heat pump
 - Need of electricity
- T_o outlet heat pump (settable), T_i inlet heat pump
 - T_o : 35°C average (for having high COP)
 - $(T_o - T_i)$ variable; average $\Delta T = 4^\circ\text{C}$
 - *Cause*: cession of heat to the building

2) **Hot sanitary water**

- T required: $50\text{-}55^\circ\text{C}$
- Need of a dedicated storage tank
- Reuse of excess heat

3) **Summer – Cooling**

- T_m inlet probes $>$ T_r outlet
 - $(T_m - T_r)$ variable; average $\Delta T = 4^\circ\text{C}$
 - *Cause*: thermal exchange in the ground
 - Two phase passages in the heat pump
 - Need of electricity
- T_o outlet heat pump (settable)
 - T_o : 15°C average (for having high COP)
 - $(T_i - T_o)$ variable; average $\Delta T = 4^\circ\text{C}$
 - *Cause*: withdraw of heat from the building

4) **Summer – Cooling (*Natural cooling*)**

- Heat pump is bypassed
- T_o reachable: $20\text{-}25^\circ\text{C}$
- $(T_i - T_o) =$ average $\Delta T = 2\text{-}3^\circ\text{C}$ max
- Need of electricity only for the circulation pumps
- Applicable if the building has a great insulating rate

Heat pump is constituted by a closed circuit in which a special fluid (refrigerant) flows; this fluid has the capacity to assume a liquid or a gas phase, depending on temperature and pressure conditions.

The closed circuit is composed by:

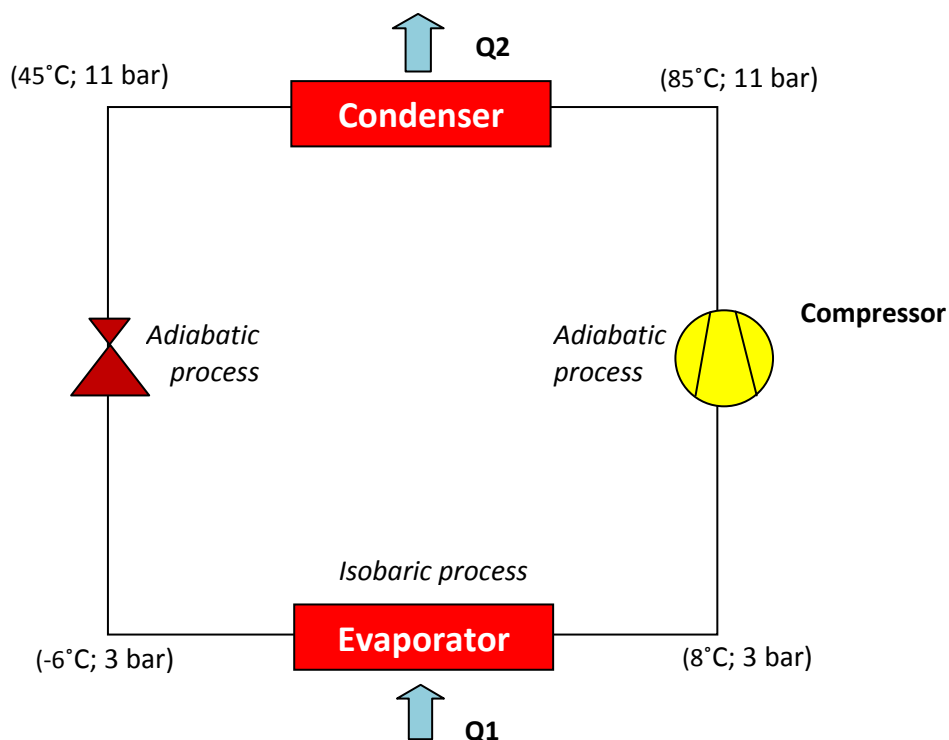
- A compressor
- A condenser
- An expansion valve

-
- An evaporator.

The condenser and the evaporator consist of heat exchanger, namely tubes in contact with a service fluid (air or water) and in which flows the refrigerant (gives heat to the condenser and subtracts heat to the evaporator). All the circuit components can be either grouped in one block, either divided into two parts (SPLIT systems) filleted from tubes in which refrigerant is flowing.

During the functioning the refrigerant, inside the circuit, is subjected to these transformations:

- **Compression:** refrigerant at gas phase and at low pressure, coming from the evaporator, is brought to high pressure; during the compression it heats up, absorbing a certain quantity of heat.
- **Condensation:** refrigerant, coming from the compressor, passes from gas phase to liquid, ceding heat.
- **Expansion:** passing through the expansion valve, the refrigerant in a liquid state transforms partially in gas and it cools down.
- **Evaporation:** the refrigerant absorbs heat from the outside and evaporates completely.



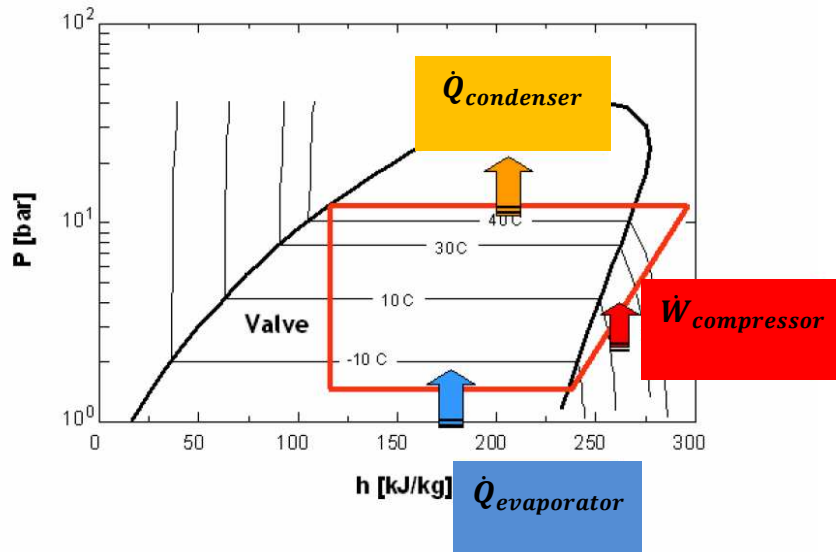


Figure 10 Heat pump circuit and its state curve (from a seminary of Padova university)

The set of these transformations constitutes the heat pump cycle: furnishing energy with the compressor to the refrigerant, this fluid, in the evaporator, absorbs heat from the surrounding mean and, through the condenser, gives it to the mean to heat up.

During its functioning, the heat pump:

- Uses electricity in the compressor
- Absorbs heat in the evaporator, from the surrounding mean (air or water)
- Gives heat to the mean to heat up in the condenser (air or water).

The advantage of using the heat pump derives from its capacity of furnishing more energy (in terms of heat) than the electricity used for its functioning, because it extracts heat from the external environment (air-water).

The efficiency of a heat pump is measured through the coefficient of performance "C.O.P." which is the ratio between furnished energy (heat given to the mean to heat up) and electricity used:

$$COP = \frac{Q_1}{W} = \frac{T_1}{T_1 - T_0}$$

Equation 1

where Q_1 is the quantity of heat obtained, W the work furnished, T_1 is the temperature of the hot source (the place where it has prevue the heating) and T_0 is the temperature of the cold source (the environment).

On the other side, if the system is used for summer conditioning, we talk about refrigeration coefficient (EER, energy efficiency ratio):

$$EER = \frac{Q_1}{W} = \frac{T_1}{T_0 - T_1}$$

Equation 2

where Q_1 is the quantity of heat given to the internal environment, W the work furnished, T_1 is the temperature of the cold source (the place it has prevue the cooling) and T_0 is the temperature of the hot source (the environment).

C.O.P. is variable considering the type of heat pump and the functioning conditions and it has, normally, values around 3. This means that for 1 kWh of electricity consumed, it will give 3 kWh (2580 kcal) of heat to the mean to heat up.

C.O.P. will be much higher the lower is the temperature at which the heat is given (in the condenser) and the higher is the temperature of the source from which heat has been absorbed (in the evaporator).

Above a certain temperature the heat pump deactivates because its performances will reduce significantly. Moreover we should take into account the fact that thermal power given from the heat pump depends on the temperature at which it absorbs heat.

Heat pumps are distinguished based on the cold source (external mean from which subtract heat) and on the hot borehole (air or water to heat up) used.

They can be of different types: air-water, air-air, water-air, water-water and soil-water.

Air as a cold source has the advantage of being available everywhere; however the power given from the heat pump diminishes with the source temperature. In case of using external air (when it is around 0°C) a defrosting system it is necessary, which means further energy consumption. Different and more advantageous is the use of internal air (extracted air) as a cold source.

Water as a cold source guarantees performances of heat pump without being influenced by the external climatic conditions; however it requires an additional cost due to the adduction system.

Underground as a cold source has the advantage of having less changes of temperature compared to the air. In case of horizontal tubes, these have to be buried at a minimum depth of 1-1.5 m in order not to be influenced too much from the outside temperature and to maintain the benefits of insulation.

1.1 Physical background

For a proper and correct simulation of a BHE, it is necessary to know the physical background of this modeling problem. In this case we will face both the thermal and the flow problem; moreover thermal problem has to be solved both along the pipe (advective heat flow) and in the surrounding ground (conduction problem). Two are therefore the phases included in this problem: solid (ground and solid parts of the borehole) and liquid (liquid flowing inside the pipes and eventual groundwater in the ground).

1.1.1 Hydraulics

1.1.1.1 Groundwater hydraulics

Groundwater flow normally is described by Darcy's law: groundwater velocity is determined by the pressure difference along a flow path (it can be density driven – convection – or forced by gravity – advection). The average velocity by Darcy is:

$$u_D = -K_g \cdot \nabla h_g$$

Equation 3

where K_g is the hydraulic conductivity, h_g is the hydraulic head (i.e. fluid level).

K_g is obtained through this equation: $K_g = \frac{k \cdot g \cdot \rho_f}{\mu_f}$ where k is the permeability, μ_f the fluid dynamic viscosity, g is gravity acceleration and ρ_f is the fluid constant density. Hydraulic conductivity is a property that depends both on the soil and fluid relative characteristics; besides as far as the fluid properties are depending on the density and viscosity, which depend on the temperature, also the conductivity depends on the temperature. Luckily, in the range of temperature of BHE performances (low enthalpy range), density and viscosity are constant.

The fluid level h_g is defined as: $h_g = \frac{P}{\rho_f \cdot g} + z$ where P is the pressure and z the z -direction vector.

Here follows a table with all the typical values of hydraulic conductivity for the soils considered in this study.

Type of soil	Hydraulic conductivity	Porosity
Gravel	$10^{-2} - 1$ m/s	0.25-0.40
Clean sand	$10^{-5} - 10^{-2}$ m/s	0.35-0.45
Sandy silt	$10^{-8} - 10^{-5}$ m/s	0.3-0.5
Clay	$10^{-12} - 10^{-8}$ m/s	0.4-0.5
Sandstone	$10^{-8} - 10^{-7}$ m/s	0.05-0.30
Limestone (not fractured)	$10^{-9} - 10^{-6}$ m/s	0-0.20

Table 1 Characteristics of soils considered in this study

Going back to Darcy's velocity, it has to be pointed out that this value is valid in a macroscopic condition and it is not comparable with the microscopic velocity, which is directly related to the actual paths of individual water particles through the grains of the matrix:

$$u_f = \frac{v_D}{\vartheta}$$

Equation 4

This average particle velocity is obtained passing through the porosity.

Darcy's law comes directly from Navier-Stokes' equation, valid at microscopic scale (dimension of pores):

$$\mu \nabla^2 \mathbf{u} = \text{grad } p \text{ and } \text{div } \mathbf{u} = 0$$

Equation 5

Where ∇^2 is the Laplace differential operator $\sum_i \frac{\partial^2}{\partial x_i^2}$, p is the microscopic fluid pressure and \mathbf{u} is the microscopic fluid velocity vector (Matheron, 1983). It can then be shown that the macroscopic Darcy's law $u_D = -K_g \cdot \nabla h_g$ derives from the linearity of the Stokes equation $\mu \nabla^2 \mathbf{u} = \text{grad } p$ and from this conservation of energy (Delhomme, et al., 2005).

1.1.1.2 Hydraulics in pipes

The flow inside a pipe is full of pressure losses, because of the presence of borehole and horizontal conduits' walls roughness, connections, changes of geometry. It is very important to know the amount of these losses in order to size the circulation pump. As far as the heat pump has been chosen based on the energy demand of the building, the volumetric flow rate is therefore determined and defines as well the flow velocity in the pipe, v_{pipe} . Considering a 1D flow in the pipe, the pressure loss ΔP along the BHE of length l in a pipe of diameter d_{pipe} is (Various, 2001):

$$\Delta P = \frac{\alpha \cdot l}{d_{pipe}} \cdot \frac{\rho \cdot v_{pipe}^2}{2} + \sum_{n=1}^i \xi_i \cdot \frac{\rho \cdot v_{pipe}^2}{2}$$

Equation 6

α is the borehole friction factor, ξ the friction factor of pipe fixtures ($\xi = 1$ for the pipe turn point fixtures at the bottom; a list of ξ for various pipe fixtures can be found in (Various, 2001)) and i is the number of pipe fixtures.

Depending on laminar or turbulent flow regimes, different are the formulations of the borehole friction factor, α , applicable. The flow regime in pipes is described by the dimensionless Reynolds Number, Re :

$$Re = \frac{v_{pipe} \cdot d_{pipe} \cdot \rho_f}{\mu_f}$$

Equation 7

Where μ_f is the fluid dynamic viscosity. Generally,

- $Re < 2300$ laminar flow
- $2300 < Re < 10^4$ transient between laminar and turbulent flow

- $Re > 10^4$ fully developed turbulent flow

For both flow regimes, α is dependent on the viscosity of the heat carrier fluid. Different are the equations for obtaining friction number α , by knowing Reynolds number, depending on the regime condition.

1.1.2 Thermal parameters and heat transfer

Different are the heat transfer phenomena involved in a borehole heat exchanger as it can be seen from the figure.

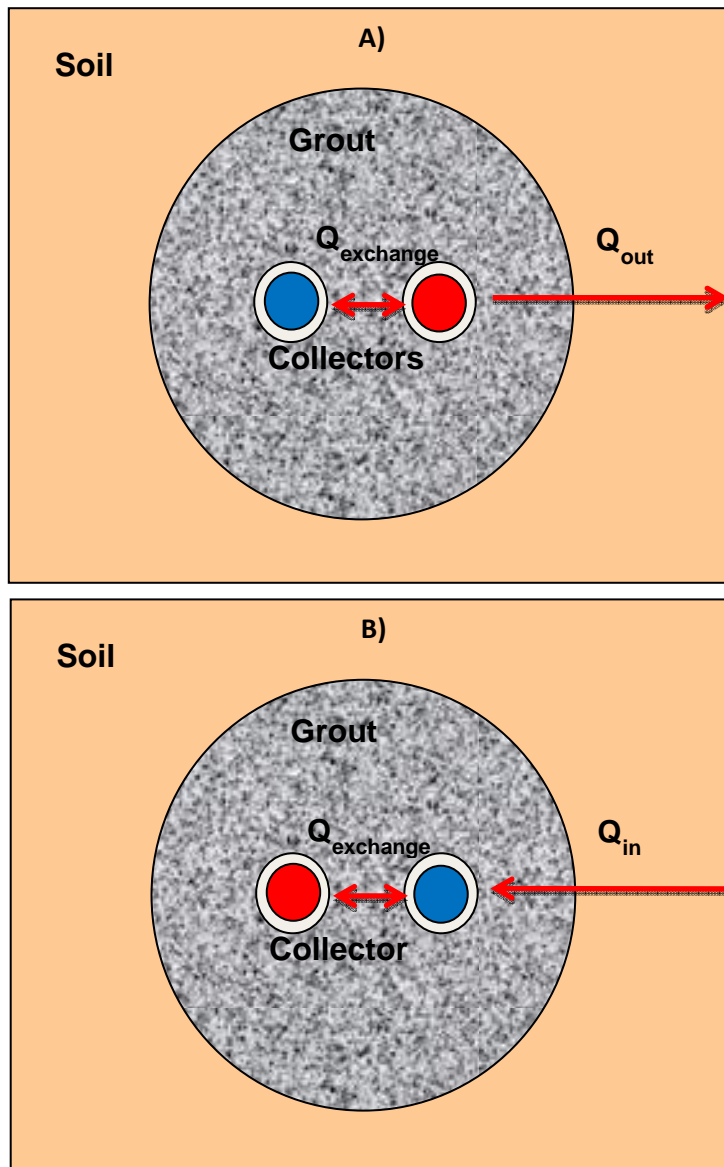


Figure 11 Types of thermal exchange existing between the heat exchanger and the ground. A) is the summer condition while B) is the winter condition.

Three are the most important ones: heat conduction, heat convection and heat advection.

1. Heat conduction which is the transfer of thermal energy between regions of matter due to a temperature gradient: heat spontaneously flows from a region of higher temperature to

a region of lower temperature, approaching thermal equilibrium. This process is the dominant one in rocks and Fourier's law is the basic equation controlling it. Given a direction x , the Fourier's law is written:

$$q_x^{con} = -\lambda_x \cdot \frac{dT}{dx}$$

Equation 8

where $\frac{dT}{dx}$ is the temperature gradient and λ_x is the thermal conductivity, i.e. the ability of transferring heat energy in a given direction by vibrations at a molecular level through a solid or fluid. The thermal conductivity changes with the direction considered, namely it is a tensor: $\vec{\lambda}$.

2. Heat convection which is the vertical movement of molecules within fluids driven by density differences due to different temperatures. Heat is transferred by convection in numerous examples of naturally occurring fluid flow, such as: wind, oceanic currents, and movements within the Earth's mantle. Convection is also used in engineering practices to provide desired temperature changes, as in heating of homes, industrial processes, cooling of equipment, etc. The equation controlling this process is the following one:

$$q_{trans} = h \cdot (T_1 - T_2)$$

Equation 9

where h is the transfer coefficient and T_i are the temperature of the bodies.

3. Heat advection which is the transport of sensible or latent heat by a moving fluid, such as air. Normally it is horizontal. In the groundwater we can have also a transport of thermal energy by advection through pores and fractures (it can affect BHE performance). Advection in chemistry, engineering and earth sciences, is a transport mechanism of a substance, or a conserved property, by a fluid, due to the fluid's bulk motion in a particular direction. The specific thermal power provided by advective mechanism can be calculated as:

$$p_{adv} = \rho \cdot c_f \cdot v_f \cdot \nabla T$$

Equation 10

where c_f is specific fluid heat capacity.

Ground can be treated as two means, solid and liquid ones, controlled by two different equations:

$$\rho_f c_f \frac{\delta T_f}{\delta t} = -\rho_f c_f v_f \nabla T_f + \nabla(\lambda_f \nabla T_f) + h \cdot \frac{A}{V} \cdot (T_s - T_f)$$

Equation 11

Time variation = advection + conduction + convection

$$\rho_s c_s \frac{\delta T_s}{\delta t} = \nabla(\lambda_s \nabla T_s) + h \cdot \frac{A}{V} \cdot (T_f - T_s)$$

Equation 12

Time variation = conduction + convection

t is the time, and A/V describes the heat transfer area A in a reference volume V .

The thermal properties of interest in these three processes are ground thermal conductivity (λ_g), ground volumetric heat capacity (c_g) and undisturbed ground temperature (T_g). These three parameters are strictly connected by the Fourier law of conduction, which in one dimension is expressed by (Carslaw, et al., 1947):

$$\frac{\partial^2 T}{\partial x^2} = \frac{c}{\lambda} \frac{\partial T}{\partial t}$$

Equation 13

All these parameters, necessary for the correct dimensioning of a BTES, are Regionalized Variables (ReV) in space or space-time and can be modeled as Random Functions.

A Regionalized Variable is a variable f that describes a characteristic in a certain point x of a phenomenon that spreads in space and exhibits a certain structure; from a mathematical point of view it is a function $f(x)$ of the point x (Matheron, 1971). Our parameters are ReV because they describe a characteristic in a specific spatial point x and the phenomenon linked exhibits a structure (think about how the temperature varies along with depth).

A Random Function is a set of random variables that have some spatial locations and whose dependence on each other is specified by some probabilistic mechanism (a random variable is a variable whose values are randomly generated according to some probabilistic mechanism). In this case our variables are random function because they do have a spatial location and they can assume some random values depending on the conditions.

- **Ground thermal conductivity** refers to the ground material's property of transmitting heat by conduction. We will explain better of its characteristics in Par. 2.
- **Ground volumetric heat capacity** is the quantity of heat necessary to produce a unit change of temperature in the ground; in natural media, as the underground, varies, but just in space (Regionalized Variable). Regarding TRT issue, it is the responsible of the transient period, characterized by the increase of fluid temperature until the steady state, when all heat has been exchanged between the borehole and the ground. It is an additive parameter.
- **Undisturbed ground temperature** refers to the temperature existing before injection/extraction of heat, which will change according to geothermal reservoir exploitation. This is a main property that quantifies the heat extraction and it is influenced by:
 - outside temperature (average over the year): in fact we will have different average ground temperature depending on where we are (the more to the north, the lower will be the temperature, and vice versa, see fig. 4 of par. 2.3, Part I);
 - geothermal gradient (average value is 3°C/100 m);
 - geothermal anomalies (instead of having the average value of gradient they can be up to 15°C /100m).

Of course the ground temperature changes during the time t when the reservoir is exploited and, in a classical BTES system, a radial configuration of temperatures distribution

around the borehole is the normal result $T(r, t)$. But such variation applies up to a limit surface, $r = [0 - r_{max}(t)]$ by simplifying a vertical cylindrical surface, from which the temperature is always undisturbed: $T(r, t) = T_g \quad r > r_{max}(t)$

The $T(r, t)$ is a Regionalized Variable, that can be modeled as a Stationary Random Function with a very low priori variance (if we consider the first 100-150 meters of depth, otherwise, changing scale to the kilometric, it is a Non Stationary one), if the ground is not thermally exploited and as a Non Stationary Random Function for $r = [0 - r_{max}(t)]$, if the ground is exploited.

Nevertheless, T_g , even in normal geological conditions (i.e. without the presence of anomalous gradients), change along the vertical and the horizontal, $T_g(x, z)$, depending on the three reasons expressed above, on a local to kilometric scale. It is the case of regions with a young geological history, as Italy is, so that each BTES system has its own T_g . Variations are not negligible with respect to the efficiency of the system. The correct knowledge of T_g over the territory is a decisive factor when designing a BTES system. Concerning the geostatistical point of view, temperature is a summable ReV.

2. THERMAL CONDUCTIVITY: STATE OF THE ART

Thermal conductivity refers to the ground material's property of transmitting heat by conduction. Even neglecting the variation of conductivity with temperature, in anisotropic materials typically it varies with orientation and it is represented by a second-order tensor. Moreover, in non-uniform materials, as are natural materials, conductivity varies with spatial location (that's why we consider it a Regionalized Variable). This is a very important issue that must be taken into account when characterizing a shallow geothermal reservoir for at least two reasons:

1. The volume interested by heat flux varies during the reservoir operation;
2. The tensorial nature of the variable makes it a non-summable variable, and therefore it is not possible to calculate an average value by the arithmetic mean.

We have to remember that by discretizing the underground domain in regular elements (support), small enough to be considered homogeneous, coupling two elementary volumes with different thermal conductivities λ_1 , λ_2 , the average conductivity is included between arithmetic and harmonic mean (Matheron, 1967).

$$\frac{2}{\frac{1}{\lambda_1} + \frac{1}{\lambda_2}} \leq \overline{\lambda_{1+2}} \leq \frac{\lambda_1 + \lambda_2}{2}$$

Equation 14

In practice we can measure thermal conductivities in laboratory on small samples, with a quasi-punctual support, resulting in a distribution of values that, given the quasi-punctual support, cannot show any anisotropy. The information at this scale allows us to model the spatial distribution of conductivity at a small scale, but any actual application works on larger scales, for example a reservoir FEM or an in situ test. The anisotropy arises from the non-linear combination of homogeneous quasi-punctual conductivities.

The common name used for identifying an average value of conductivity on a large scale domain is "effective" ground thermal conductivity. But we prefer to deepen the analysis and introduce the terminology "equivalent conductivity" defined according to the analogous definition of equivalent permeability given by Matheron (Matheron, 1967), as the fictitious conductivity of a homogeneous medium which conveys the same heat flux \vec{q} as the real one. In fact two operational interpretations exist of the equivalent conductivity: the effective conductivity and the block conductivity (De Lucia, 2008).

λ_{ef} : The effective conductivity refers to a medium statistically homogeneous on a large scale, with a correlation distance small with respect to the domain dimension. It appears when a heat flow uniform in average exists and it is an intrinsic property, independent on macroscopic boundary conditions.

λ_{eq} : This is the equivalent conductivity attributed to a block of finite dimensions for a specific geothermal problem. It is not an intrinsic property of the conductive medium, but just a computing intermediary defined by boundary conditions and by the numerical method

adopted to solve the differential equation problem, in such a way that coherence would be assured between actual results of large scale applications and the upscaling results of small scale modeling. There is not a unique solution, so that equivalence criteria are needed. This definition has been applied in most of cases when modeling a shallow geothermal reservoir, because volumes at hand have at least one dimension regarded as small.

There are heuristic upscaling solutions able to give a unique and plausible value of the equivalent conductivity. They apply when boundary conditions are not affecting the equivalent thermal conductivity field. We can adopt the classical result of the power mean

$$\lambda_{eq} = \left(\frac{1}{V} \int_V \lambda(x)^p dv \right)^{\frac{1}{p}} \quad -1 \leq p \leq 1$$

Equation 15

When $p = -1$ the harmonic mean is obtained, when $p=1$ the result is the arithmetic mean and for $p \rightarrow 0$ the geometric mean is got. By adopting the results of Matheron and Noetinger (Noetinger, 1994) we can state that in case of media statistically homogeneous, then $p = 1-2/n$, where n is the space dimension. In 2D, the geometric mean results.

In general, it is possible to define inequalities. The above introduced inequality is the base one: the equivalent conductivity lies between the harmonic and arithmetic means

$$\lambda_h \leq \lambda_{eq} \leq \lambda_a$$

Equation 16

Many other and stricter inequalities have been introduced. Of interest is the result known as the “Matheron’s conjecture” for λ_{ef} computation:

$$\lambda_{ef} = \lambda_a^\alpha \lambda_h^{1-\alpha} \quad \alpha \in [0,1]$$

Equation 17

If the medium is isotropic and statistically homogeneous, then $\alpha = (n-1)/n$.

When treating permeability values, the differences between the types of upscaling is dramatical (see fig. 12) and it can be also of one or two order of magnitude. In case of thermal conductivity, we cannot really know how big the difference will be because we do not have realistical values of thermal conductivity along space (example different values on radial direction of measured thermal conductivity) and we don’t know how much effectively these values can be different. In any case, mathematically, it is obvious that the difference will be slightly lower than the permeability one.

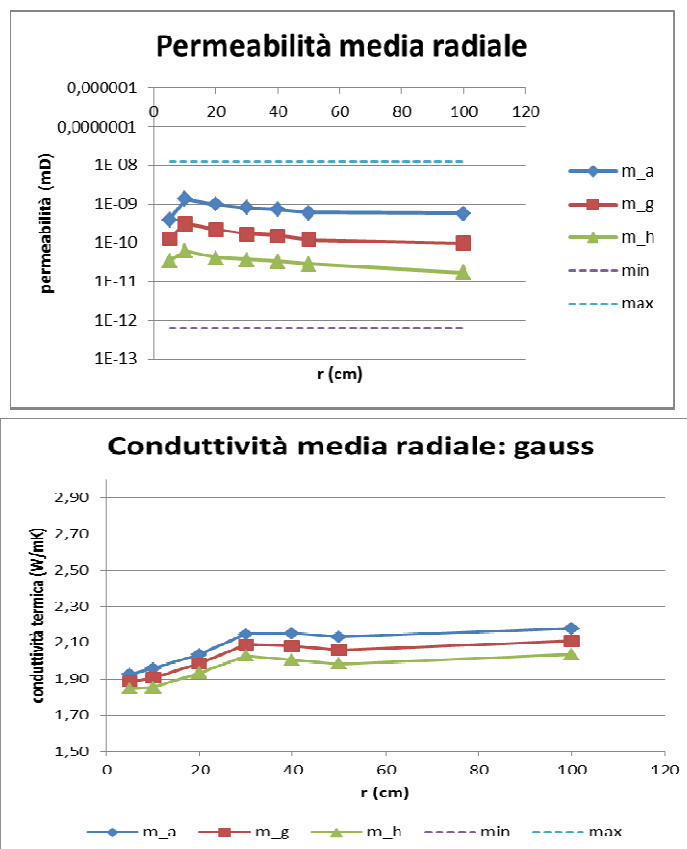


Figure 12 Permeability and conductivity radial averages

2.1 Theoretical studies on thermal conductivity

Thermal conductivity has been studied from a lot of researchers, concerning how to measure it and how it is related to other parameters. The first wide research made on the subject was developed by Woodside and Messmer (Woodside, et al., 1961) and their considerations and results can be resumed in the following:

- The line heat source (probe) method (a thin internally heated cylindrical sensor is inserted into the sample material and the thermal conductivity is deduced from the observed temperature rise in the sensor and the heating power applied) is satisfactory for the determination of effective thermal conductivities of unconsolidated sands under a variety of test conditions. The measurements are rapid and reproducible to within one or two percent.
- Effective thermal conductivities vary with porosity, saturating fluid conductivity, pressure of the gas filling the pores and overburden pressure. In particular the higher the porosity, the lower the thermal conductivity, while the higher is the saturating fluid conductivity, the higher is thermal conductivity. Özkahraman et al. (Özkahraman, et al., 2004) affirm that porosity is inversely proportional to thermal conductivity, whilst P-wave velocity, bulk density and compressive strength are directly proportional to thermal conductivity.
- Comparing the effect of overburden pressure and of degree of saturation, it is clear that the effect of the overburden pressure will be little on the conductivities of rocks with a high degree of saturation in water. The effect of overburden pressure is visible

only in not saturated rocks and the higher is the pressure, the higher will be thermal conductivity.

- Weighted geometrical mean of thermal conductivities predicts rock thermal conductivities which are in good agreement with those measured.

In the following years, several were the equations/models proposed for obtaining thermal conductivity from other parameters; Brailsford and Major (Brailsford, et al., 1964) derived equations for the thermal conductivity of the two-phase media from simple physical models corresponding to various types of structure, while Yang (Yang, 1998) proposed a linear inverse model to estimate thermal conductivity in a 1D heat conduction problem. Lu et al. (Lu, et al., 2007) developed a model describing the relationship between thermal conductivity and volumetric water content of soils: a simple linear relationship was applied to calculate the λ_{dry} , dry thermal conductivity, from soil porosity.

Bulk density and soil water content were parameters considered always related to thermal conductivity (Özkahraman, et al., 2004; Lu, et al., 2007) as Abu-Hamdeh (Abu-Hamdeh, 2003) confirmed with his studies about the effect of water content and bulk density on the specific heat, volumetric heat capacity, and thermal diffusivity: he verified that specific heat increases with increased moisture content and volumetric heat capacity increases with increased moisture content and soil density. Other researchers deepened this study a bit more, using a numerical modeling approach (Cosenza, et al., 2003) which shows that the microscopic arrangement of water influences the relation between λ and θ (volumetric heat content): simulated values for n (porosity) ranging from 0.4 to 0.6, λ_s (thermal conductivity of the solid fraction) ranging from 2 to 5 W/(m·K) and θ from 0.1 to 0.4 can be fitted by a simple linear formula that takes into account n , λ_s and θ . The results given are in satisfactory agreement with published data both for saturated rocks and for unsaturated soils. An analysis mostly statistical and geostatistical was applied for understanding this relation by Usowicz et al. (Usowicz, et al., 1996), revealing that there is a distinct impact of soil water content and bulk density on the spatial variability of soil thermal properties. In fact volumetric heat capacity is linearly dependent upon soil water content and it depends on soil bulk density to a lower degree. Soil thermal conductivity and thermal diffusivity have a nonlinear dependence on soil water content.

Some authors demonstrated that there is also a relation from thermal conductivity and compressive strength of the rock specimen (Özkahraman, et al., 2004; Demirci, et al., 2004), showing as well that thermal conductivity of the rocks under three-dimensional stress increases compared with the thermal conductivity coefficient under uniaxial stress.

An important contribution to the study of thermal conductivity was made by Côté and Konrad (Côté, et al., 2005). They realized a new model relying on:

- two relationships to compute the porosity and the degree of saturation that consider the effect of volume change as water turns to ice in frozen soils

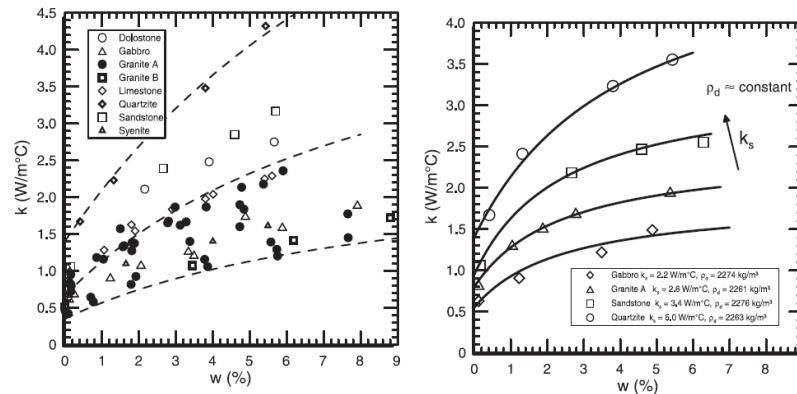


Figure 13 a) Thermal conductivity of frozen base-course materials as a function of water content; b) Thermal conductivity of unfrozen base-course materials as a function of water content and thermal conductivity of solid particles

- the geometric mean model for the computation of the thermal conductivity of solid particles and for the saturated base-course materials in the unfrozen and frozen states;
- a modified form of the geometric mean model for the computation of the thermal conductivity of dry base-course materials;
- two simple relationships between the normalized thermal conductivity and the degree of saturation for base-course materials in the unfrozen and frozen states.

An inverse model was applied for getting thermal conductivity in case of repositories by Sundberg and Hellström (Sundberg, et al., 2009): a 3D finite difference model of the repository is used to calculate the transient temperature increase due to the heat generation in the canisters and a homogeneous thermal conductivity value is chosen to obtain the best fit with temperature measured data.

It is clear after this review that thermal conductivity and its measure were deeply studied, but this area still seems to need more investigation. As it can be seen, a main drawback is that every research has obviously been performed concerning a specific soil/rock mostly because thermal conductivity has a different “behavior” in each of them. From one side the basic relations are always the same (thermal conductivity depends on the saturation degree, on the bulk density, etc.), but there is no general relationship to express them (we have different ones from soil to soil and from rock to rock).

Thermal properties depend on saturation degree and bulk density, but they also have a spatial variability, as well as a temporal one (for example saturation degree can vary along time): therefore it is necessary to define a spatial-temporal variability. The main problem is that we cannot define a spatial variability, theoretical or empirical formulation are lacking in this case.

Concerning indirect measures, useful tests for thermal properties characterization can hardly refer to direct measures (ex. direct measure on a small sample) and therefore it would be better to find some fast method to have a spatial characterization of thermal properties. In any case it is still difficult to make a correlation between the spatial characterization and its temporal evolution (for example with the varying saturation degree).

Concluding, there are no general equations and moreover it's not clear the spatial variability of thermal conductivity; at most we can have time-series of thermal conductivity, for example through the geothermal heat pumps' monitoring, fiber optic measures (most probably the spatial variability will be less than the temporal, but it has not yet been demonstrated).

2.2 Thermal conductivity laboratory measurement

Thermal conductivity can be measured both by in situ and laboratory tests. In this section it is deepened the state of art concerning laboratory tests.

The principal methods of measuring thermal conductivity from sub - ambient temperatures up to 1500°C on solid materials exhibiting a very wide range of conductivity are axial flow, radial flow, guarded hot plate and hot-wire method (ANTER).

1) **Axial Flow Methods** It is the method chosen for cryogenic temperatures. Key measurement issues are mainly concentrated on reduction of radial heat losses in the axial heat flow developed through the specimen from the electrical heater mounted at one end (the power dissipation of this heater is used in calculating column heat flux). These losses are minimal at low temperatures. In practice only, cylindrical symmetry heat transfer is used. In addition to guarded and unguarded solutions, other categories are separated:

a) *Absolute axial heat flow*, which is mostly used in sub ambient environments. Systems of this nature require very precise knowledge of the electrical power feeding the heater. Consequently, the losses from the hot heater surfaces also play a major role.

b) *Comparative cut bar* (ASTM E1225 Test Method). This is perhaps the most widely used method for axial thermal conductivity testing. The principle of the measurement lies in passing the heat flux through a known and an unknown sample and comparing the respective thermal gradients, which will be inversely proportional to their thermal conductivities. Most commonly, the unknown is sandwiched between two known samples, "the references", to further account for minor heat losses that are very difficult to eliminate.

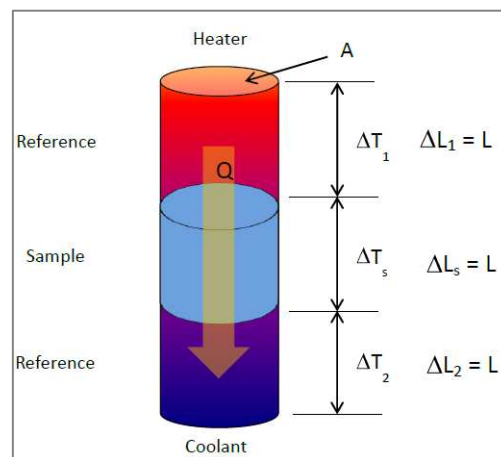


Figure 14 Comparative cut bar (ASTM E1225 Test Method) (ANTER)

where K_R is the thermal conductivity of the references. From this, the thermal conductivity of the unknown sample (K_S) can be calculated as:

$$\frac{Q}{A} = K_S \frac{\Delta T_S}{L} = K_R \frac{\Delta T_1 + \Delta T_2}{2} \frac{1}{L}$$

Equation 18

c) *Guarded or unguarded heat flow meter method* (ASTM C518, E1530 Test Methods). It involves the use of a flux gauge, whose purpose is similar to the references in the comparative cut bar method. In practice, the reference material has a very low thermal conductivity and, therefore, it can be made very thin.

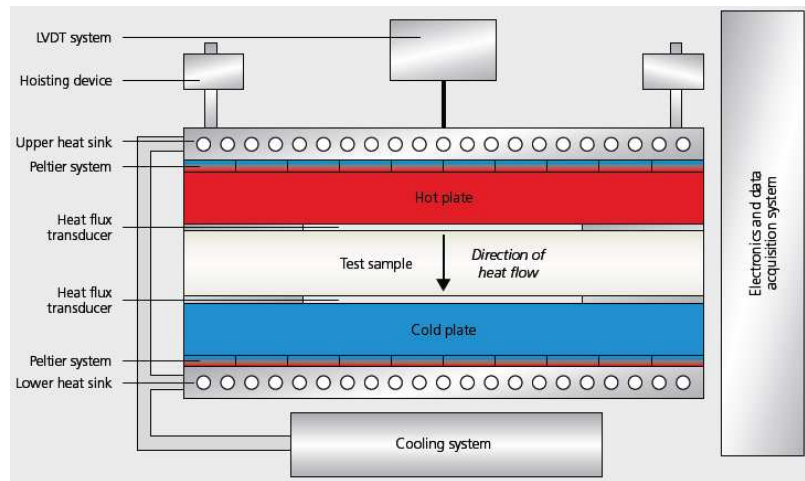


Figure 15 Guarded heat flow meter (Netzsch)

Usually, a large number of thermocouple pairs are located on both sides of the reference plate, connected differentially to yield directly an electrical signal proportional to the differential temperature across it.

$$K_S = K_R \frac{\frac{\Delta T_1 + \Delta T_2}{2}}{\Delta T_S}$$

Equation 19

The assembly is cast into a protective coating for durability. This type of flux gauge is mostly used with instruments testing very low thermal conductivity samples, such as building insulations. In a similar fashion, flux gauges can be constructed from just about any material, thick or thin, depending on the material's thermal conductivity. Common requirements for all flux gauges are that the material used for the measuring section is stable, not affected by the thermal cycling, and the gauge has been calibrated by some method independently.

2) **Guarded Hot Plate Method** (ASTM C 177 Test Method). Guarded hot plate is a widely used and versatile method for measuring the thermal conductivity of insulations. A flat, electrically heated metering section surrounded on all lateral sides by a guard heater section controlled through differential thermocouples, supplies the planar heat source introduced over the hot

face of the specimens. The most common measurement configuration is the conventional, symmetrically arranged guarded hot plate where the heater assembly is sandwiched between two specimens. In the single sided configuration, the heat flow is passing through one specimen and the back of the main heater acts as a guard plane creating an adiabatic environment.

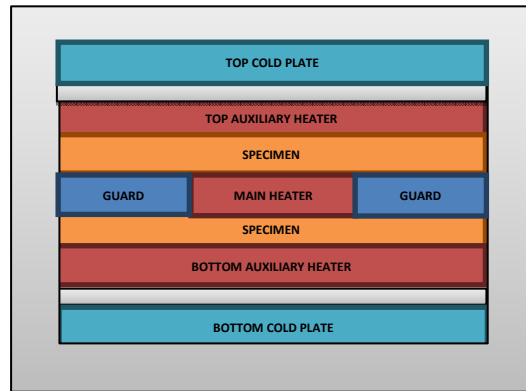


Figure 16 Guarded hot plate method: the main heater is sandwiched in the middle of the specimens.

This is an absolute method of measurement and its applicability requires:

- the establishment of steady-state conditions
- the measurement of the unidirectional heat flux in the metered region, the temperatures of the hot and cold surfaces, the thickness of the specimens and other parameters which may affect the unidirectional heat flux through the metered area of the specimen.

3) **Hot Wire Method** (ASTM C1113 Test Method) Hot wire methods are most commonly used to measure the thermal conductivity of "refractories" such as insulating bricks and powder or fibrous materials. Because it is basically a transient radial flow technique, isotropic specimens are required. The technique has been used in a more limited way to measure properties of liquids and plastics materials of relatively low thermal conductivity.

4) Relatively recent modification of this long-established technique is the "**probe**" method. This configuration is particularly practical where the specimen conductivity is determined from the response of a "hypodermic needle" probe inserted in the test specimen. Thus the method is conveniently applied to low-conductivity materials in powder or other semi rigid form. A probe device can be used to measure the thermal properties of soils in situ, but most commonly a closely controlled furnace is used to contain the sample and produce the base temperatures for the tests. The probe contains a heater and a thermocouple attached to it.

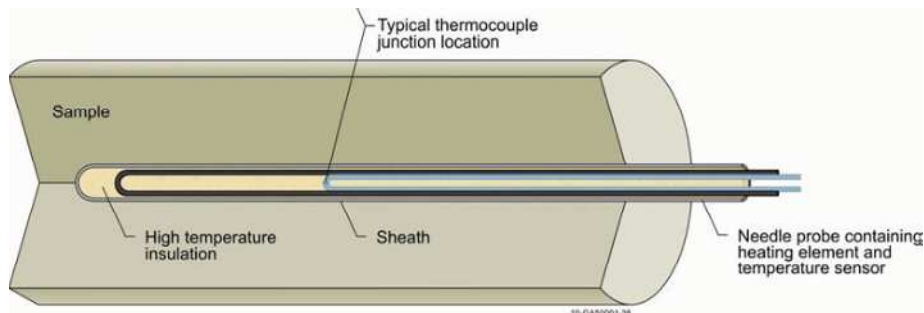


Figure 17 Schematic diagram of thermal conductivity needle probe (Daw, et al., 2010).

When a certain amount of current is passed through the heater for a short period of time, the temperature history of the heater's surface will take on a characteristic form. In the initial phase, the temperature will rapidly rise, and as the heat begins to soak in, the rate of rise becomes constant. When the thermal front reaches the outer boundary of the sample, the rise will slow down or stop altogether due to losses into the environment. From the straight portion of the rate curve (temperature vs. time) the thermal conductivity can be calculated.

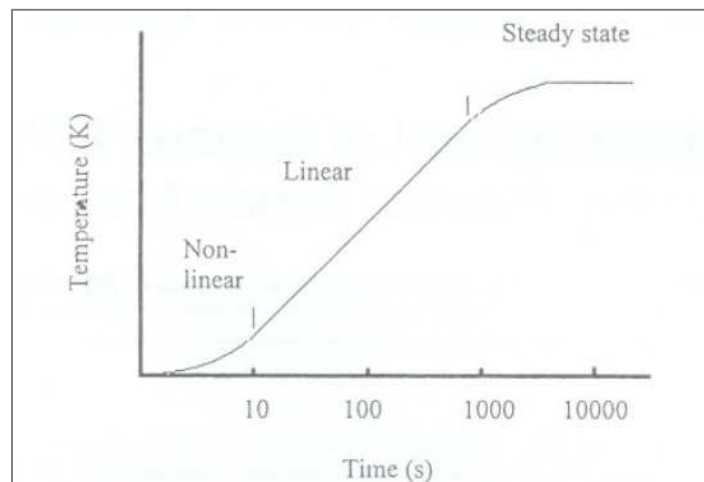


Figure 18 Typical experimental probe method test results (this an idealized curve) (Manohar, et al., 2000)

The finite radius of the probe has the effect of a time delay before the theoretical rate of radial heat flow through the surface of the probe is equal to the heat dissipated by the heater filament (Manohar, et al., 2000).

Other authors developed their own technology in order to measure thermal conductivity of their samples: here follow some examples.

Munoz (Munoz, 2006) used a laboratory heating test in order to measure the thermal and hydraulic conductivity in saturated condition of argillaceous rocks by means of a heater pulse. The evolution of temperatures in the inner of the sample is measured with two sensors diametrically opposed to the pore water pressure sensors.

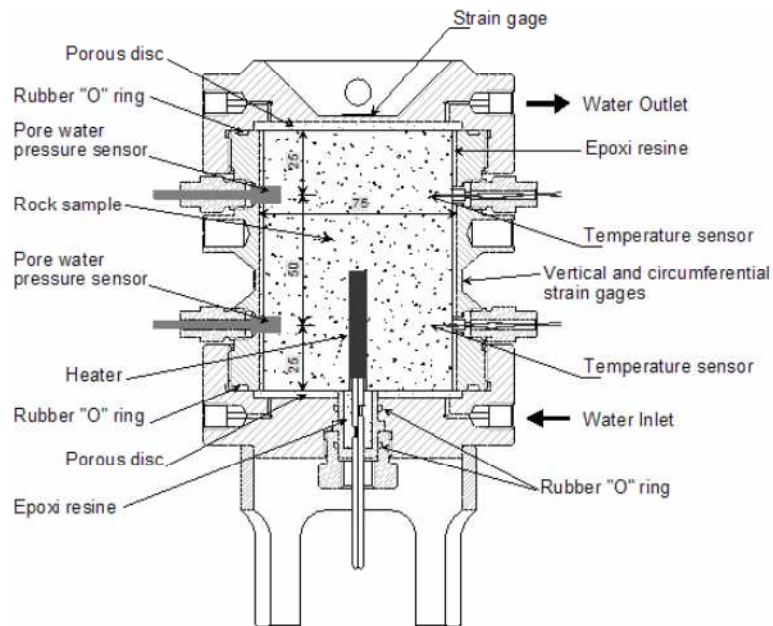


Figure 19 Munoz laboratory heating test to measure thermal and hydraulic conductivity in saturated condition of argillaceous rocks by means of a heater pulse.

Lu & al. (Lu, et al., 2007) used a thermo-time domain reflectometry (thermo-TDR) probe (developed by Ren & al. 1999) to measure the thermal properties of packed soil columns.

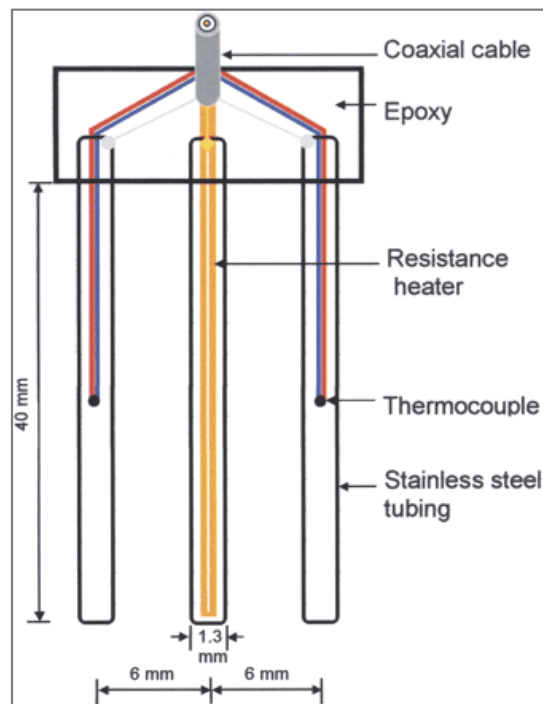


Figure 20 Schematic view of the thermo-time domain reflectometry

To determine λ , thermo-TDR probe has to be inserted into the soil sample, and current has to be applied to the heater in the middle needle for 15 s to produce a heat pulse. Soil thermal properties (thermal conductivity, thermal diffusivity, and volumetric thermal capacity) are determined with a nonlinear regression technique (Welch et al., 1996) involving the temperature increase vs. time in the outer rods.

Antriasian (Antriasian, 2010) created a Portable Electronic Divided Bar (PEDB) which is an electronic apparatus that produces a temperature gradient across a specially prepared rock sample; it allows thermal conductivity of a rock sample to be determined via the application of Fourier's Law.

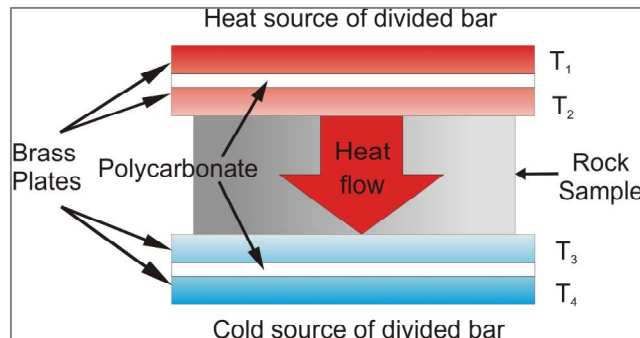


Figure 21 Principal components of the plates of the PEDB: each brass plate is fitted with a separate thermocouple. ΔT is the ratio of the temperature of the plates of the PEDB: $\Delta T = (T_2 - T_3) / ((T_1 - T_2) + (T_3 - T_4))$. The heat source is above the top pair of brass plates, and the cold source is below the bottom pair; the consequence is that heat flows across the rock sample (Antriasian, 2010).

Measurements are rapid, taking from 5 to 15 minutes per sample. In addition to uniaxial thermal conductivity measurements, biaxial and triaxial measurements can be made with the PEDB, allowing for studies of thermal conductivity anisotropy.

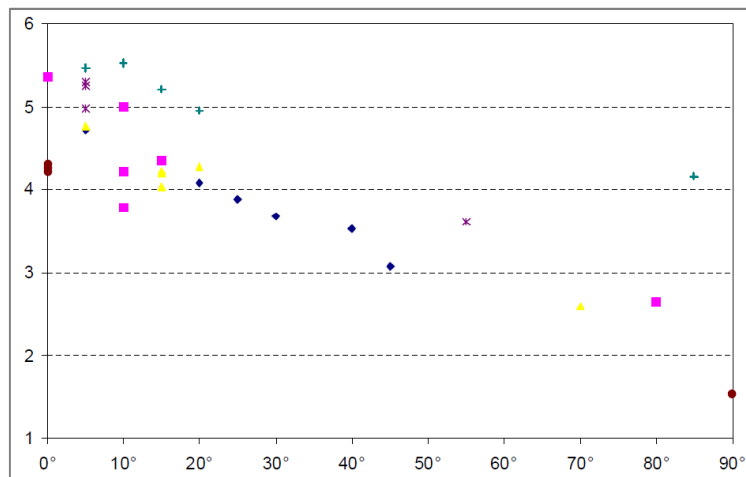


Figure 22 Summary of thermal conductivity data from six meta-sedimentary rock specimens; the six differently shaped symbols indicating the different specimens studied. Each specimen was measured for thermal conductivity at several angles with respect to the specimen's foliation. The vertical axis is thermal conductivity in W/m·K; the horizontal axis is the angle between the foliation of the rock sample, and the direction of heat flow across the rock sample while within the PEDB, measured in degrees (°). A relationship exists between the magnitude of thermal conductivity and the direction of heat flow with respect to the specimen's foliation (Antriasian, 2010).

Demirci & al. (Demirci, et al., 2004) developed a new device for measuring the thermal conductivity coefficient of a rock specimen, based on the combination of devices developed by Mousset-Jones and McPherson, Duruturk, Demirci and Keçeciler and a modification of the Hoek cell. This set-up consists of:

- Hydraulic press.
- A cylinder-shaped stainless-steel body and insulation cover to provide a linear and steady heat flow from bottom to top of the column.

- Heat source incorporated into the steel body connected with a digital DC-power source providing a steady heat flow.
- Thermocouples used to measure the temperature difference between top and bottom of the rock samples and heat source levels.
- A multi-channel temperature read-out system is used to read the temperatures in thermocouples.
- Rock sample.
- A cylinder-shaped stainless steel body for cooling and cooling set-up.
- Confining pressure-supplying unit (a hydraulic pump with a pressure transducer).

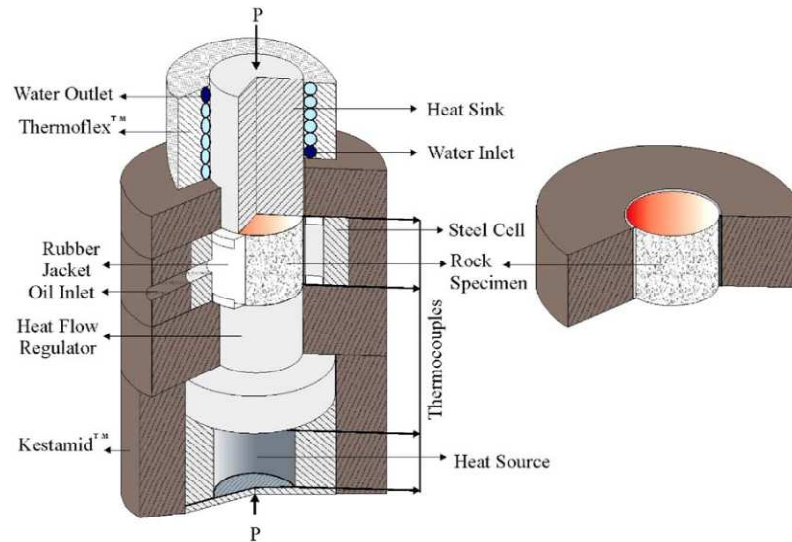


Figure 23 Device for measuring the thermal conductivity coefficient of a rock specimen

Tests normally are run following this sequence:

- Preparation of rock core samples. The specimen prepared is subsequently set in the test device.
- Connections between thermocouples and the multi-channel temperature read-out system are made. At the same time, the input and output ends of the cooling system are connected to the water utility system in the laboratory.
- Heat source temperature reached 100°C.
- Thermal conductivity coefficient of the rock specimens is calculated according to the Fourier Law using the recorded rock parameters and temperatures obtained from the tests.

Tavman (Tavman, 1996) used a modified hot wire method to measure the effective thermal conductivity of granular porous materials. The heating wire is placed between two rectangular shaped materials, the first one is an insulating material of known thermal properties which is a part of the measuring probe and the second one is the granular sample placed in a rectangular shaped sample holder of dimensions 10cm length, 3cm width and 4cm height.

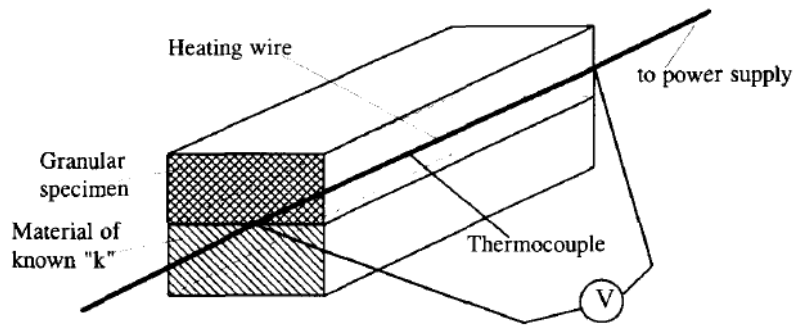


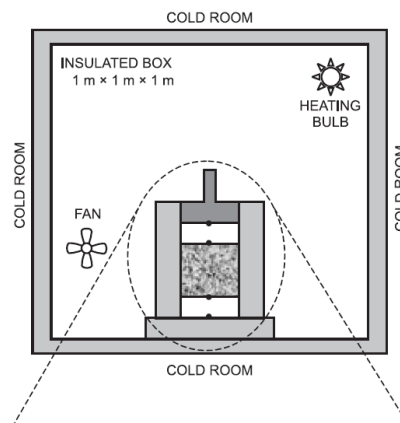
Figure 24 Modified hot wire method

The error which may be introduced by the variation in the resistance of the heating wire with temperature, causing a non-constant power input, is made negligible by using, as heater, a wire with a low temperature coefficient of resistance. The measuring process requires only 10 to 90 seconds after heating starts at the wire. In this case, the thermal conductivity of the

sample is given by the following equation: $k = F \cdot \frac{Q \cdot \ln(t_2/t_1)}{T_2 - T_1} - H$

where F and H are specific constants of the probe, to be determined with materials of known thermal conductivities. By this method the thermal conductivity is measured with an accuracy of +5 % and reproducibility of +2%.

Côté and Konrad (Côté, et al., 2005) used a system composed by a thermal conductivity cell surrounded by an insulated and temperature-controlled box, placed inside a large cold room maintained at a constant temperature of about 4 °C below the average temperature used in the test cell. The samples are compacted into a cylindrical PVC mold (101.6 mm of diameter and 75 mm of height) and then placed between two Pyrex disks 101.6 mm in diameter and 30 mm high. Each Pyrex disk is instrumented with two thermistors embedded in the center, at a few tenths of a millimeter, from the planar faces.



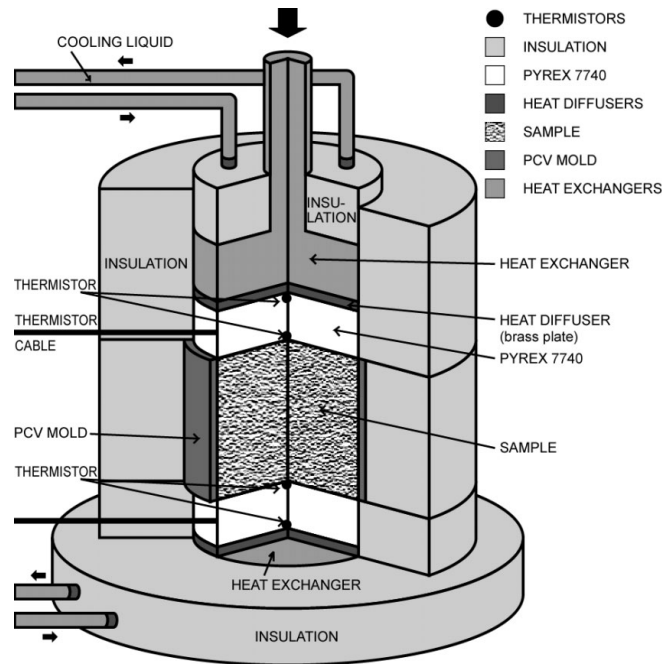


Figure 25 Experimental setup used by Coté and Konrad

The temperature boundary conditions at the top and bottom of this three-layer system are maintained constant with two independent heat exchangers to create a constant vertical heat flow through both the sample and the Pyrex disks. The sample and the Pyrex disks are tightly surrounded with a 50 mm thick polystyrene jacket to reduce radial heat losses. The ambient temperature of the insulated box is maintained equal to the mean value of the temperatures applied at both extremities of the system. The heat flux in the thermal conductivity cell is measured through the Pyrex disks. The temperatures of the top and bottom of each Pyrex heat flux meter are recorded every 15 min through an acquisition system and plotted as a function of time. When temperatures become constant with time, steady state heat flow is reached. The thermal conductivity (in W/m°C) of the tested sample is approximated as

$$k = \frac{q_{uf} + q_{lf}}{2} \frac{\Delta h}{\Delta T} = \left[\left(k_{uf} \frac{\Delta T_{uf}}{\Delta h_{uf}} + k_{lf} \frac{\Delta T_{lf}}{\Delta h_{lf}} \right) \frac{\Delta h}{\Delta T} \right] / 2$$

where q is the heat flux (W/m°C); Δh is the distance between two temperature measurements (m); ΔT is the temperature difference (°C); and the subscripts "uf" and "lf" refer to the upper and lower heat flux meters, respectively.

Abu-Hamdeh (Abu-Hamdeh, 2001) exploited the single and dual-probe methods to measure the thermal conductivity of the soils. In the single-probe method, an electrical wire is implanted in the soil sample; a steady current is supplied to the electrical wire and the temperature rise and fall of the heating wire is measured by a thermocouple and recorded during a short heating and cooling.

The dual-probe heat-pulse device used for making measurements in this study consisted of parallel heater and sensor needle probes made from thin stainless steel tubing 100 mm long and 2 mm in diameter. The needles were fixed on an acrylic plate by epoxy glue. The heater to

sensor probe spacing was 7-5 mm. The diameter, length, and spacing of the needles were such that the assumptions of a probe of infinite length would produce negligible errors in the calculated thermal conductivity. The heater resistance R was $300 \text{ } \Omega/\text{m}$. The temperature sensor consisted of copper- constantan thermocouple junction, which was pulled into and centered in the sensor needle. The needles were filled with high thermal conductivity epoxy glue to minimize radial temperature gradients through the probe and to provide a water-resistant, electrically insulated probe. Heat was generated by applying voltage from a 9 V DC power supply to the heater for a fixed period of time. Lower power inputs were used to minimize the effects of heating on soil water movement and, hence, thermal conductivity.

2.3. Thermal conductivity in situ measurement

After the description of the laboratory tests for thermal conductivity, it will be deepened the topic of in situ measurements.

2.3.1 Thermal response test

One of the most used technique for measuring the effective thermal conductivity of a borehole is thermal response test At the current state of technology, the Thermal Response Test (TRT) is the in situ test for the characterization of ground thermal properties with the higher degree of accuracy. This consists of simulating the BTES operation of heat injection/extraction for a limited time (Gehlin, 1998).

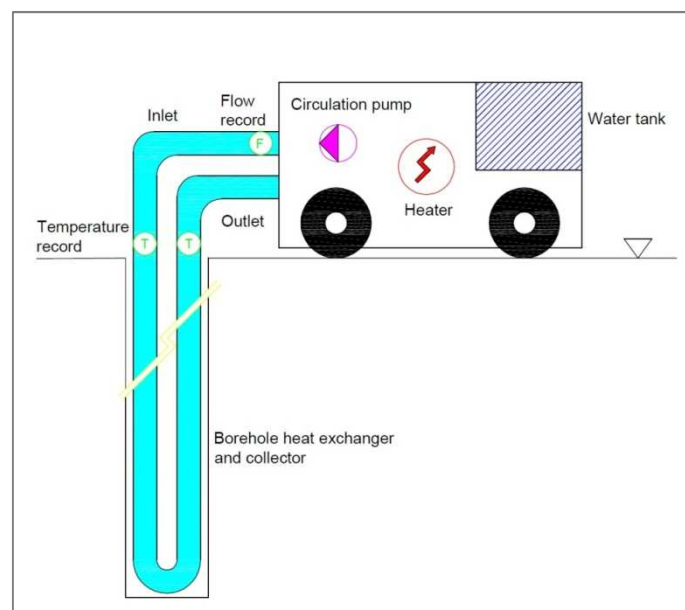


Figure 26 TRT apparatus

By analysing the temperature variation of the circulating heat carrier fluid, it is possible to estimate the equivalent thermal properties of the quasi-cylindrical ring of soil affected by the heat exchanger. The cylindrical ring is composed by several materials; some of them are artificial and have constant thermal properties, while others, the natural ones, have variable ones. The perfect cylindrical geometry of the borehole depends on drilling procedure. The impossibility to have a perfect vertical borehole adds another source of

variability. Normally the test lasts 3 days and the investigated radius around the borehole is within 10 and 30 cm.

We can calculate the radius influenced by the Thermal Response Test by applying the penalty temperature formulation. In literature the so called penalty temperature normally refers to the variation of temperature occurring in a geothermal field where there are a lot of boreholes:

$$T_p = \frac{1 \cdot N_4 + 0.5 \cdot N_3 + 0.25 \cdot N_2 + 0.1 \cdot N_1}{N_{tot}} \cdot T_{p1}$$

Where N is the number of boreholes surrounded by boreholes respectively on 4-3-2-1 sides, N_{tot} is the total number of boreholes, while T_{p1} is the penalty temperature of a single borehole surrounded on all sides by other boreholes.

Penalty temperature T_{p1} of a single borehole is calculated in the following way:

$$T_{p1} = \frac{Q_{stored}}{c_g \cdot d_s^2 \cdot L}$$

where Q_{stored} is the heat accumulated in the ground after a certain time the system works (J), c_g is the thermal capacity of the ground (J/(m³·K)), d_s is the reciprocal distance between two heat exchangers (m), L is the length of the borehole (m). Q_{stored} is calculated as:

$$Q_{stored} = \sum_{i=1}^n c_g \cdot \pi \cdot L \cdot [(R_i + \Delta R)^2 - R_i^2] \cdot \Delta T_{gi}$$

where R_i is the internal radius of the annulus and ΔR is the radius increment (m), ΔT_{gi} is the i-th temperature variation of the undisturbed ground temperature (°C). In the following figure the difference between the radiuses is better explained.

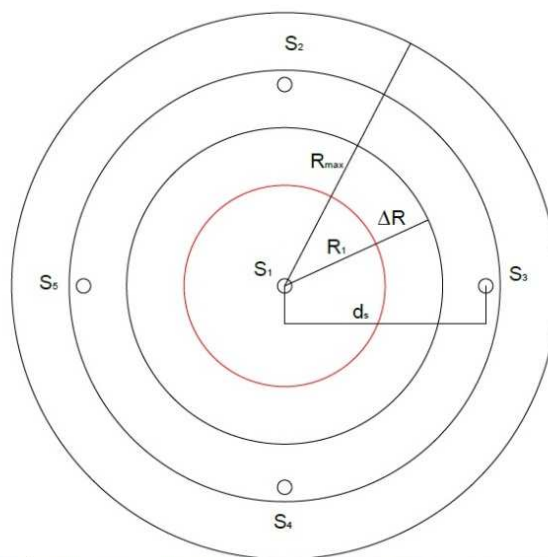


Figure 27 Scheme with the different radius used, boreholes' and concentric surfaces used for the calculation.

For calculating ΔT_{gi} these are the equations needed:

$$\begin{aligned} \text{a) } \Delta T_{gi} &= \frac{Q \cdot I(X)}{2 \cdot \pi \cdot \lambda_g \cdot L} & \text{b) } I(X) &= -0.577078 \cdot \ln(X) - 0.1 \quad 0.5 \leq X < 1 \\ & & I(X) &= -0.932002 \cdot \ln(X) - 0.14601 \quad 0.01 < X < 0.5 \\ \text{c) } X &= \frac{R}{2 \cdot \sqrt{\alpha_g \cdot \tau}} \end{aligned}$$

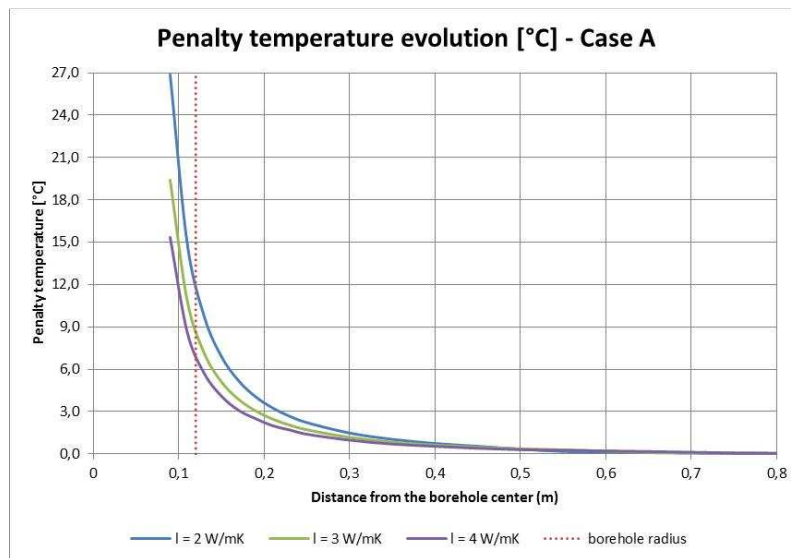
where Q is the average injected power (W), X is a coefficient dependent on R which is the average radius of the annulus $(= (R_i + \Delta R)/2, \text{ in m})$, α_g is the thermal diffusivity of the ground, τ is the time for which the penalty temperature is calculate (s) and I(X) is dependent on X.

We tried to adapt this calculation on a single borehole not surrounded by other boreholes; the data we used as an input are reported in the following table:

Case	a	b	c	d
c_g [J/m ³ K]	2,20E+06	2,20E+06	2,50E+06	2,50E+06
D_{borehole} [m]	0,13	0,13	0,13	0,13
L [m]	100	100	100	100
ΔR [m]	0,01	0,01	0,01	0,01
Q [W]	5400	6200	5400	6200
λ_g [W/mK]	2- 3- 4	2- 3- 4	2- 3- 4	2- 3- 4
α_g [m ² /s]	9,091E-07	9,091E-07	9,091E-07	9,091E-07
τ [days]	3	3	3	3

Table 2 Different cases of BHE conditions

In each of these cases penalty temperature has been calculated for increasing distances from the borehole centre, up to the distance for which the penalty temperature reaches 0,01 °C.



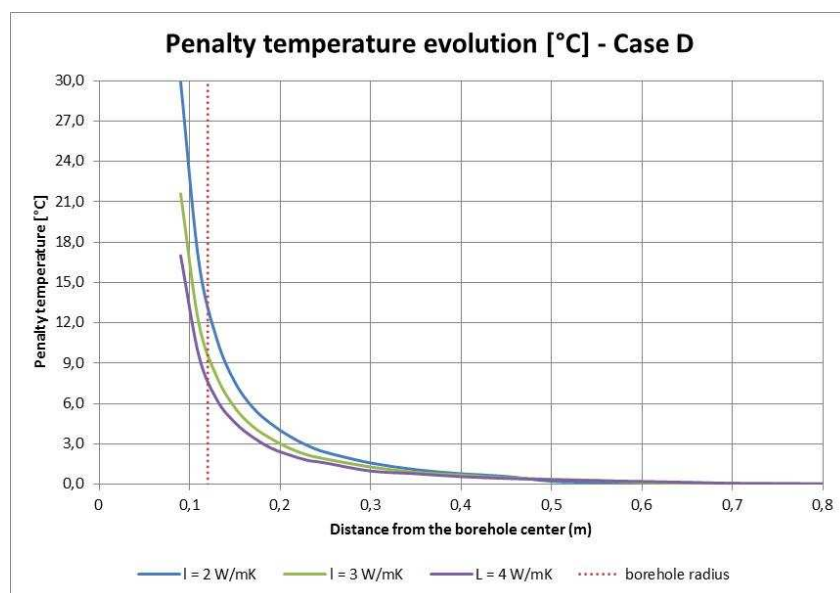
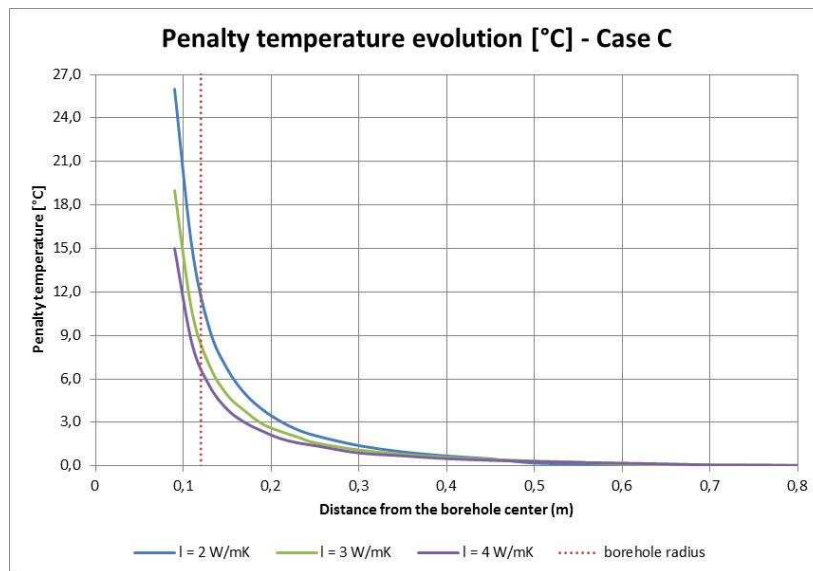
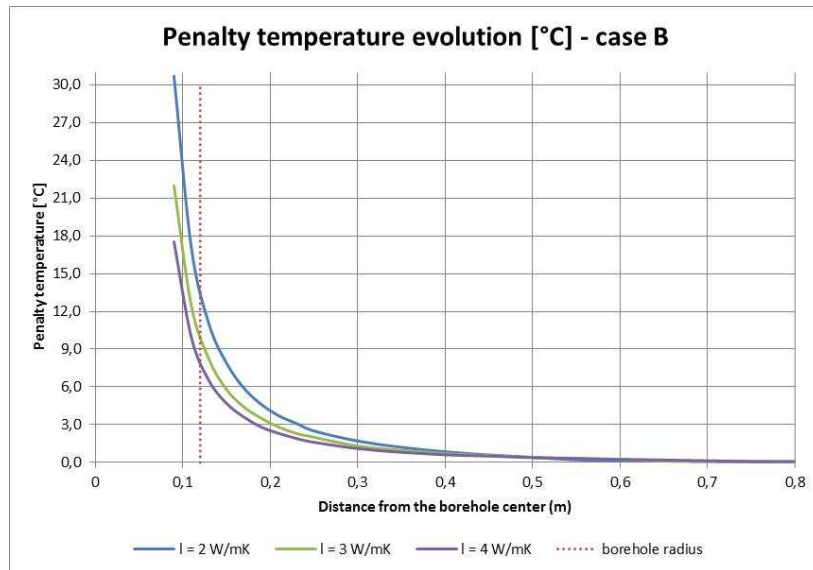


Figure 28 Penalty temperature in the 4 cases for the 3 different values of thermal conductivity

By comparing the 4 graphs of figure 28, it is visible that the higher penalty temperature is always connected to the lower thermal conductivity. By fixing the thermal conductivity we notice that the higher the power injected is the higher of course will be the penalty temperature; moreover the lower is the ground thermal capacity (fixed the power and the thermal conductivity), the higher will be the penalty temperature.

The following graph shows the evolution of penalty temperature on the borehole wall by changing the thermal conductivity.

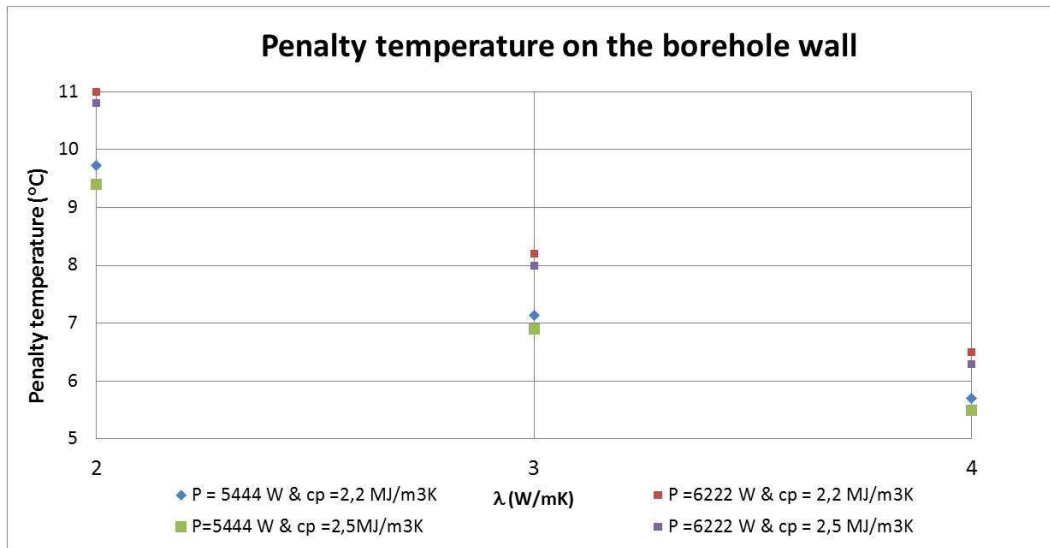


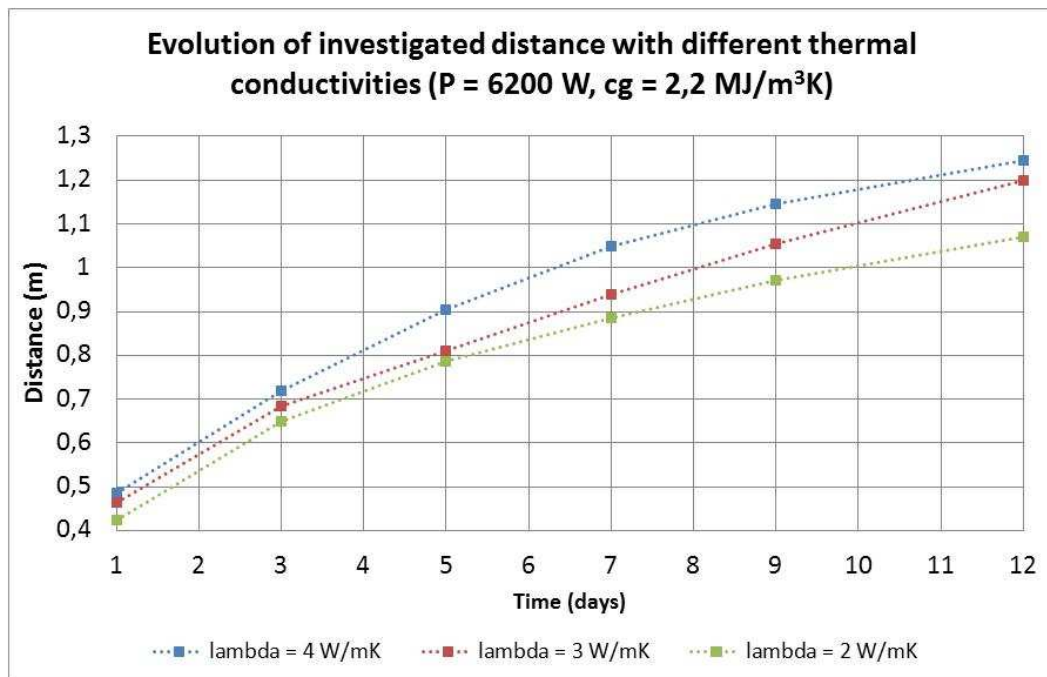
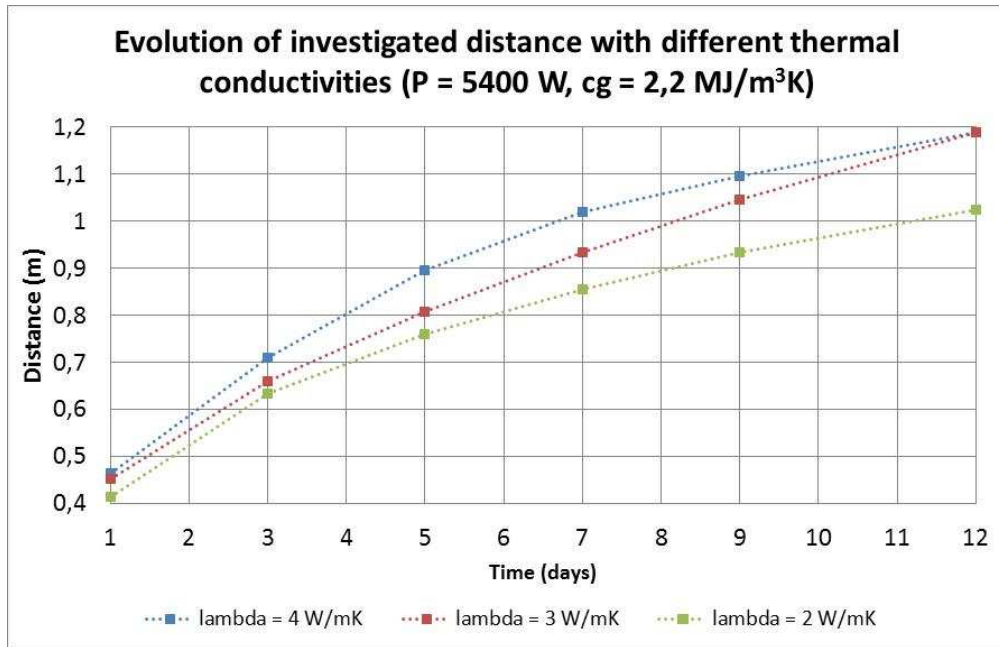
Figure 29 Evolution of penalty temperature by changing the ground thermal conductivity.

As it is clear from the graph, the higher the power injected is the higher will be the penalty temperature; taking as constant the power, the lower the thermal capacity is, the higher will be the penalty temperature. In fact, by increasing the thermal capacity, the thermal diffusivity lowers, which means that the thermal flux is much more difficult (we need “more heat” to fill up the ground before it lets other heat pass); that’s why if the thermal capacity is higher the penalty temperature is lower because it’s more difficult for the heat to pass. Another clear trend is that if we increase ground thermal conductivity, penalty temperature will decrease.

Distance at which Tpen = 0,1°C				
lambda	c _g = 2,2 MJ/m3 K		c _g = 2,5 MJ/m3 K	
W/mK	P= 5444 W	P= 6222 W	P= 5444 W	P= 6222 W
2	0,6	0,65	0,6	0,6
3	0,65	0,7	0,65	0,65
4	0,7	0,75	0,7	0,7
Distance at which Tpen = 0,01°C				
lambda	c _g = 2,2 MJ/m3 K		c _g = 2,5 MJ/m3 K	
W/mK	P= 5444 W	P= 6222 W	P= 5444 W	P= 6222 W
2	0,8	0,8	0,75	0,8
3	0,95	0,95	0,9	0,9
4	1,05	1,05	1	1

Table 3 Distance at which the penalty temperature goes to 0,01 °C or to 0,1°C with an injecting time of 3 days

In case of a TRT run for 3 days, therefore, the investigated radius around the borehole is within 60-70 cm (considering as maximum influence a penalty of 0, 1°C). If we run the test for more time (for example 5 days) we will obtain a different radius of influence, obviously bigger (ex. 90 cm for $\lambda = 4 \text{ W/mK}$, $P = 5400 \text{ W}$ and $c_g = 2,2 \text{ MJ/m}^3\text{K}$, 110 cm for 9 days at the same conditions).



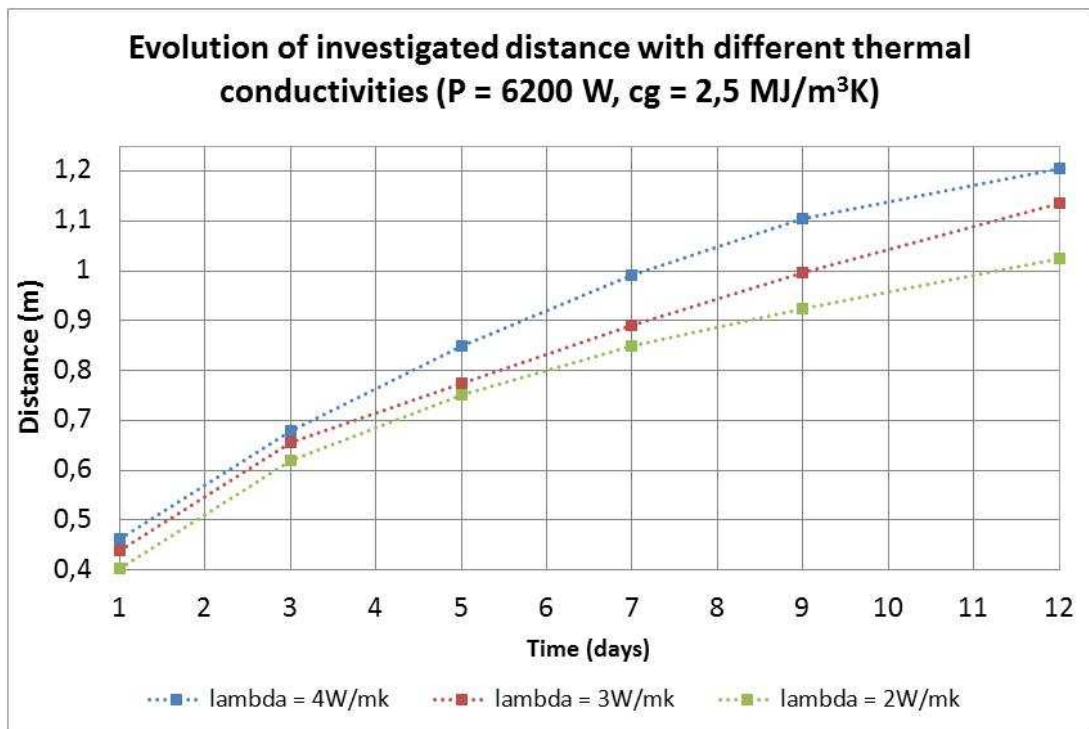
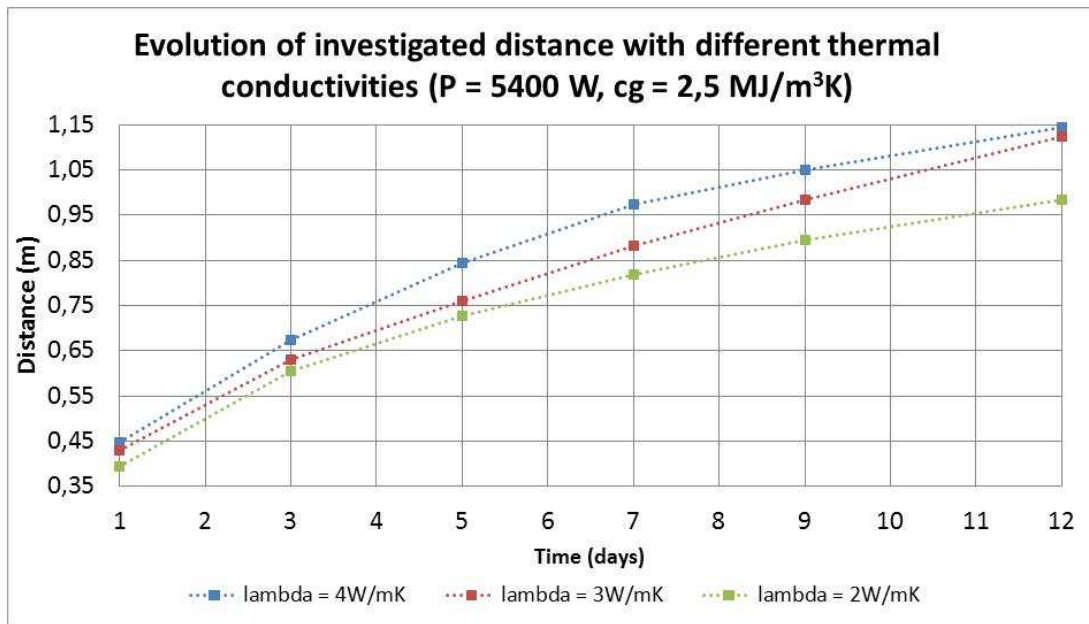


Figure 30 Evolution of the investigated distance, with constant power injected equal to 5400 W – 6200 W , constant ground thermal capacity equal to 2,2 – 2,5 MJ/m³K and variable thermal conductivity.

As it can be seen from Fig. 30, by varying ground thermal conductivity and keeping constant power and ground thermal capacity, the investigated distance is higher the higher is the thermal conductivity (of course, the heat will pass more easily where the thermal conductivity is higher). Moreover it is noticeable that the higher is the power injected the higher is the investigated distance, by keeping constant the time; this distance increases the lower is the thermal capacity of the ground (investigated distance is higher with low ground thermal capacity because we have to stock less heat before it can pass through a defined volume of ground).

Considering only a 3 days time (a normal TRT), the difference of investigated distance changing thermal conductivity and keeping constant the power and thermal capacity is 5%, while, if we keep constant thermal conductivity and thermal capacity and vary the injected power, is within 1% to 4%. The difference is within 4,5 % and 6 % if the keep constant the thermal conductivity and the power and we change the ground thermal capacity.

The TRT doesn't fully solve the problem of characterizing the thermal properties of a shallow geothermal reservoir, simply because it characterizes just the neighbourhood of the heat geo-exchanger at hand and just for the test duration. In fact, the 3D/2D variability of thermal properties through the whole reservoir cannot be studied if just one test is available, which is the normal practice. Such variability can be an important concern if a multi-borehole geothermal field has to be implemented. Moreover, the temporal variability of groundwater level could change the equivalent thermal properties of each heat exchanger (Clauser, et al., 1995). Nevertheless TRT is the most adequate, popular and efficient tool for identifying the parameters to be considered when designing the BTES system.

2.3.2 Other in situ measurements

One of the fastest methods is a needle-shaped thermal sensor developed by Hukseflux (company of Delft, Netherlands).

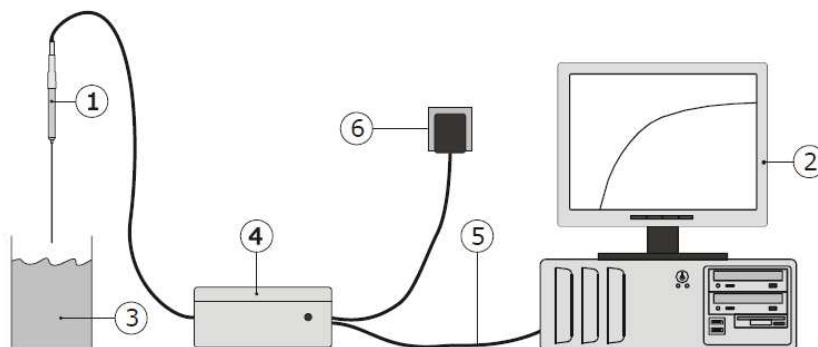


Figure 31 This is the system diagram of this kind of measurement: the main components are the thermal properties sensor (1), the measurement control unit (4) and a computer (2). (3) is the sample of soil on which we are performing the measure. This tool gives an estimation of thermal conductivity and an associated standard deviation.

The measurement method is based on the so-called Non-Steady-State Probe technique (NSSP), which uses a probe (thermal needle) in which both a heating wire and a temperature sensor are incorporated. The probe is inserted into the soil. From the response to a heating step the thermal resistivity (or the inverse value, the conductivity) of the soil can be calculated. The NSSP principle relies on a unique property of a line source: after a short transient period the temperature rise, ΔT , only depends on heater power, Q , and medium thermal conductivity, λ :

$$\Delta T = \left(\frac{Q}{4\pi\lambda} \right) \cdot \{ \ln(t_0) - \ln(t_1) \}$$

Equation 20

with ΔT in K, Q in W/m, λ in W/m·K, t the time the heater is on in s. By measuring the heater power, and tracing the temperature in time, λ can be calculated. This method can be used only for measuring thermal parameters of the first meters of soil.

Ronher et al. (Rohner, et al., 2005) developed a novel wireless borehole probe which consists of pressure and temperature sensors and mini-data logger/programmed microprocessor in a closed metal tube water-tight up to 100 bars.

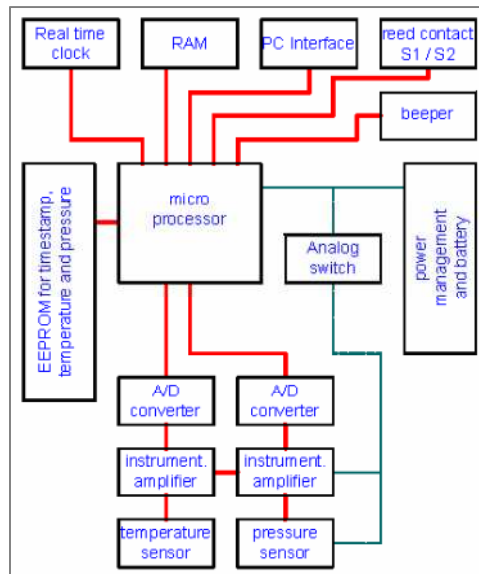


Figure 32 Block diagram of the probe: all the components are inserted in a probe with a length of 235 mm, a diameter of 23 mm and weighs only 99.8 g.

The measurement run for 300 m depth BHE takes less than 60 minutes; the resolution of temperature is 0.003°C.

Rybach & al. (Rybach, et al., 2005; Rohner, et al., 2008) developed a wireless borehole probe (Nimo-T) which consists of pressure and temperature sensors and a mini-data logger microprocessor in a closed metal tube. The probe sinks in completed (not yet working) BHE through its own weight to the bottom and records pressure and temperature at defined intervals, while descending. After completion of the logging the probe is flushed back to the surface by a small pump (length of measurement is less than 60 minutes for 300 meters depth). In the data processing the thermal conductivity profile of the logged BHE is calculated (based on pure conduction) from the temperature gradient along the BHE (derived from the measured temperature log). This technique is therefore very useful in case we need thermal conductivity measures all along the borehole considered.



Figure 33 Appearance of miniature data logger "Nimo-T"

Fujii (Fujii, et al., 2006) developed a fiber optic sensor that is inserted in the U-tube or coaxial pipe. The thermal medium (water or antifreeze liquid) is circulated under the condition that the flow rate and heating rate is constant. The procedure is the same as common TRT. The vertical distribution of soil effective thermal conductivity around the BHE can be estimated on the basis of temperature measurements with the optical fiber thermometer.

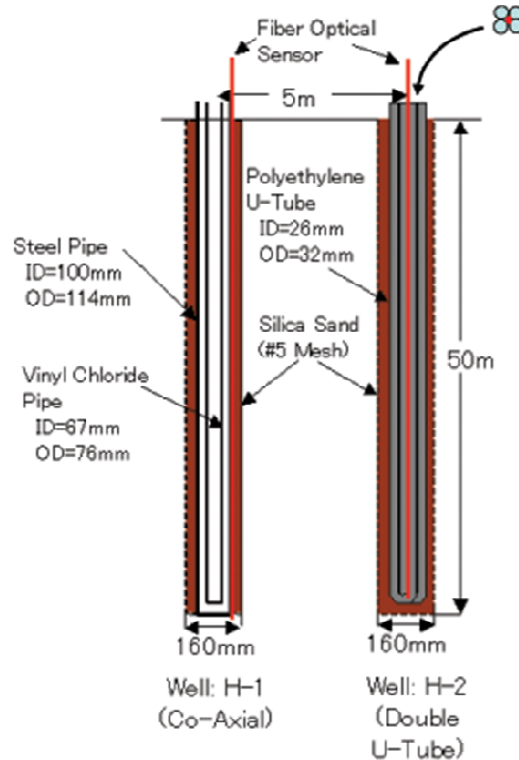


Figure 34 Fiber optic sensor is inserted in the U-tube or coaxial pipe

The equation below this measure is the cylindrical source function G (Ingersoll, et al., 1954): an average heat exchange is used to calculate the outer surface temperature of the U-tube and the U tubes were considered as a single pipe with an equivalent radius (internal is r_i , while external is r_o). To model the vertical temperature profile, the ground is divided into 1–2 m thick sub-layers (Fujii, et al., 2009).

Gustafsson & al. (Gustafsson, et al., 2003) developed a thermal response test performed while drilling (TRTWD): a constant heat power is injected into the borehole and the thermal response of circulating fluid is measured. In this case, differently from a normal TRT, energy is in the form of heat dissipation from drilling work.

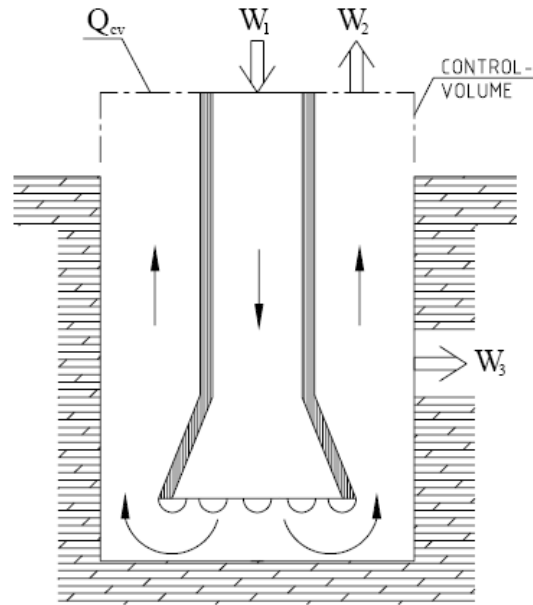


Figure 35 Energy flow through a control volume during drilling. W1 is injected energy, W2 is energy leaving the borehole, and W3 is energy transferred to the formation. Q_{cv} represents the internal energy of the control volume (Gustafsson, 2006)

The equation controlling the heat exchange (Q is the energy that has reached the formation) in this case is the following one:

$$Q = \int \rho c_v T \cdot dV - \int \rho c_v T_0 \cdot dV$$

Equation 21

Where ρ is the rock density, c_v is the rock's heat capacity, T is the rock temperature, T_0 is the initial undisturbed rock temperature, and V is the affected volume. Normally this equation is solved by using a CFD-analysis software, Fluent.

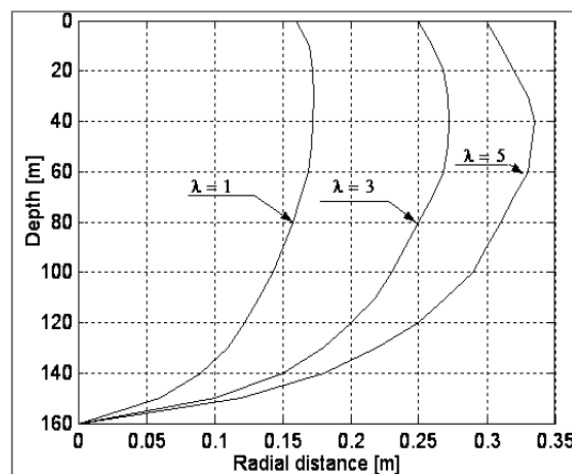


Figure 36 Isothermal curves showing the position where the formation's temperature has increased by 1°C (to 11°C) at t=320 min (drilling at 160 meters depth). The different curves represent formations with thermal conductivity $\lambda=1$, $\lambda=3$ and $\lambda=5$ W/(m· K).

The affected volume is different depending on the thermal conductivity involved, as it can be seen from Fig. 30. But although the differences in conductivity, we can easily affirm that not more than 0.5 meters can be investigated through a TRTWD, by using an injected power of 150 kW.

Witte & al. (Witte, et al., 2006) are involved in the development of a step pulse test, in which sequential pulses of different heat flux (injecting and extracting heat) are used. The system used for giving the pulses is the same used for running thermal response tests. The test results (interpreted through the finite line source model) can be used to calibrate the heat transfer of the model used for the final design.

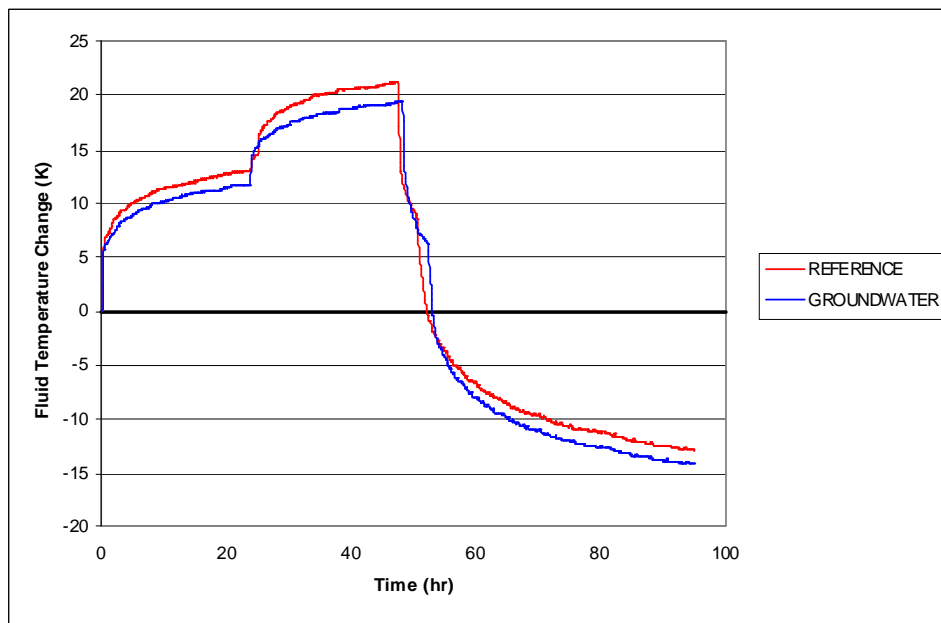


Figure 37 Fluid temperature evolution during the sequential pulses of heat flux

Nagano (Annex 21, 2010) proposed a method exploiting a hot wire cable inserted in the tube of a BHE. PT-100¹ sensors are disposed on the surface of the hot wire cable and connected to a data logger for registering temperature variations. The heating time is 50-100 hours. The temperature measuring is continued for several days after the heating.

The effective thermal conductivity of soil surrounding the borehole heat exchanger is estimated basis on the following equation, directly obtained from the line source theory.

$$\text{In the case of } t \leq t', \theta \cong \frac{q}{4\pi\lambda} \left(-0.5772 + \ln \frac{4at}{r^2} \right)$$

$$\text{In the case of } t > t', \theta \cong \frac{q}{4\pi\lambda} \left(\ln \frac{4at}{r^2} - \ln \frac{4a(t-t')}{r^2} \right) = \frac{q}{4\pi\lambda} \ln \frac{t}{(t-t')}$$

¹ Pt100 is the common abbreviation for the most common type of resistance temperature sensor used in industry. It has a specified resistance of 100.00 ohms at 0°C and is made of Platinum which has an accurately defined resistance vs. temperature characteristic.

Where t' correspond to the moment we stop the injection/extraction of heat and the recovery part starts; θ is the power injected/extracted from the borehole.

2.4 Comments on the actual ways of measuring thermal conductivity

The most important things needed to obtain suitable measures of thermal conductivity are:

- 1) to have georeferenced samples (in order to study their spatial variability), in case we are working with undisturbed ones (otherwise, if they don't reproduce real conditions, the measure is not consistent anymore)
- 2) to have samples small enough to consider the measured parameter as a Regionalized Variable homogenous and isotropic. This means that if we have a core we should keep its 3D geo-reference (its coordinates and depth) and we should do a higher number of measures on it (not only thermal conductivity, but saturation as well for example).

Knowing that, it is useful to go again through all the measurement methods explained so far in order to check if they can guarantee all these features to the measure. Concerning the laboratory measures we can divide into groups the types of measurements:

- Guarded Hot Plate Method and Probe Method are both for low conductivity values (which limits a lot the range of measures). The dimension of samples, however, is small enough to consider the measures as a RV.
- PEDB method (Antriasian, 2010) and Demirci method (Demirci, et al., 2004) are both for rocks, while in our case we are mostly interested in soils. In any case, the dimension of the samples can be considered suitable for obtaining data as a RV; moreover PEDB lets us estimate samples' anisotropy as well. The duration of the test is too long in case of Demirci, while with PEDB method it can be in between 5 and 15 minutes per each sample.
- Heater pulse (Munoz, 2006), Côté and Konrad method (Côté, et al., 2005) and axial flow methods are characterized by a long duration, even though samples' dimension can be considered suitable for obtaining a regionalized variable. The high length of the tests forces us to choose another methodology for finding thermal conductivities.
- Hot wire developed by Tavman (Tavman, 1996) is a fast measure (10 to 90 seconds per sample) with a proper dimension of samples. There are, nevertheless, some problems with the measure: first of all it's completely in air, with absolutely no protection for the sample, and second the material, as far as it has no protection outside, has to maintain its shape during the entire test. Considered that, it is clear that a normal soil cannot preserve its shape moreover when it is dry or not enough cohesive.
- Classic hot wire method measures thermal conductivity in transient and it is valid only for isotropic materials, which is not good for us because we want to estimate anisotropy as well.
- Abu Hamdeh method (Abu-Hamdeh, 2001) and thermo TDR used by Lu (Lu, et al., 2007) are both fast measurements (the first takes 200 seconds, while the second takes only 15 seconds) and they both deal with soil. These two methods can be considered perfect for our purposes if they are applied on a set of georeferenced sample and undisturbed ones.

Concerning the in situ measurements, a part from the Hukseflux method (needle), which gives us measures only from the first meters of soil, all the other mentioned method are measuring equivalent thermal conductivity of a specific part of soil. In particular TRT method, step pulse test (Witte, et al., 2006) and the hot wire cable proposed by Nagano are measuring equivalent conductivity of all the borehole's length (they are basically measuring an equivalent conductivity of 100-150 meters depth, with a different involved area depending on the power injected/extracted), while TRT-while-drilling (Gustafsson, et al., 2003), registering TRT while increasing the depth, is measuring a lot of equivalent thermal conductivity of different packs of soils (for example, only the first 10 meters, then first 15, then 20 etc.). Wireless probe of Rohner (Rohner, et al., 2005), Nimo-T of Rybach (Rybach, et al., 2005) and the fiber optic sensor of Fujii (Fujii, et al., 2006) are all punctual measures obtained all along the borehole; both Rohner and Rybach measures take 1 hour to do 300 m of measures. There is something very important to be taken into account while considering these measures: the investigated volume is different as we change the power injected, therefore we cannot consider as Regionalized Variable these values because of the changing of volume and because these volumes cannot be considered as punctual as the one of laboratory measurements. Therefore these measures are good to know in a more precise way thermal conductivity of the studied borehole, but it is important to consider their values as related to some support, which is different every time we are using a different power in the test.

2.5 Which are the values used for designing a BHE in common practice?

In normal practice values of thermal conductivity are taken from VDI norms (Ingenieure, 2004): the table below is taken directly from the VDI norms.

Ground type	Thermal conductivity		Density	Specific heat capacity per unit volume	Thermal diffusivity
	λ_E in W/(m·K)	Typical calculated value	ρ_E in 10 ³ kg/m ³	$\rho_E \cdot c_E$ in MJ/(m ³ ·K)	a in m ² /s·10 ⁻⁶
Sand, dry	0,3 to 0,8	(0,4)	1,16 to 1,7	1,3 to 1,6	0,28
Sand, water-saturated	1,7 to 5,0	(2,4)	1,6 to 2,2	2,2 to 2,9	0,94
Gravel, dry	0,4 to 0,5	(0,4)	1,5 to 1,8	1,4 to 1,6	0,27
Gravel, water-saturated	approx. 1,8	(1,8)	approx. 2,2	approx. 2,4	0,75
Clay or silt, dry	0,4 to 1,0	(0,5)	0,93 to 1,3	1,5 to 1,6	0,32
Clay or silt, water-saturated	0,9 to 2,3	(1,7)	1,2 to 1,7	1,6 to 3,4	0,68
Peat	0,2 to 0,7	(0,4)	n.a.	0,5 to 3,8	0,19

Table 4 Thermal properties for different soils (Ingenieure, 2004)

As it is clear from the table, values of thermal conductivity for each ground type are expressed in a range (minimum to maximum value) and it is reported the "typical calculated value" as well, which is a sort of average value of the distribution of possible values. In the norm it is not clearly defined how they obtain those values, there is only a reference to the Fourier's equation. We don't know therefore which was the method used for obtaining these data and which was the support investigated. We already start from a biased case if we use these parameters for designing our systems; moreover we have to choose one value in the middle of

the range, something which is or completely arbitrary or picked up because we have some info about the soil (degree of saturation for example). In any case, one question rises by seeing the values in the table: how is “typical calculated value” obtained? In fact we don’t know if these “typical values” are referred to a small laboratory samples’ dimension or to a bigger one. Moreover thermal conductivity values vary with degree of saturation, speed of the aquifer, porosity, compressive strength and bulk density (as it was seen in the previous paragraphs): it is a very sensitive value and it cannot be considered as a mere “typical value”.

The best thing to do for having a consistent value of thermal conductivity for the considered soil is to extract it from a probability distribution that takes into account also its variability. In this case two are the ways of considering the distribution: as the distribution of the equivalent parameter (statistical approach) or as a probability function of a stationary random function (geostatistical approach). The most correct is the geostatistical approach, but it needs measures made at a small support in order to have a homogenous regionalized variable. By knowing distributions and variogram, we can simulate values of thermal conductivity over a volume and therefore calculate the equivalent value of thermal conductivity, which is not the simple arithmetic mean, but it’s the harmonic one because in our case (borehole) the flux is radial (in any case, as seen before in Part II Par.2, differences between harmonic and arithmetic values are not as big as it happens with permeability instead). What is important to point out is that thermal conductivity is a non summable variable, as permeability is, and its equivalent value is variable in time because the support involved is different.

All these considerations are valid in static and dry conditions; in case there is an aquifer, if it is static we can just consider conductivity distribution for saturated soil or rocks, if not we have to consider aquifer velocity that is changing our equivalent values also in time.

3. OVERVIEW ON THE BOREHOLE HEAT EXCHANGERS' MODELS

Our geothermal system can be seen as different parts joined together: in fact we have a borehole heat exchanger (underground part) linked to a heat pump (external part). In this script we will focus on the underground part (dimensioning of boreholes system), which is the part of the system directly connected to underground properties and therefore to their modeling.

We can in principle make a distinction between the techniques that have been used so far in a stationary analysis of the problem and those used in a transient analysis. Basically this difference is the same we are facing if we consider the thermal response test (which can be seen as a stationary situation, after an initial transient time) on one side and the borehole condition while being used in a complete installation.

In this chapter we are going to deepen all the methods used to model our geothermal system, focusing on the one treating data coming out from thermal response test (because so far it is the most reliable in situ method for measuring thermal conductivity) for having stationary results and on the methods used for a transient analysis.

In both cases the existing methods are divided into analytical and numerical: in thermal response test analysis they are basically used simply for finding soil's thermal conductivity, while in the "condition of use" case they are used for dimensioning the system considering its load & time characteristics.

Before explaining our proposal, it can be useful to clarify which are the models existents up to now starting from the analytical and then switching to the numerical.

3.1 Analytical models

3.1.1 *Infinite Line Source model for TRT analysis*

In order to obtain average thermal conductivity of the underground and thermal resistance of the borehole (heat exchanger + grouting), a borehole heat exchanger must be approximated by a thermal model that allows estimating indirectly these parameters, starting from the results obtained by the Thermal Response Test, namely: input temperature, output temperature, circulation fluid flow. There are several possible models, among them the most used and popular is the Infinite Line Source model (Ingersoll, et al., 1948), which is based on the following initial approximations:

- the temperature along the borehole is taken constant as its variability is minimal compared to the radial field (minimal means that the influence on the radial field is more relevant than the one in the vertical direction: we can consider the vertical temperature as not affected by the circulation of fluid during the TRT, while the radial temperature will suffer an increase/decrease);
- the borehole is considered of infinite length for short periods of time because this value is much higher than the radius of the borehole itself;
- the power injected during the test has to be kept constant;
- heat exchange between the fluid and the surrounding ground refers to a purely conductive problem.

The problem was solved by the simplified equation of Hellström, Eskilson and Mogensen (Eskilson, 1987):

$$\Delta T(r_b, t) = q \cdot R_g = \frac{q}{4 \cdot \pi \cdot \lambda} \cdot \left(\ln \frac{4 \cdot a \cdot t}{r_b^2} - \gamma \right)$$

Equation 22

where:

$\Delta T(r_b, t)$ = temperature difference around the borehole; it is a function of the borehole radius and of the time and it is equal to $T_b - T_g$ [K];

r_b = borehole radius [m];

t = test duration [s];

T_b = average temperature on the borehole walls [K];

T_g = undisturbed ground temperature [K];

q = thermal power per meter injected in the heat exchanger [W/m];

R_g = thermal resistance of ground around the borehole [K/(W/m)]

λ = thermal conductivity of ground considered constant [W/(m·K)];

a = thermal diffusivity; it is equal to λ/c [m²/s];

$c = \rho C$ = volumetric thermal capacity [J/(m³·K)];

γ = Euler's constant, equal to 0,5772.

The ground is inhomogeneous so that any chemical-physical parameter cannot be constant. Nevertheless the most popular simplification is to consider an effective value that, for the problem at hand, allows satisfying the theoretical relationships. This is the case for the thermal conductivity here considered (Witte, 2009).

The accuracy of the line source model increases with test time, so the curve gradually leaves the transient condition (after an initial time called t_0) resulting in the stabilization of the temperature. Several experimental investigations have confirmed the theoretical suggestion that the simplified equation is acceptable for times $t \geq (5r_b^2)/a$. However the optimal condition is obtained for $t \geq (20r_b^2)/a$, value that guarantees a theoretical accuracy around 2,5% (Eklof, et al., 1996). These accuracies are obtained starting from the not simplified equation of line source: $T(r, t) = \frac{q}{4\pi\lambda} \int_{r^2/4at}^{\infty} \frac{1}{s} e^{-s} ds = \frac{q}{4\pi\lambda} E_1 \left(\frac{r^2}{4at} \right)$ where $E_1 \left(\frac{r^2}{4at} \right) = \int_{r^2/4at}^{\infty} \frac{1}{s} e^{-s} ds$. E_1 gives us temperature variations with time and with distance from the borehole center. If we call $\tau = r^2/a_b t$, then we can study E_1 for different τ intervals and see how $T(r, t)$ changes therefore. Eklof and Gehlin analyzed the equation for $\tau \geq 0,5$ and they found out that the equation is valid up to an error of 1% and $T(r, t)$ has a simplified version. If $\tau \geq 5$ $T(r, t)$ equation assumes a less complicated form and it has a maximum error of 2%. Therefore it has been normally used this simplified equation for evaluating in a faster way thermal conductivity for time $t \geq 5r_b^2/a_b$.

Another factor of extreme importance is the thermal resistance R_b between the circulation fluid and outer surface of the borehole, in contact with the ground. Normally it is approximated by the thermal resistance of cement type used in the borehole and it is considered constant.

The following relation applies:

$$T_f - T_b = R_b \cdot q$$

Equation 23

where:

T_f = average temperature of the circulation fluid; $T_f = (T_{fin} + T_{fout}) / 2$ [K];

T_b = temperature at the borehole wall [K];

q = thermal power inject per meter [W/m];

R_b = borehole thermal resistance [K/(W/m)].

The two resistances R_g and R_b are arranged in series (Fig. 8), so the amount of power injected is constant (see hypothesis), while the overall temperature variation is the addition of the two ΔT (Fig. 9), i.e. $T_f - T_g$ (Eq.6).

$$\Delta T(r_b, t) = q \cdot (R_b + R_g) = q \left[R_b + \frac{1}{4 \cdot \pi \cdot \lambda} \cdot \left(\ln \frac{4 \cdot a \cdot t}{r_b^2} - \gamma \right) \right]$$

Equation 24

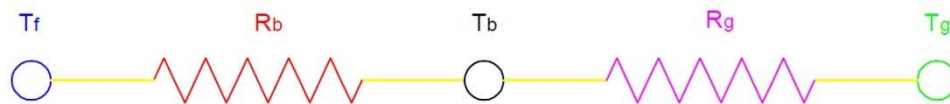


Figure 38 Resistances arranged in series representing the borehole and the ground

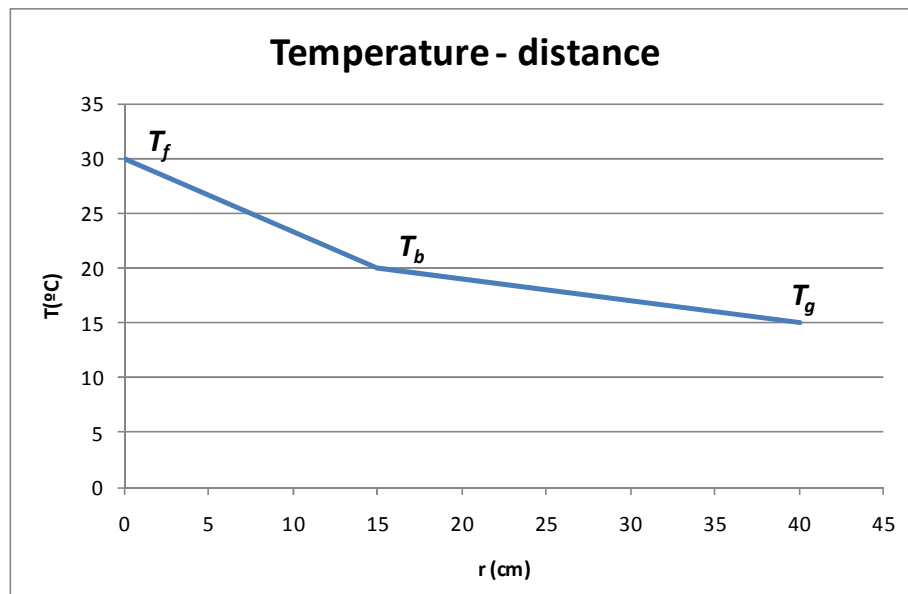


Figure 39 Evolution of temperature distance from the borehole center.

After several steps, it is possible to express the average temperature of the fluid in the following form:

$$T_f = \frac{Q}{4 \cdot \pi \cdot \lambda \cdot H} \cdot \ln(t) + \left[\frac{Q}{H} \cdot \left(\frac{1}{4 \cdot \pi \cdot \lambda} \cdot \left(\ln \left(\frac{4 \cdot a}{r_b^2} \right) - \gamma \right) + R_b \right) + T_g \right]$$

Equation 25

where H is the borehole length. This equation turns into a line in the dimension of the time logarithm:

$$T_f = K \ln t + m$$

Equation 26

So, knowing the slope K, we can derive the effective thermal conductivity of the ground λ , independently of time (if the support interested by the heat flux doesn't vary too much):

$$\lambda = \frac{Q}{4\pi HK}$$

Equation 27

The line intercept, in turn, allows estimating the thermal capacity through this formulation:

$$R_b = \frac{H}{Q} (m - T_g) - \left(\frac{1}{4\pi\lambda} \left(\ln \frac{4a}{r_b^2} - \gamma \right) \right)$$

Equation 28

in which we use the above estimated thermal conductivity λ .

There is a circular analysis concerning the current procedure for borehole resistance identification: borehole thermal resistance (R_b) is a function of borehole radius (r_b) and diffusivity (a_b), $R_b(r_b, a_b)$, and it is estimated by the regression analysis which applies to steady state conditions, i.e. from a time actually identified by the inequality $t \geq 20 (r_b^2)/a_b$ (Gehlin, 2002). To identify this initial time, a tentative value of grouting thermal diffusivity a_b^G is requested, which means, implicitly, a tentative value of borehole thermal resistance R_b^G has been adopted. Neglecting this issue, we can find the slope K and the intercept m by operating a linear regression (Fig.41) on the experimental T_f .

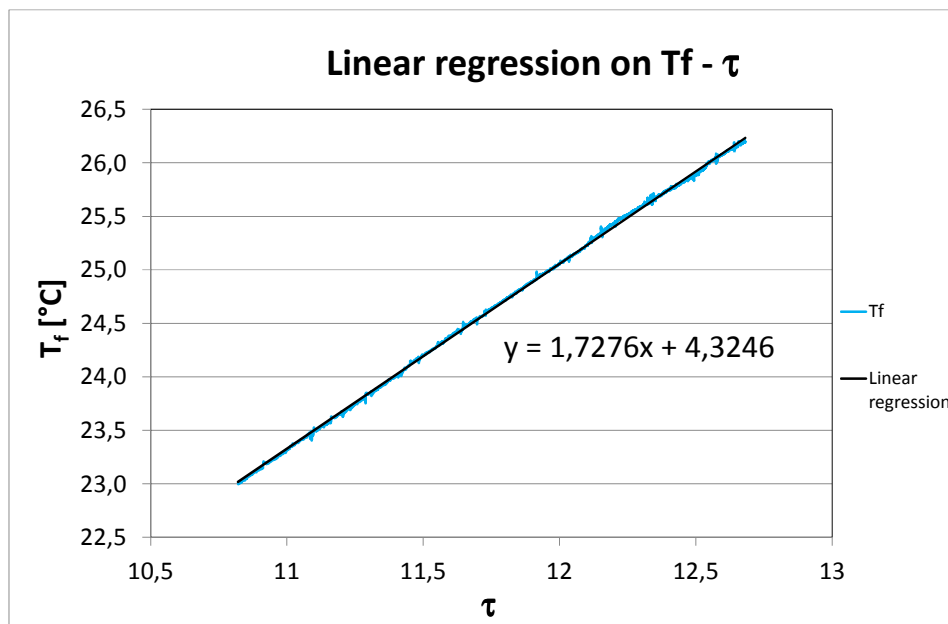


Figure 40 Linear regression of fluid temperature T_f on time_log scale, $\ln(t)$

Once known thermal conductivity, and once estimated volumetric heat capacity on the underground stratigraphic succession, the thermal resistance R_b is obtained by using the same equation.

3.1.2 Cylindrical source model for TRT analysis

Another model for the interpretation of TRT data is the cylindrical source model, which is based, for a constant heat transfer rate, on Carslaw and Jaeger's (Carslaw, et al., 1947) and Ingersoll's (Ingersoll, et al., 1948) works.

This method provides a classical solution for the radial transient heat transfer from a cylinder pipe with infinite length surrounded by an infinite homogeneous medium with constant properties (Javed, et al., 2009). The cylinder, which usually represents the borehole outer boundary, is assumed to have a constant heat flux across its outer surface; it is also assumed that the heat transfer between the borehole and soil with perfect contact is of pure heat conduction (Yang, et al., 2010). Based on the governing equation of the transient heat conduction along with the given boundary and initial conditions, the temperature distribution of the ground can be easily given in the cylindrical coordinate:

$$\begin{cases} \frac{\partial^2 t}{\partial r^2} + \frac{1}{r} \frac{\partial t}{\partial r} = \frac{1}{a} \frac{\partial t}{\partial \tau} & r_b < r < \infty \\ -2\pi r_b k \frac{\partial t}{\partial r} = q_l & r = r_b, \tau > 0 \\ t - t_0 = 0 & \tau = 0, r > r_b \end{cases}$$

where r_b is the borehole radius.

The cylindrical source solution is given as follows:

$$T - T_0 = (q_l/k) \cdot G(z, p)$$

Where $z = \alpha\tau / r_b$ and $p = r/r_b$.

The expression $G(z, p)$ is only a function of time and distance from the borehole center.

The temperature on the borehole wall, where $r = r_b$, i.e. $p = 1$, is of interest as it is the representative temperature in the design of GHEs. However, the expression $G(z, p)$ is relatively complex and involves integration from zero to infinity of a complicated function.

3.1.3 Others analytical models for TRT analysis and new proposals

Other authors have treated the analysis of TRT data through analytical models, mostly contesting the infinite line source model and its approximations.

Eskilson (Eskilson, 1987) in his PhD thesis was the first conducting analytical studies about the formulas concerning conductive heat extraction from boreholes and in particular about finite line source model.

Zeng et al. (Zeng, et al., 2002) derived an analytical solution of the transient temperature response in a semi-infinite medium with a line source of finite length. The assumptions made are the following:

- Ground is a homogeneous semi-infinite medium, with constant thermo-physical properties with temperature.
- The initial temperature T_0 is uniform in the space.
- The ground surface keeps a constant temperature throughout the considered period.

-
- The radial dimension of the borehole is neglected so that it may be approximated as a line source stretching from the boundary to a certain depth, H .
 - The heating rate per length of the source, q_l , is constant.

Bandos et al. (Bandos, et al., 2009) sustain that infinite line source models have some limitations, mostly for long time periods because the finite size effects are to be taken into account in order to reach a steady state value for ground temperature. They propose then to use the finite line source (FLS) model, whose solution has been expressed as an integral (Eskilson, 1987; Carslaw, et al., 1947) given zero temperature at the boundary of the semi-infinite medium. The heat flow along the vertical has a constant temperature gradient k_{geo} ; it is considered a variable ground surface temperature as well. Heat is released at a constant rate along the BHE and it is transferred by conduction. This method consists of averaging the borehole temperature, instead of using its value at the mid-point of the borehole, by properly accounting for the influence of ground surface and of BHE's bottom conditions.

Previously this model had also been studied and improved by Lamarche and Beauchamp (Lamarche, et al., 2007), who studied as well the short time response of vertical boreholes with an analytical approach that solves the exact solution for concentric cylinders and is a good approximation for the familiar U-tube configuration (Lamarche, et al., 2007). Lamarche's method is valid just for a short time response which corresponds to the transient period of a thermal response test; this method can be used for real time simulations of heat pump systems for time less than an hour, peak load effect for the length calculations of vertical heat exchangers and for the evaluation of the ground thermal properties in short period of time.

Yang et al. (Yang, et al., 2009) divide the heat transfer region of BHE into two parts at the boundary of borehole wall; these two parts are coupled by the temperature of borehole wall. The transient borehole wall temperature is calculated for the soil region outside borehole by use of a variable heat flux cylindrical source model (adapted from Ingersoll model which was for constant flux). The model considered the effect of fluid temperature along the borehole length and heat interference between two adjacent legs of U-tube simultaneously. Both steady and transient heat transfer method are used to analyze the heat transfer process inside and outside borehole, respectively.

3.1.4 Comments to the actual models of TRT

The problem of all these methods is principally that they are all setting initial hypotheses in order to be true and valid in some precise condition. None of them is valid in any time and in any condition of power, length.

Starting from the first one, infinite line source method, it has a lot of initial hypotheses that could be easily denied:

- the temperature along the borehole is taken constant as its variability is minimal compared to the radial field \rightarrow this is not completely true. It is true that the variability is bigger on the radial direction, but at the same time on the vertical direction we will have a variation of temperature, even if small, due to the thermal gradient;
- the power injected during the test has to be kept constant \rightarrow this is something very difficult to have, at least during normal TRT test. The machine test unlikely is going to maintain a constant injection/extraction power moreover because the amount of

power is varied along with the varying difference between input temperature and output temperature from the borehole (if the flow keeps constant);

- heat exchange between the fluid and the surrounding ground refers to a purely conductive problem → this is not true. As it was seen before, the heat exchange is not only due to conduction but also to convection and advection.

Cylindrical heat source model (Ingersoll, et al., 1948; Javed, et al., 2009; Yang, et al., 2010) assumes to have a constant heat flux across its outer surface and that the heat transfer between the borehole and soil is of pure heat conduction. In this case as well we can comment that the heat transfer will not be just of heat conduction, but we have to consider convection and advection as well.

Finite line source model proposed by Bandos (Bandos, et al., 2009) has some advantages compared to the other because it takes into account more variability (ground surface temperature variable, existence of a temperature gradient along the vertical), but it still considers a constant power injected/extracted which is not completely realistic and a pure conductive model (see previous comments).

The short time response model proposed by Lamarche and Beauchamp (Lamarche, et al., 2007) is interesting because it deals with the transient period in an analytical way, which is something much more rapid than a numerical simulation of it. On the other hand, it gives us information about the transient period and not the steady state period and the assumptions made are the same as the finite line source method.

Zeng model (Zeng, et al., 2002), as some of the other, makes some assumptions that are not completely acceptable (ground is a homogeneous with constant properties and constant temperature along the considered period, heating rate is taken as constant).

3.2 Numerical methods

Besides the analytical solutions, there is also a numerical way for interpreting TRT data and for modeling a borehole heat exchanger. Generally numerical models handle any kind of power input and they allow the evaluation of effects of BHE on smaller time scales and lower the time minimum criterion. Also the heat transfer considered in the ground is not restricted to heat conductance, but includes for example ground water flow.

Actually the techniques that can be used are different and we are going to resume the most important in this paragraph.

Yavuzturk (Yavuzturk, 1999) proposed a numerical model for the simulation of *transient heat transfer* in vertical ground loop heat exchangers based on a two-dimensional fully implicit finite volume formulation. The model has two main applications: first it is used in a parameter estimation technique to find the borehole thermal properties from short time scale test data; second it is the calculation of non-dimensional temperature response factors for short time scales that can be used in annual energy simulation.

Schonder and Beck (Schonder, et al., 1997) proposed a parameter estimation method based on numerical solutions to the heat conduction equation in cylindrical coordinates (for a TRT data analysis); this method includes the effect of grout inside the borehole, allowing the estimation of soil thermal conductivity and also borehole thermal resistance. There are three

main advantages of this method, namely: its accuracy is not affected by short-term variations in power input to the heat exchanger; it's more accurate at early times so it doesn't require early data to be discarded as the analytical method normally does; finally, a qualitative estimate of the accuracy of the thermal properties is given.

Al-Khoury et al. (Al-Khoury, et al., 2005) developed a computationally efficient finite element tool for the analysis of 3D steady state flow in geothermal heating systems. This model has then been implemented on FEFLOW software as the numerical solution.

Nagano et al. (Nagano, et al., 2006) created a new design and performance prediction tool for the ground source heat pump (GSHP) system, which applies cylindrical heat source theory with high speed calculation algorithm. It is applied in the TRT analysis.

Signorelli (Signorelli, et al., 2006) used the 3D numerical model of FRACTure code (used for TRT as well), developed between 1988 and 1995 by the Institute of Geophysics and Polydynamics Ltd of Zurich (Kohl, et al., 1995): it is a finite element model created to simulate the long-term behavior of an elementary HDR (hot dry rock) system to prolonged circulation. Some were the models included in its realization: hydraulic flow, transport of heat energy by diffusion and advection and elastic deformation. The fact that it includes so many physical models makes it suitable for modeling a geothermal area as well.

Wagner and Clauser (2005) used the FD simulation code SHEMAT (Clauser 2003), which was customized to perform parameter estimation and to use load-time functions for time-dependent source/sink terms. SHEMAT (Simulator for HEat and MAss Transport) is an easy-to-use, general-purpose reactive transport simulation code for a wide variety of thermal and hydrogeological problems in two or three dimensions.

Lee and Lam (Lee, et al., 2008) proposed a three-dimensional finite-difference method using rectangular coordinate system was employed to discretize the ground around a borefield, with each borehole represented by a square column to avoid using fine grids inside the borehole. Allowing the vertical heat transfer, the actual borehole temperature and loading profile could be estimated. Some assumptions characterize the model:

- homogeneous ground
- constant thermal properties
- no contact resistance between the borehole and the ground
- ground temperature constant at the top surface and below the borehole (vertically and transversally)
- borehole in quasi steady state (TRT analysis)
- same fluid flow rate for all the boreholes and the tubes.

Nam et al. (Nam, et al., 2008) developed a model that combines heat transport model with groundwater flow and a heat exchanger model with an exact shape; they also propose a method for estimating soil properties based on ground investigations to obtain accurate simulation results. In this research, FEFLOW is adopted in order to calculate heat exchange rate between ground heat exchanger and its surrounding ground and to estimate the distribution of subterranean temperature.

Pasquier set up a 3D finite element numerical model which was then constructed within the COMSOL environment (Marcotte, et al., 2008) for simulating the behavior of a BHE. It

comprises a geological media, a heat carrier fluid circulating inside a U-loop and a borehole filled with a conductive material (i.e. grout). Note that the fluid velocity inside the pipes is assumed constant and, therefore, it does not take into account the convective resistance occurring at the tube wall.

Fujimitsu et al. (Fujimitsu, et al., 2009) conducted demonstration and performance assessment of the ground coupled heat pump (GCHP) system through numerical simulations in FEFLOW (application of Al-Khoury method).

He et al. (He, et al., 2010) developed a 3D numerical model to simulate transient fluid transport and heat transfer in and around Borehole Heat Exchanger. The model is being used to develop improved simplified models of BHEs.

More information concerning the choice of the simulator will be in Part III.

3.2.1 Finite length source

This numerical method was presented the first time from Eskilson (Eskilson, 1987) who used non-dimensional thermal response functions (g-functions) for modeling the thermal response of a borehole heat exchanger. In practice he divided the response in unit step pulse calculated using a finite difference approach (Javed, et al., 2009), so the temperature response of the boreholes is obtained from a sum of step responses. This model is the only one that takes into account the long-term influence between boreholes.

$$T - T_0 = \sum_i \frac{\Delta q_i}{2\pi\lambda} \cdot g\left(\frac{t - t_i}{t_s}, r_H^*, \dots\right), \quad t_s = \frac{H^2}{9a}$$

Equation 29

where the change in extraction time t_i is Δq_i .

PART III

Inverse Modeling of a Geothermal Reservoir

1. INTRODUCTION TO INVERSE MODELING TECHNIQUE

Inverse modeling is a simulation process of a parameter, conditioned to data of a variable related to this parameter through a partial difference equation. The algorithm of inverse modeling allows us to determine reservoir properties using a limited number of *in situ* observations, by an iterative process in which the differences between observed values and simulated ones are minimized (application of a transfer function F).

Practically in the iterative process, we impose some perturbations to the property investigated by the inverse problem with the objective of minimizing successively the objective function (subsequent perturbations to obtain an optimized solution that honors the known data).

In order to better describe the investigated property, we can express it in a more complex way: by using geostatistical simulations to create realistic images of it.

First of all, it's necessary to explain why we use geostatistics in our study:

- 1) For giving heterogeneity to our reservoir (accurate grids)
- 2) For quantifying uncertainty through different models with the same heterogeneity
- 3) For integrating different types of data at different scale and precisions (hard and soft data) through cokriging and co-simulations.

For modeling the reservoir we could use:

- Kriging, but it reduces the variance, thus it will not reproduce in a good way our heterogeneity (it squeezes extreme values that, in this case, are important)
- Simulation reproduces the histogram, respects the variogram and furnishes the uncertainty through multiples images equiprobable and real of the phenomena.

The resolution method proposed for this kind of problem is an algorithm of inverse modeling whose objective is reservoir characterization by the integration of dynamic data in stochastic modeling using Direct Sequential Simulation (DSS) and Co-simulation (CoDSS) as a convergent process of global and regional perturbation of permeability images. This algorithm lets us obtain a spatial distribution of reservoir permeability which respects both static data (variogram and histogram of permeability distribution in the stochastic model) and dynamic ones (flux in the observations' boreholes).

The procedure followed requires:

- Stochastic modeling of reservoir properties is made by the *facies* geometry simulation and by the petrophysical properties distribution in the *facies* exploiting geostatistics
- Dynamic modeling of reservoir's fluids, based on energy and mass conservation's laws, Darcy's law, dynamic models' equation (state equation) and relationship between relative permeability and capillary pressure. This simulation model is composed by:
 - a. Equation regulating fluid dynamics
 - b. Maps to define study area
 - c. Data describing the area and the parameters
 - d. Initial and boundary conditions.

Deepening a bit our inverse problem, it follows these steps:

- a) Definition of the stochastic model, which is in practice a geostatistical modeling exploiting borehole data (hard data). Through this model, reference permeability images are simulated.
- b) Numerical simulation of fluids flux in the reservoir, one per each different permeability image simulated in the previous step, considering as a boundary condition null flux. This step corresponds to a determinist modeling.
- c) Successively we perform perturbations through a co-simulation using an image of step 1 as secondary information to generate new realizations in order to have numerical simulation flux results respecting observed production data. In this step we apply the objective function to verify the reproduction of dynamical behavior (production data). Following perturbations performed on permeability images maintain spatial variability of predefined stochastic model; therefore permeability images respect both spatial variability and production data.
- d) Everything is repeated until c) until we find permeability images creating dynamic results matching boreholes' production data, according to the objective function.

There are different objective functions for performance evaluation (i.e. ability to reproduce observed data); for example, sum of square differences have been used in a lot of works (Landa, 1997; Valeo, et al., 2000; Hu, 2002; Hu, et al., 2004) as a method of performance evaluation of simulation algorithms.

In general an objective function (OF) is an optimization function that determines the strength of a solution (Mata-Lima, 2006) and it has to be minimized in order to choose the best solution among all the existing alternatives.

Equation	Terms	Comments	Bibliography
$AE = \sum_{i=1}^n \frac{O_i - S_i}{n}$	AE is the average error; n is the number of observations used for the optimization; O_i , S_i are observed and simulated values and O_m is the average of observed values.	Best value is 0.	(Loague, et al., 1991; Chanasyk, et al., 2003)
$RMSE = \frac{\left(\sum_{i=1}^n \frac{(O_i - S_i)^2}{n}\right)^{1/2}}{O_m}$	RMSE is the square root of quadratic mean error and O_m is the average of observed values.	Best value is 0.	(Loague, et al., 1991; Chanasyk, et al., 2003; Eching, et al., 1993; Willmott, 1982)
$RMS = \left(\sum_{i=1}^n \frac{(O_i - S_i)^2}{n}\right)^{1/2}$	RMS is the square root of square average.	Best value is 0.	(Loague, et al., 1991; Chanasyk, et al., 2003; Li, 1988; Barringer, et al., 1997; Matthias, et al., 2000)
$SSD = \sum_{i=1}^n (O_i - S_i)^2$	SSD is the sum of square differences.	Best value is 0.	(Gomez-Hernández, et al., 1997; Landa, 1997; Valeo, et al., 2000; USACE, 2001; Castano, et al., 2006)
$SMS = \sum_{i=1}^n \frac{(O_i - S_i)^2}{n}$	SMS is the sum of mean quadratic error.	Best value is 0.	(Boken, et al., 2004; Goovaerts, 2000; Hu, et al., 2004)
$SAR = \sum_{i=1}^n O_i - S_i $	SAR is the sum of absolute error.	Best value is 0.	(USACE, 2001; Pandey, et al., 1999)

$WRMS = \frac{\left(\sum_{i=1}^n \frac{(O_i - S_i)^2}{n}\right)^{1/2}}{O_m}$	WRMS is the square root of weighted squares.	Best value is 0.	(USACE, 2001; USACE, 1994)
$MARE = \frac{\sum_{i=1}^n \frac{O_i - S_i}{O_i}}{n}$	MARE is a relative error.	Best value is 0.	(Panigrahi, et al., 2003)
$RE = \left \frac{O_i - S_i}{O_i} \right $	RE is a relative error.	Best value is 0.	(USACE, 2001; Yue, et al., 2000)
$CRM = \frac{\sum_{i=1}^n O_i - \sum_{i=1}^n S_i}{\sum_{i=1}^n O_i}$	CRM is the coefficient of error between simulated and observed values.	Best value is 0.	(Chanasyk, et al., 2003; Loague, et al., 1991)
$EF = 1 - \frac{(O_i - S_i)^2}{n}$	EF is the model efficiency and O_m is the average of observed values.	Best value is 1.	(Loague, et al., 1991; Nash, et al., 1970; ASCE, 1993; Hvilshoj, 1998; Antonopoulos, et al., 1998; Sharma, et al., 2003)
$\chi^2 = \sum_{i=1}^n \frac{(O_i - E_i)^2}{E_i}$	χ^2 is the sum of the squared difference between observed (O) and the expected (E) data	Best value is 0.	(Pearson, 1900)

Table 5 Résumé of all the minimization function

2. GEOSTATISTICAL SIMULATION OF THERMAL PARAMETERS

In order to represent the variability of the natural mean, we need to perform geostatistical simulation of the parameters characterizing the soil. In our case study the most important parameter we need to simulate is thermal conductivity.

Different are the simulations that we could perform in order to obtain our domain of thermal conductivities. In the following pages the most common ones are summarized.

2.1 Sequential Gaussian Simulation (SGS)

The main principle besides simulations in general is that, in order to reproduce real images, when data follow a Gaussian distribution, we estimate average and variance of the probability distribution function for each point of the domain considered and we create randomly a value starting from this distribution.

The first step followed by Sequential Gaussian Simulation is, therefore, that all the values are transformed in Gaussian values, through the following relation $Y(x) = \phi[Z(x)]$, and their variogram is calculated. All the simulation process is therefore run in a “Gaussian environment”; data transformation to their original distribution is made at the end of the simulation process.

The simulation process follows then these steps:

- choice of a random point on the regular grid that will be simulated
- through a multigaussian kriging, using known data and variogram, kriging average and variance are calculated for this point. These two values are considered average and variance of the local Gaussian probability distribution of the point
- choice of a random value for this point, following the normal law (kriging average and variance)
- that point (from now on called simulated) is therefore considered as a known point for conditioning the next point (besides real data obviously)
- repetition of these steps for all the unknown points.

Simulated values are conditioned to true values: they have the same distribution and the same variogram. Finally, an inverse transformation is performed to restore the original data distribution in case it is not the Gaussian.

This kind of simulation is used for porosity, but not for permeability.

2.2 Direct Sequential Simulation (DSS) and Co-Simulation (Co-DSS)

In this simulation (Soares, 2001) no transformation of the original variable into a Gaussian one is needed. The simulation has the objective of using local average and variance for resampling the global distribution law (and not for defining local laws as it was in the SGS). It is mostly used with permeability to avoid problems derived from the Gaussian transformation of the variable.

Whichever is the probability distribution chosen, if the local cumulative distribution function is centered on the simple kriging estimator $[Z(x_u)]^* = m + \sum_{\alpha} [Z(x_{\alpha}) - m]$ then the model of Spatial Covariance and Variogram are reproduced in the image simulated in the end. Cumulative distribution function $F_z(Z)$ is maintained over all the algorithm steps.

Z intervals are extracted from $F_z(Z)$ defining a new $F'_z(Z)$: simulated values $Z^s(x_u)$ are sampled from $F'_z(Z)$ distribution. Intervals are centered in the simple kriging estimator $[Z(x_u)]^*$ and the interval limit depends on the estimation variance of simple kriging $\sigma^2_{ks}(x_u)$.

These intervals are defined selecting a subset of $Z(x_i)$ values from the experimental histogram in order to have average and variance of these n values equal respectively to $[Z(x_u)]^*$ and to $\sigma^2_{ks}(x_u)$:

$$\frac{1}{n} \sum_{i=0}^N Z(x_i) = [Z(x_u)]^*$$

$$\frac{1}{n} \sum_{i=0}^N [Z(x_i) - [Z(x_u)]^*]^2 = \sigma^2_{ks}(x_u)$$

Equation 30

In this way the simulated value $Z^s(x_u)$ is generated from $F'_z(Z)$ of the n selected values. We can also recourse to a Gaussian distribution to define sampling intervals' limits according with $\sigma^2_{ks}(x_u)$.

ϕ is the result of the Gaussian transformation of $z(x)$ values, thus $Y(x) = \phi(z(x))$, $G(Y(x))=F_z(z(x))$. The local simple kriging estimator $[Z(x_u)]^*$ has its Gaussian equivalent in $[Y(x_u)]^* = \phi([Z(x_u)]^*)$, which, together with $\sigma^2_{ks}(x_u)$, defines a Gaussian cumulative distribution function $G([Y(x_u)]^*, \sigma^2_{ks}(x_u))$.

This Gaussian distribution is useful only for sampling the intervals and doesn't influence the estimation local distribution function.

After calculating transformed $Z(x)$, these are the steps to follow:

1. Defining a random path all over the regular grid of x_u points on which run the simulation
2. Estimating local mean and variance of $Z(x_u)$ with simple kriging, conditioning them to $Z(x_i)$ data and to the potential simulated data $Z^s(x_i)$
3. Defining the interval of $F_z(Z)$ to sample, referring to Gaussian cumulative distribution $G([Y(x_u)]^*, \sigma^2_{ks}(x_u))$
4. Choosing a value $Z^s(x_u)$ of cumulative distribution function $F_z(Z)$ in this way:
 - a. Generate a value p starting from a uniform distribution $U(0,1)$
 - b. Obtain a value Y^s from $G([Y(x_u)]^*, \sigma^2_{ks}(x_u))$ being $Y^s = G^{-1}([Y(x_u)]^*, \sigma^2_{ks}(x_u), p)$
 - c. Deduce $Z^s(x_u)$ from the inverse transformation ϕ^{-1}
5. Going back to the initial point and doing again all the procedure for all the points to simulate.

In case we have two variables $Z_1(x)$ and $Z_2(x)$, one of which is a primary variable (ex. $Z_1(x)$), we will use a co-simulation process. The iter is the following:

- Choosing a path on the grid to simulate
- Simulating $Z_1^s(x_u)$ value in x_u points (see 2-3-4 of direct simulation)
- At this point simulating $Z_2(x)$ with a direct sequential simulation considering previously calculated $Z_1(x)$ as a secondary variable.
- $[Z_2(x)]^*$ and $\sigma_{ks}^2(x_u)$ are calculated through collocated cokriging conditioned on data near to $Z_2(x)$ and to the collocated value $Z_1^s(x_u)$:

$$[Z_2(x)]^*_{CKS} = \sum_{\alpha=1}^n \varphi_{\alpha}[Z_2(x_{\alpha}) - m_2] + \varphi_{\beta}[Z_1^s(x_u) - m_1] + m_2$$

- Then we need to transform $[Y(x_u)]^* = \phi_2([Z_2(x_u)]^*)$ (ϕ_2 is the result of the Gaussian transformation of $Z_2(x)$). Now a value p is generated starting from a uniform distribution $U(0,1)$, then Y^s is generated from $G([Y_2(x_u)]^*, \sigma_{ks}^2(x_u))$ and from it we obtain $Z_2^s(x_u) = \phi_2^{-1}(Y^s)$.

2.3 Building up the synthetic data

Thermal conductivity of our soils is taken from the VDI norms (maximum, minimum and average values are shown) and per each has been done a bibliographical study for understanding their distribution in soils.

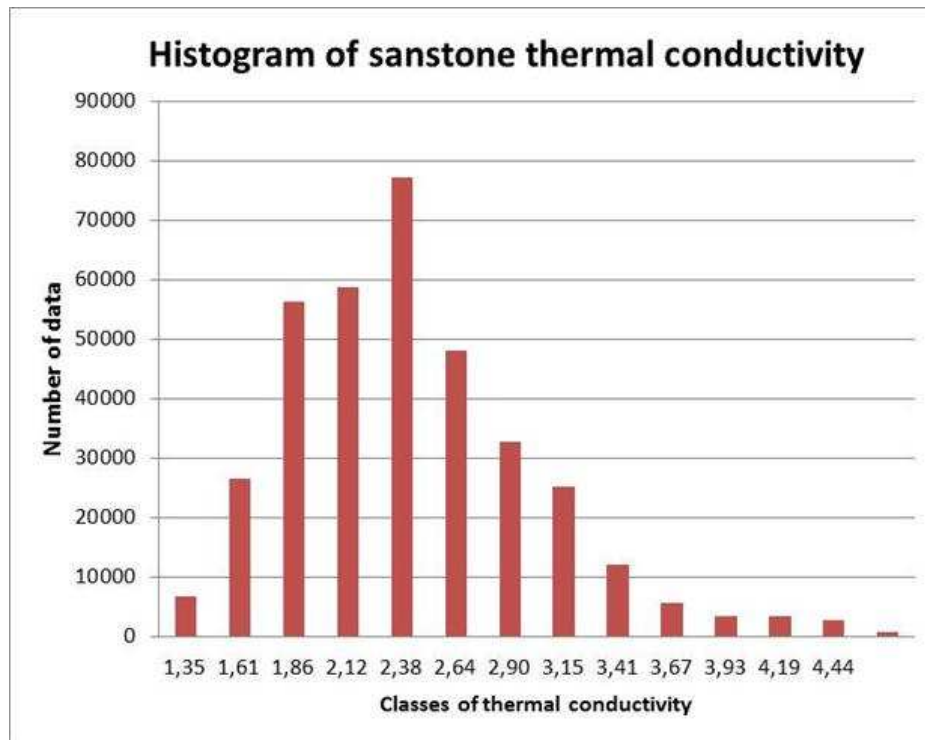


Figure 41 Example of a histogram of frequency of sandstone thermal conductivity

Simulation of thermal conductivity has been run on a domain 60x60x100 meters, using some fictitious data obtained from a borehole.

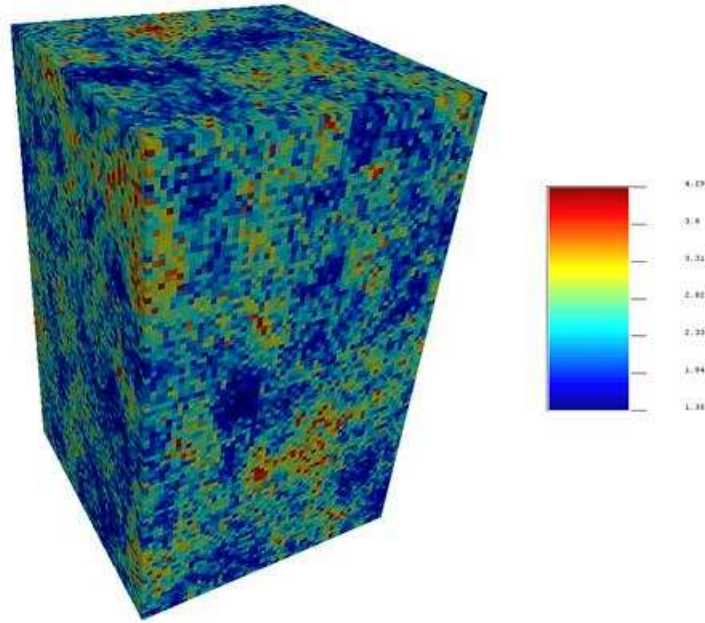


Figure 42 Image of a simulation 60x60x100 m3 of sandstone thermal conductivity obtained by using borehole data.

After that, 6 boreholes have been extracted from the simulation and from now on they will be considered as real data (they are on a symmetrical position in the field). Then these data have been analyzed geostatistically (average, variance and variogram) and by using them other simulations have been run (DSS – direct sequential simulation) obtaining different realizations related to boreholes’ data.

All the procedure has been done for different types of soil (sandstone, dry and saturated clay, saturated sand, marl, clay schist) and for two different structures of variogram (spherical and Gaussian model).

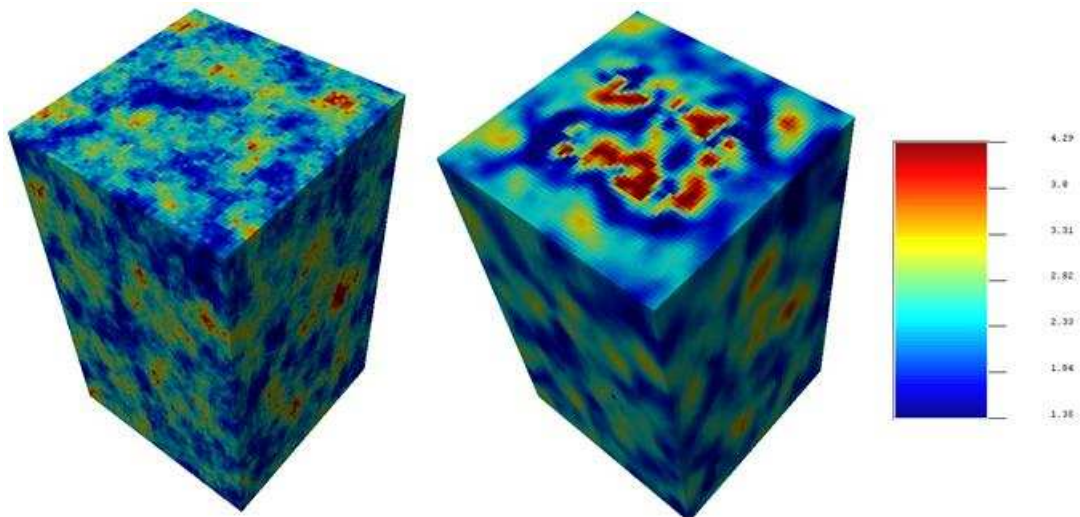


Figure 43 Simulation of thermal conductivity with a spherical model and with a gaussian one.

3. DYNAMIC SIMULATION OF A GEOTHERMAL SYSTEM

3.1 State of the art

Our purpose is to model the geothermal system (underground + borehole) through the simulator chosen (namely FEFLOW). Before starting to create the synthetic model, it has been necessary to study deeply the bibliography concerning numerical simulation of geothermal systems.

Four are the examples considered in this study:

- “Numerical evaluation of thermal response tests”- S. Signorelli et al. (Signorelli, 2007)
- “Evaluating thermal response tests using parameter estimation for thermal conductivity and thermal capacity” - R. Wagner & C. Clauser (Wagner, et al., 2005)
- “On the estimation of thermal resistance in borehole thermal conductivity test” - D. Marcotte & P. Pasquier (Marcotte, et al., 2008)
- “Efficient numerical modeling of borehole heat exchangers” – Al-Khoury et al. (Al-Khoury, et al., 2010).

In the following table the most relevant features are summarized and compared.

GEOMETRICAL CHARACTERISTICS	Signorelli et al.	Wagner & Clauser	Marcotte & Pasquier	Al-Khoury et al.
<i>Dimension of model</i>	1500x1500x500 m ³	150 m radius x 100 m depth	150 m height	100x100x150 m ³
<i>Number of layers</i>	More than 25	10	8	12
BOREHOLE CHARACTERISTICS	Signorelli et al.	Wagner & Clauser	Marcotte & Pasquier	Al-Khoury et al.
<i>Borehole length [m]</i>	160	150	40	100
<i>Borehole diameter[m]</i>	0.152	0.15	0.5	0.15
<i>Outer pipe diameter [m]</i>	0.04	0.034	0.04	0.032
<i>Outer pipe wall thickness [m]</i>	0.0037	0.003	0.0037	0.0029
<i>Grouting material</i>	Quartz sand cement	Not specified	Not specified	Not specified
<i>Heat carrier fluid</i>	Water	Water +refrigerant	Water +refrigerant	Water +refrigerant
THERMAL CHARACTERISTICS	Signorelli et al.	Wagner & Clauser	Marcotte & Pasquier	Al-Khoury et al.
<i>Average soil thermal conductivity [W/mK]</i>	3	2.0	2.1	1.7
<i>Soil volumetric thermal capacity [J/m³K]</i>	2.5 · 10 ⁶	2.0 · 10 ⁶	2.2 · 10 ⁶	2.2 · 10 ⁶
<i>Grout thermal conductivity[W/mK]</i>	0.8	0.8	Various	2.65
<i>Grout volumetric thermal capacity [J/m³K]</i>	2 · 10 ⁶	2 · 10 ⁶	1.5 · 10 ⁶	2.2 · 10 ⁶
<i>Fluid thermal conductivity</i>	0.58	0.502	0.49	0.48

[W/mK]				
Fluid volumetric thermal capacity [J/m ³ K]	4.186 · 10 ⁶	3.98 · 10 ⁶	4.4 · 10 ⁶	3.99 · 10 ⁶
Pipe thermal conductivity [W/mK]	0.4	0.42	0.42	0.42
Pipe volumetric thermal capacity [J/m ³ K]	1.62 · 10 ⁶	2.19 · 10 ⁶	2.6 · 10 ⁶	Not specified
HEAT PUMP	Signorelli et al.	Wagner & Clauser	Marcotte & Pasquier	Al-Khoury et al.
Heat pump capacity [kW]	6.2	0.96	7.5	5
Flow rate [l/h]	810	730	various	1440

Table 6 Most relevant features for defining a model

The 4 authors used different simulation software and different are the problems solved. Signorelli has developed her model in FRACTure, solving an inverse problem for individuating the thermal conductivity of best fit; she choose as objective function the sum of square errors (SSE). Wagner and Clauser calculated the response temperature of a synthetic TRT experiment as a reference for a subsequent joint estimation of rock thermal conductivity and thermal capacity (parameter estimation problem) using SHEMAT. Marcotte and Pasquier proposed a new method for finding the borehole thermal resistance and they applied it on a model developed in COMSOL. Al-Khoury presented a new finite element modeling technique for double-U tube borehole heat exchangers; this model has been implemented on FEFLOW.

Considering boundary and initial conditions, the following table will help in resuming the choices made by the authors.

BOUNDARY CONDITIONS	Signorelli et al.	Wagner & Clauser	Marcotte & Pasquier	Al-Khoury et al.
	Base flux of 90 mW/m ² Dirichlet and Neumann conditions tested are different.	Dirichlet condition: $T_i(0,t) = 13,75^{\circ}\text{C}$ Temperature on the surface is the same as the initial ground temperature.	Dirichlet condition: $T_i(0,t) = \text{cost}$ Temperature at the bottom and on the borders is the same as the initial ground temperature. Neumann condition: Vertical flux in the borehole is null.	Dirichlet condition: $T_i(0,t) = T_{in}(t)$ Pipe-in temperature is equal to the refrigerant temperature at the moment it enters into the pipe-in. Neumann condition: $-\lambda_g \delta T_g / \delta n = b_{gs}(T_g - T)$ Along the borehole there is a heat flow between it and the neighboring soil mass.
INITIAL CONDITIONS	Signorelli et al.	Wagner & Clauser	Marcotte & Pasquier	Al-Khoury et al.
	$T_i(z,0) = 12,4^{\circ}\text{C}$ Temperature gradient of 2,5 °C /100 m	$T_i(z,0) = 13,75^{\circ}\text{C}$ Applied to top, bottom and lateral bounds.	$T_p(z,0) = T(z,0)$ where $T(z,0)$ is the ground undisturbed temperature	$T_p(z,0) = T(z,0)$ (steady state condition)

Table 7 Boundary and initial conditions used in different models.

3.2 Choice of the simulator

Before starting the work on the simulation of our geothermal system, it is necessary to choose which one is the best software for our purposes. As we've seen before, different are the software used in this domain. Let's deepen a bit their characteristics.

SHEMAT (Simulator for HEat and MAss Transport, Clauser, 2003) is a general purpose reactive transport simulation code for a wide variety for thermal and hydrogeological problems, 2D or 3D. It does not include any package for entering directly BHE characteristics.

COMSOL Multiphysics is a finite element analysis, solver and Simulation software for various physics and engineering applications, especially coupled phenomena. In addition to conventional physics-based user-interfaces, COMSOL Multiphysics also allows for entering coupled systems of partial differential equations (PDEs). If you want to create a BHE model into this software, you have to create it by yourself: Prof. Pasquier and Marcotte (Marcotte, et al., 2008) developed a model of single BHE with a single U-tube, but it is suitable only with some versions of COMSOL. In any case it's a simple model, with one borehole, and it should have been implemented for creating different scenarios.

TOUGH2-MP (Transport Of Unsaturated Groundwater and Heat) is a massively parallel (MP) version of the TOUGH2 code (Pruess, et al., 1999), which is a three-dimensional numerical simulator for heat and fluid flow in geothermal systems. It is based on the integral finite difference method (IFDM) (Narasimhan, et al., 1976) and it uses the U-mesh program for creating the spatial discretization (Kim, et al., 2008). To take thermal and hydraulic processes related to the vertical closed-loop GHP system into account, three modules were developed and added to TOUGH2-MP (Kim, et al., 2010). With this integration, mesh and input files are suitable to simulate the vertical closed loop ground heat pump system.

FRACTure (Flow, Rock And Coupled Temperature effects) is a 3D Finite Element Program developed with the specific aim of studying the coupling of interactive mechanisms in geoscience and in particular those relevant to the long term behavior of a Hot Dry Rock reservoir (Kohl, et al., 1995). It is characterized by a flexible modular structure that lets us add further processes and elements to its library.

GEMS3D (General Elliptical Multi-block Solver in 3 Dimensions) is a simulator that applies the finite volume method to solve the partial differential equation for heat transfer on three-dimensional boundary fitted grids. Subdividing the solution domain into a finite number of small control volumes, and then integrating the partial differential equation to form an algebraic equation in terms of fluxes at the boundaries of the control volume allows the temperatures and heat fluxes to be calculated (He, et al., 2010).

TRNSYS (TRaNsient SYstem Simulation program) (Klein, 2010) is a transient system simulation program with a modular structure that was designed to solve complex energy system problems by breaking the problem down into a series of smaller. Its library includes the components commonly found in a geothermal system (ground heat exchanger, heat pump, circulation pump, etc) and the program allows to directly join the components implemented using other software (e.g. Matlab or Excel) (Magraner, et al., 2010). This program allows the simulation of all the system, principally the surface part (and all the connections with the building).

FEFLOW (Finite Element Flow simulator) has a specific part for modeling and simulating borehole heat exchangers: it includes both an analytical and a numerical model for BHE (Authors, 2010).

The analytical model is based on Eskilson and Claesson (Eskilson, et al., 1988) theory with significant extensions (generalized formulations for 2U, 1U, CXA and CXC type BHE, improved relationships for thermal resistances, effective coupling to 3D FE-discretization of porous matrices). The only restriction is that the steady-state conditions are *local* and appropriate for long-term predictions (robust and fast procedure).

The numerical model, instead, is based on Al-Khoury model (Al-Khoury, et al., 2005; Al-Khoury, et al., 2006), extended as well (generalized formulations for 2U, 1U, CXA and CXC type BHE, multiple grout points, improved relationships for thermal resistances, essentially non-iterative coupling method).

After comparing all the possible software, it has been chosen FEFLOW first of all because University of Bologna already had a previous version of it and a license, second because it has some features useful for our purposes:

- It has a 3D module that couples heat and mass transport, which is very important for us because we will face also coupled problem of heat transfer linked to groundwater flow
- It gives us the possibility of realizing as many layers as needed and of uploading punctual database information for each layer (thermal conductivity, thermal capacity, hydraulic conductivity, etc.)
- It gives us the possibility of putting different temperatures for each layer and therefore to express the vertical thermal gradient
- It has already implemented a module for BHE borehole heat exchangers, which relieves us from the problem of creating a model for BHE in all its characteristics. In this module we can in fact define all the figures characterizing a BHE: total heat input rate, coordinates of the borehole, computational method applied to BHE (analytical or numerical), type of BHE (1U, 2U, CXA, CXC), information about the borehole (diameter, pipe distance, pipe-in and pipe-out diameter, thickness and thermal conductivity), information about the refrigerant (flow discharge, volumetric heat capacity, thermal conductivity, dynamic viscosity, mass density), information about the grout (volumetric heat capacity, thermal conductivity). The biggest advantage of this module is that it will take care of all the modeling of the borehole, in the sense that we don't need to "design" the different part of the borehole in the model, neither to insert the refrigerant fluxes because everything is included in the module.

4. FEM: FINITE ELEMENT METHOD

The finite element method (FEM) is a numerical technique for finding approximate solutions of partial differential equations (PDE) as well as integral equations. The solution approach is based either on eliminating the differential equation completely (steady state problems), or rendering the PDE into an approximating system of ordinary differential equations, which are then numerically integrated using standard techniques such as Euler's method, Runge-Kutta, etc.

We consider here a model problem, elliptical and stationary defined on $\Omega \in \mathbb{R}^2$ which is a limited, open and connected dominium, and $\delta\Omega$ is the border divided into Γ^N e Γ^D .

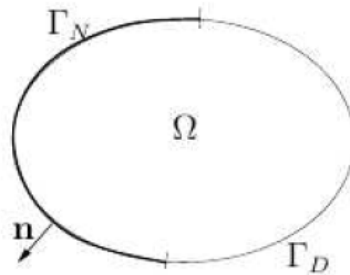


Figure 44 Dominium of our problem.

u is our variable and f is an assigned function. Initial conditions are the following:

$$\begin{cases} -\Delta u = f & \text{in } \Omega, \\ u = g & \text{on } \Gamma^D \text{ (Dirichlet condition)} \\ \frac{\partial u}{\partial n} = \psi & \text{on } \Gamma^N \text{ (Neumann condition)} \end{cases}$$

There are some hypotheses:

$$\begin{cases} f \in L^2(\Omega), \psi \in L^2(\Gamma^N) \text{ where } L^2(\Omega) = \{f: \Omega \rightarrow \mathbb{R}, \int_{\Omega} |f|^2 d\Omega < \infty\} \\ \Gamma^D \neq \emptyset \\ g \in H^{1/2}(\Gamma^D) \text{ }^2 \text{ where } H^1(\Omega) = \{f: \Omega \rightarrow \mathbb{R}, f \in L^2(\Omega) \text{ and } \delta f / \delta x_i \in L^2(\Omega), i = 1, 2\}. \end{cases}$$

If $\Gamma^D = \emptyset$ then f and ψ have to verify the compatibility condition: $\int_{\Omega} f d\Omega = - \int_{\delta\Omega} \psi d\gamma$. We will therefore have one solution, but non unique because it will depend on a constant. For having a unique solution Γ^D has to be different from \emptyset .

² H are Sobolev spaces, which means vector space of functions equipped with a norm that is a combination of L^p -norms of the function itself as well as its derivatives up to a given order. $H^{1/2}$ is the space of the traces of H^1 which is, instead, the space where solutions have to be found. The trace of a function $v \in H^1(\Omega)$ is given by the function $\mathbb{Q}_0: H^1(\Omega) \rightarrow L^2(\delta\Omega)$ such that $\mathbb{Q}_0(v) = v|_{\delta\Omega}$ (it is basically the function on the border). For more information about that see Mark Gockenback – “Understanding and implementing the finite element method”, SIAM 2006

In order to solve this problem $-\Delta u = f$, the integral is solved on the domain and multiplied per a test function (see Gauss Green theorem). After some simplifications this is the equation:

$$\int_{\Gamma_N} \nabla u \nabla v \, d\Omega = \int_{\Gamma_N} \psi v \, d\gamma + \int_{\Omega} f v \, d\Omega \quad \forall v \in V$$

Equation 31

Where $V = H^1_{\Gamma_D}(\Omega) = \{v \in H^1(\Omega) : v|_{\Gamma_D} = 0\}$ is the test function space and $V_g = \{v \in H^1(\Omega) : v|_{\Gamma_D} = g\}$ is the solutions space. The problem is not symmetric (solution space is different from the initial solution space) and it should be found a way to make it symmetric: it can be performed a change of variable and solve the problem as a “boundary value problem”. A function called R_g , that detects data on the borders, was defined as: $R_g \in H^1(\Omega)$ and $R_g|_{\Gamma_D} = g$. This is the function that let the problem become symmetric. We will define then $\bar{u} = u - R_g$, where $\bar{u}|_{\Gamma_D} = 0$ (therefore $\bar{u} \in H^1(\Omega)$) and $\nabla u = \nabla \bar{u} + \nabla R_g$. By substituting in the equation (a) we will obtain:

$$\int_{\Gamma_N} \nabla \bar{u} \nabla v \, d\Omega = \int_{\Gamma_N} \psi v \, d\gamma + \int_{\Omega} f v \, d\Omega + \int_{\Gamma_N} \nabla R_g \nabla v \, d\Omega \quad \forall v \in H^1_{\Gamma_D}(\Omega)$$

Equation 32

Moreover I can simplify the equation by introducing two functional³, $a: V \times V \rightarrow \mathbb{R}$ and $F: V \rightarrow \mathbb{R}$:

$$\begin{cases} a(u, v) = \int_{\Omega} \nabla u \nabla v \, d\Omega \\ F(v) = \int_{\Omega} f v \, d\Omega + \int_{\Gamma_N} \psi v \, d\gamma + \int_{\Gamma_N} \nabla R_g \nabla v \, d\Omega \end{cases}$$

and it results therefore that $a(u, v) = F(v)$.

There are a lot of problems in which we can apply this type of solution and different are the methods that can be used to solve it.

4.1 Galerkin Method

By using Galerkin’s method we can solve in a discrete way our integral problem into a domain of finite dimension (V_h is a finite space included in V and approximating it; its dimension is $N_h < \infty$): $a(u_h, v_h) = F(v_h) \quad \forall v_h \in V_h$.

As we are in a finite space, we can define the solution as a linear combination of bases and a new formulation of the problem is obtained: $Au = f$ which is a linear problem. A is the stiffness matrix, f is the vector of known values and u is the solution of our problem. If the problem is stationary we can reduce the integral form into a discrete one (with h as dimension of the discretization) and the solution will depend on the choice of the bases. Basically we want that for h tending to zero (the smaller the h the more continue is the space) discrete solution can approximate in a proper way continue solution.

Resuming, two are the most important choices to do in solving the problem in a discrete way:

1. How to choose the h (therefore how to discretize physically my domain)
2. How to choose the bases.

³ Functional is a function that takes a vector as its input argument, and returns a scalar.

The techniques for discretizing our domain are different: we can use a Delaunay triangulation or an advancing front technique. A triangulation has to respect some rules: intersection between triangles has to be only on a vertex or only on a side (conformity); triangles should not be too much squeezed (regularity).

Then the choice of the bases is important: we can choose our bases in a polynomial space of grade $r = 1, \dots, n$ and depending from the grade chosen we will have to solve them on different nodes on our discretization (the most common polynomial used is the Lagrangian type).

Once chosen the bases and the discretization, we can start solving our problem considering that there will be an approximation error depending on how fast the method is converging. Exact solution of the integral problem is $u \in V$, while u_h is the approximated finite element solution. In order to lower the error and increase the accuracy, we can refine our mesh (decreasing h values) or use a higher grade r of the polynomial space for the bases (in any case it should not be higher than the p of $H^p(\Omega)$).

The procedure to follow in solving one of these problems is the following:

- 1) Definition of the domain
- 2) Construction of the triangulation
- 3) Definition of boundary conditions
- 4) Assembling of A and f
- 5) Calculation of the solution of $Au = f$
- 6) Plotting the solution and calculation of errors.

5. FEFLOW MODEL OF THE BOREHOLE

The borehole heat exchanger can be modeled in two different ways in FEFLOW: analytical (Eskilson, et al., 1988) or numerical (Al-Khoury, et al., 2010).

5.1 Analytical solution of BHE

It is normally valid for local steady-state heat transport (it is therefore used not for short time analysis but for long term analysis of borehole functioning) and given temperature at borehole wall. The equations for local steady-state balance were developed by Eskilson and Claesson (Eskilson, et al., 1988) for fluid in pipe-in and in pipe-out:

$$-A^i \rho^r c^r u (\nabla_z T_{i1}) = \frac{T_{i1} - T_s}{R_1^\Delta} + \frac{T_{i1} - T_{o1}}{R_{12}^\Delta}$$

$$A^i \rho^r c^r u (\nabla_z T_{o1}) = \frac{T_{o1} - T_s}{R_2^\Delta} + \frac{T_{o1} - T_{i1}}{R_{12}^\Delta}$$

Equation 33

Where T_{i1} is the input temperature of the pipe, T_{o1} is the output temperature, T_s is the temperature at the borehole wall at steady state, A^i is the internal cross-sectional area of the pipe (pipe in and out have the same area), u is the refrigerant fluid velocity, c^r is the specific heat capacity of the refrigerant, ρ^r is the density of the refrigerant, R_1^Δ is the thermal resistance of pipe in, R_2^Δ is the thermal resistance of pipe out and R_{12}^Δ is the thermal resistance of both pipes considered as one single pipe.

The boundary conditions applied are:

$$T_{i1}(0,t) = T_i(t)$$

$$T_{i2}(L,t) = T_{oi}(L,t)$$

Equation 34

where $T_i(t)$ is the inlet temperature and $T_o(t)$ is the outlet temperature.

The couple of equations 24 can be solved by using Laplace transforms and we obtain:

$$T_{i1}(z,t) = T_{i1}(0,t)f_1(z) + T_{o1}(0,t)f_2(z) + \int_0^z T_s(\xi,t) f_4(z-\xi) d\xi$$

$$T_{o1}(z,t) = -T_{i1}(0,t)f_2(z) + T_{o1}(0,t)f_3(z) - \int_0^z T_s(\xi,t) f_5(z-\xi) d\xi$$

Equation 35

Valid for $0 \leq z \leq \bar{L}$.

The functions f_1, \dots, f_5 are given by the following expressions:

$$f_1(z) = e^{\beta z} (\cosh \gamma z - \delta \sinh \gamma z)$$

$$f_2(z) = e^{\beta z} \frac{\beta_{12}}{\gamma} \delta \sinh \gamma z$$

$$f_3(z) = e^{\beta z} (\cosh \gamma z + \delta \sinh \gamma z)$$

$$f_4(z) = e^{\beta z} \left[\beta_1 \cosh \gamma z - \left(\delta \beta_1 + \frac{\beta_2 \beta_{12}}{\gamma} \right) \sinh \gamma z \right]$$

$$f_5(z) = e^{\beta z} \left[\beta_2 \cosh \gamma z - \left(\delta \beta_2 + \frac{\beta_1 \beta_{12}}{\gamma} \right) \sinh \gamma z \right]$$

Equation 36

where:

$$\beta_1 = \frac{1}{R_1^\Delta A^i \rho^r c^r u} \quad \beta_2 = \frac{1}{R_2^\Delta A^i \rho^r c^r u} \quad \beta_{12} = \frac{1}{R_{12}^\Delta A^i \rho^r c^r u} \quad \beta = \frac{\beta_2 - \beta_1}{2}$$

$$\gamma = \sqrt{\frac{(\beta_1 + \beta_2)^2}{4} + \beta_{12}(\beta_1 + \beta_2)} \quad \delta = \frac{1}{\gamma} \left(\beta_{12} + \frac{\beta_1 + \beta_2}{2} \right)$$

Equation 37

As far as our simulation are all run on single or double U tubes, just the formulation relates to these cases are shown.

It is assumed that the pipes are arranged symmetrically in the borehole so that it results:

$$R_2^\Delta = R_1^\Delta$$

Equation 38

This leads us to a lot of simplifications:

$$\beta_2 = \beta_1 = \frac{1}{R_1^\Delta A^i \rho^r c^r u} \quad \beta_{12} = \frac{1}{R_{12}^\Delta A^i \rho^r c^r u} \quad \beta = 0$$

$$\gamma = \sqrt{\beta_1^2 + 2\beta_{12}\beta_1} \quad \delta = \frac{1}{\gamma} (\beta_{12} + \beta_1)$$

Equation 39

And therefore:

$$f_1(z) = \cosh \gamma z - \delta \sinh \gamma z \quad f_2(z) = \frac{\beta_{12}}{\gamma} \delta \sinh \gamma z$$

$$f_3(z) = \cosh \gamma z + \delta \sinh \gamma z \quad f_4(z) = \beta_1 \cosh \gamma z - \left(\delta \beta_1 + \frac{\beta_2 \beta_{12}}{\gamma} \right) \sinh \gamma z$$

$$f_5(z) = \beta_2 \cosh \gamma z - \left(\delta \beta_2 + \frac{\beta_1 \beta_{12}}{\gamma} \right) \sinh \gamma z$$

Equation 40

Using all these simplifications, we can solve the equations and obtain the outlet temperature $T_o(t)$:

$$T_o(t) = T_i(t) \frac{f_1(\bar{L}) + f_2(\bar{L})}{f_3(\bar{L}) - f_2(\bar{L})} + \int_0^{\bar{L}} \frac{T_s(\xi, t)[f_4(\bar{L} - \xi) - f_5(\bar{L} - \xi)]}{f_3(\bar{L}) - f_2(\bar{L})} d\xi$$

Equation 41

Knowing the inlet temperature through the boundary conditions and the outlet temperature from the previous equation, the temperature distribution T_{i1} and T_{o1} as a function of z and t are obtained after solving the integrals in eq. 34:

$$T_{i1} = T_i(t)f_1(z) + T_o(t)f_2(z) + \int_0^z T_s(\xi, t)f_4(z - \xi)d\xi$$

$$T_{o1} = -T_i(t)f_2(z) + T_o(t)f_3(z) - \int_0^z T_s(\xi, t)f_5(z - \xi)d\xi$$

Equation 42

The integrals are then performed elementwise, where the solid temperature T_s at the borehole wall is numerically approximated as a linear function from the nodal finite element solution at time t .

The temperature for the grout zones for 1U configuration are:

$$T_{g1}(z, t) = \frac{\left[\frac{T_s(z, t)}{R_{gs}^{1U}} + \frac{T_{o1}(z, t)}{R_{fig}^{1U}} + \left(\frac{T_s(z, t)}{R_{gs}^{1U}} + \frac{T_{i1}(z, t)}{R_{fig}^{1U}} \right) u_1 R_{gg}^{1U} \right] R_{gg}^{1U}}{(R_{gg}^{1U})^2 u_1^2 - 1}$$

$$T_{g2}(z, t) = \left(\frac{T_{g1}(z, t)}{R_{gg}^{1U}} + \frac{T_{o1}(z, t)}{R_{fig}^{1U}} + \frac{T_s(z, t)}{R_{gs}^{1U}} \right) \frac{1}{u_1}$$

Equation 43

Where $u_1 = \frac{1}{R_{gs}^{1U}} + \frac{1}{R_{fig}^{1U}} + \frac{1}{R_{gg}^{1U}}$, R_{gg}^{1U} and R_{gs}^{1U} are thermal resistances due to intern grout exchange and due to grout-soil exchange, while R_{fig}^{1U} is the following:

$$R_{fig}^{1U} = R_{adv}^{1U} + R_{cond a}^{1U} + R_{cond b}^{1U}$$

where R_{adv}^{1U} is the thermal resistance due to the advective flow of the refrigerant, $R_{cond a}^{1U}$ is the thermal resistance due to the pipes wall material and $R_{cond b}^{1U}$ is the thermal resistance due to the grout transition.

For the 2U configuration it gives:

$$T_{g1}(z, t) = T_{g2}(z, t) = \frac{\left[\frac{2T_s(z, t)}{R_{gs}^{2U}} + \frac{2T_{o1}(z, t)}{R_{fig}^{2U}} + \left(\frac{2T_s(z, t)}{R_{gs}^{2U}} + \frac{2T_{i1}(z, t)}{R_{fig}^{2U}} \right) u_2 v \right] v}{v^2 u_2^2 - 1}$$

$$T_{g3}(z, t) = T_{g4}(z, t) = \left(\frac{T_{g1}(z, t)}{v} + \frac{2T_{o1}(z, t)}{R_{fig}^{2U}} + \frac{2T_s(z, t)}{R_{gs}^{2U}} \right) \frac{1}{u_2}$$

Equation 44

With:

$$R_1^\Delta \equiv R_{fig}^{1U} + R_{gs}^{1U}$$

$$u_2 = \frac{2}{R_{fig}^{2U}} + \frac{2}{R_{gs}^{2U}} + \frac{1}{v}$$

$$v = \frac{R_{gg1}^{2U} R_{gg2}^{2U}}{2(R_{gg1}^{2U} + R_{gg2}^{2U})}$$

$$R_{12}^\Delta = \frac{(u_1 R_{fig}^{1U} R_{gg}^{1U})^2 - (R_{fig}^{1U})^2}{R_{gg}^{1U}}$$

Equation 45

Thermal resistances are given for 2U pipes:

$$R_1^\Delta = \frac{R_{fig}^{2U} + R_{gs}^{2U}}{2}$$

$$R_{12}^\Delta = \frac{(R_{fig}^{2U})^2}{4} \left(u_2^2 v - \frac{1}{v} \right)$$

Equation 46

The matrix that has to be solved is the following one:

$$([A_s^*] + [R_{BHE}]) \cdot \{T_s\}^{n+1} = \{B_s\}^{n+1} + \{B_{BHE}(T_s^{n+1})\}$$

Equation 47

Where

$$R_{BHE} = \int_z \left(\frac{1}{R_1^\Delta} + \frac{1}{R_2^\Delta} \right) dz l$$

And

$$B_{BHE}(T_s^{n+1}) = \int_z \left(\frac{T_{i1}^{n+1}}{R_1^\Delta} + \frac{T_{o1}^{n+1}}{R_2^\Delta} \right) dz$$

The matrix system is solved through an iterative procedure according to:

$$\text{Starting solution } \tau = 0 \quad ([A_s^*] + [R_{BHE}]) \cdot \{T_s\}^{n+1} = \{B_s\}^{n+1} + \{B_{BHE}(T_s^n)\}$$

$$\text{Iteration } \tau + 1 \quad ([A_s^*] + [R_{BHE}]) \cdot \{T_s\}^{(n+1),(\tau+1)} = \{B_s\}^{n+1} + \{B_{BHE}(T_s^{(n+1),\tau})\}$$

Equation 48

which is stopped when a satisfactory convergence is achieved.

The analytical model shows better responses if used in a long term simulation (1 year simulations) while for short term conditions it's better to use the numerical solution.

5.2 Numerical solution of BHE

In FEFLOW each borehole is discretized by a number of K nodes; Cauchy boundary conditions require the solution of the grout temperatures T_{gi} ($i = 1, \dots, G$) at the K nodes, which is obtained by solving the local matrix system.

For the soil temperatures $T_s^{n+1} = T_s(t^{n+1})$ the matrix to solve is the following one:

$$[A_s] \cdot \{T_s\}^{n+1} = \{B_s\}^{n+1} - \sum_{i=1}^G [R_s] \cdot \{T_{gi}\}^{n+1}$$

Equation 49

With $[A_s] = [A_s^*] - G[R_s]$ where $[A_s^*]$ is the soil matrix without the soil-grout transfer condition.

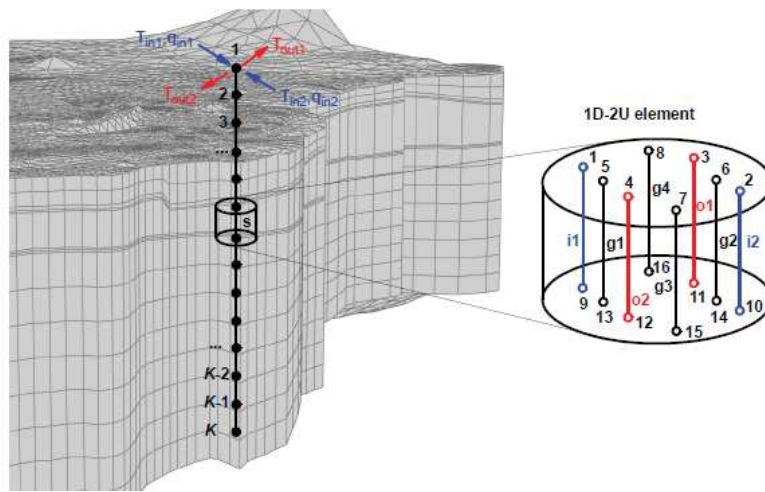


Figure 45 Discretized 2U exchanger borehole.

We can express the matrix in a compact way:

$$\begin{bmatrix} A_{pipe} & R_{ps} \\ R_{ps}^T & A_s \end{bmatrix} \cdot \begin{Bmatrix} T_{pipe} \\ T_s \end{Bmatrix}^{n+1} = \begin{Bmatrix} B_{pipe} \\ B_s \end{Bmatrix}^{n+1}$$

Equation 50

For the solution of the system it has to be applied a static condensation strategy (it lets us obtain an exact solution), where the internal pipe variables T_{pipe}^{n+1} can be eliminated from the matrix system. The reduced system is therefore:

$$(A_s - A_{ps}) \cdot T_s^{n+1} = B_s^{n+1} - B_{ps}^{n+1}$$

$$A_{ps} = R_{ps}^T \cdot (A_{pipe}^{-1} \cdot R_{ps})$$

$$B_{ps}^{n+1} = R_{ps}^T \cdot (A_{pipe}^{-1} \cdot B_{pipe}^{n+1})$$

Equation 51

for solving only the soil temperature T_s^{n+1} at the new time stage $n+1$. The modified matrix $(A_s - A_{ps}) = (A_s^* - GR_s - A_{ps})$ represents the *Schur complement*.

A_{pipe}^{-1} can be easily computed by a direct Gaussian matrix solution for each pipe.

As far as the system is particularly stiff and can lead to roundoff errors, the matrix system is combined with an iterative correction strategy:

Starting solution $\tau = 0$: $(A_s - A_{ps}) \cdot T_s^{(n+1),\tau} = B_s^{n+1} - B_{ps}^{n+1}$

$$T_{pipe}^{(n+1),\tau} = A_{pipe}^{-1} \cdot (B_{pipe}^{n+1} - R_{ps} \cdot T_s^{(n+1),\tau})$$

Iterative correction $\tau+1$: $(A_s^* - GR_s) \cdot T_s^{(n+1),(\tau+1)} = B_s^{n+1} - B_{ps}^{n+1}$

$$T_{pipe}^{(n+1),(\tau+1)} = A_{pipe}^{-1} \cdot (B_{pipe}^{n+1} - R_{ps} \cdot T_s^{(n+1),(\tau+1)})$$

Equation 52

where τ corresponds to an iteration counter. At each time level we start with the Schur complement solution⁴. It results the soil temperature $T_s^{(n+1),\tau}$ and the pipe temperature $T_{pipe}^{(n+1),\tau}$ at initial state $\tau=0$. With known $T_{pipe}^{(n+1),\tau}$ the global soil matrix system is solved to find the new iterate for temperatures of soil $T_s^{(n+1),(\tau+1)}$ and accordingly of pipe $T_{pipe}^{(n+1),(\tau+1)}$. The iteration τ (see 1-151) is repeated until a satisfactory convergence is achieved.

It is important for the numerical solution to be careful while realizing the mesh: it is, as a matter of fact, compulsory to create the mesh close to the BHE (which is treated as a 1D element) with a particular distance from it. The minimum distance from BHE and the nodes in the vicinity is $\Delta = a \cdot r_b$ where a is 4.81 if we have 4 nodes near the BHE, 6.13 if the nodes are 6 and 6.66 if the nodes are 8.

There are indeed some differences between original Al-Khoury model and its implementation on FEFLOW. Namely (Diersch, et al., 2010):

- Integrating the 1D BHE pipe element into FEFLOW's finite element matrix system similar to fracture elements
- Generalization of the formulations for single and double U-shape as well as coaxial pipe configuration
- Direct and non-sequential (non-iterative) coupling of the 1D pipe elements to the porous medium discretization
- Extending FEFLOW's boundary conditions for BHE pipes similar to multi-well borehole conditions.

⁴ In numerical analysis, the Schur complement method is the basic and the earliest version of non-overlapping domain decomposition method, also called iterative sub structuring. A finite element problem is split into non-overlapping subdomains, and the unknowns in the interiors of the subdomains are eliminated. The remaining Schur complement system on the unknowns associated with subdomain interfaces is solved by the conjugate gradient method.

5.3 Upscaling of underground properties

For any numerical calculation, porous media representation passes through a spatial discretization of the domain to describe. Medium properties are defined on every elementary volume of this spatial discretization, whose name is support (it has to be of a dimension equal or bigger than REV Representative Elementary Volume). When characterizing geologically and geostatistically our domain, we have data on a small and regular support (typically centimeters to meters); when we are simulating dynamically our system, instead, we are using a spatial discretization with a bigger dimension (tens to hundreds meters) (Wen, et al., 1996). So basically the support used in dynamic simulations is different from the one used in geostatistical simulations: the operation of deriving porous media properties for the bigger scale from the lower one is called scale changing or upscaling (De Lucia, 2008).

Upscaling method depends on the type of variable we are considering: if it is a summable variable (porosity, mineral volume), upscaled value is the arithmetical mean of the small scale values; if it is not summable, as the permeability is, the problem is more complicated and the upscaled value is not the simple arithmetical mean.

One of the most used algorithms for the upscaling is the *Simplified Renormalization* proposed for rectangular uniform grids, 2D or 3D, with variable tensor diagonal (anisotropy axes are directed as grid axes).

This method groups iteratively two by two adjacent cells, interchanging at every pace the direction chosen for averaging (alternating, therefore, arithmetic mean, done in parallel, and harmonic mean, done in series among the flux). This technique is reiterated until the moment we obtain a single value for the expected dimension of the grid. In the end, I will obtain 2 extremes values' from which I will get tensor values of k through specific formulas. These two values constitute two of the components of equivalent k tensor:

$$K_b = \begin{pmatrix} K_{rs}^{xx} & 0 \\ 0 & K_{rs}^{yy} \end{pmatrix} \quad (\text{from scalar values of permeability we obtain a vector}).$$

The main disadvantage of this method is its dependence on the direction of flow.

5.3.1 FEFLOW and data interpolation: Akima interpolation

The Akima interpolation is a mathematical method for interpolation from a given set of data points in a plane and for fitting a smooth curve to the points (Akima, 1970). It is a continuously differentiable sub-spline interpolation, built from piecewise third order polynomials. Only data from the next neighbor points are used to determine the coefficients of the interpolation polynomial. There is no need to solve large equation systems and therefore this interpolation method is computationally very efficient. For a set of data points

$$s_i = s(x_i), \quad 1 \leq i \leq k$$

Equation 53

the interpolation function is defined as

$$s(x) = a_0 + a_1 \cdot (x - x_i) + a_2 \cdot (x - x_i)^2 + a_3 \cdot (x - x_i)^3, \quad x_i \leq x \leq x_{i+1}$$

Equation 54

To determine the coefficients a_0 , a_1 , a_2 , and a_3 of the interpolation polynomial for each interval $[x_i, x_{i+1}]$ the function values s_i and s_{i+1} , and the first derivatives s_i' and s_{i+1}' at the end points of the interval are used.

The first derivative s_i' of the interpolation function at x_i is estimated from the data for this point and the next two points on each side of x_i . Using the ratios

$$d_j = \frac{s_{j+1} - s_j}{x_{j+1} - x_j} \quad j = i - 2, i - 1, i, i + 1$$

Equation 55

and the weighting coefficients

$$w_{i-1} = |d_{i+1} - d_i|, \quad w_i = |d_{i-1} - d_{i-2}|, \quad \dots$$

Equation 56

the estimated derivative s_i' is defined as

$$s_i' = \frac{w_{i-1}d_{i-1} + w_i d_i}{w_{i-1} + w_i}$$

Equation 57

Several special cases for s_i' have to be considered.

$$\begin{array}{ll} s_i' & = d_{i-1} & d_{i-2} = d_{i-1}, d_i \neq d_{i+1} \\ s_i' & = d_i & d_i = d_{i+1}, d_{i-2} \neq d_{i-1} \\ s_i' & = d_{i-1} = d_i & d_{i-1} = d_i \\ s_i' & = (d_{i-1} + d_i)/2 & d_{i-2} = d_{i-1} \neq d_i = d_{i+1} \end{array}$$

Equation 58

To be able to use (Eq.15) for calculating the derivatives s_1' , s_2' , s_{k-1}' , and s_k' additional ratios d_{-1} , d_0 , d_k , and d_{k+1} have to be estimated.

$$d_{-1} = 2 \cdot d_0 - d_1 \quad ; \quad d_0 = 2 \cdot d_1 - d_2 \quad ; \quad d_k = 2 \cdot d_{k-1} - d_{k-2} \quad ; \quad d_{k+1} = 2 \cdot d_k - d_{k-1}$$

Equation 59

The order of the interpolation function reduces to 2 for these intervals.

Similar algorithms can be used for the interpolation of two-dimensional data on rectangular grids and on unstructured grids by bicubic and cubic polynomials, respectively.

6. BOREHOLE HEAT EXCHANGER SYNTHETIC COMPUTATIONAL MODEL

Once chosen the simulator to use, we have to set our computational model. First of all boundary and initial conditions have been chosen.

Concerning the boundary conditions we applied:

- Dirichlet condition $T_i(0, t) = \text{cost}$ for which the temperature at the bottom and on the borders is the same as the initial ground temperature;
- No water flow entering or exiting from our domain
- Neumann condition $-\lambda_g \cdot \delta T_g / \delta n = b_{gs}(T_g - T)$: along the borehole there is a heat flow between it and the neighboring soil mass.

Concerning the initial conditions, these are the choices we made:

- $T_i(z, 0)$ = temperature of undisturbed ground, applied to top, bottom and lateral bounds
- Groundwater flow equal to 0 at sea level.

The area involved in the simulation is different varying the case study; we can have a different number of BHE and therefore the dimension of the area changes.

Our first case study was a synthetic one composed of 6 boreholes distributed on an area of 60 m x 60 m on the plane and 125 m depth. The length of the borehole is 100 m and the power injected is the same in every borehole and equal to $4.2 \cdot 10^8$ J/d.

Basically the synthetic procedure that has been developed is organized as follows:

1. Using thermal conductivity data of a fictitious borehole (see fig. 39 a)) and its statistical parameters, we simulate our conductivities on a field of 60 m x 60 m x 120 m (we will use direct simulations)
2. We extract n boreholes (n can be a number bigger than 2, in this case we have 6 boreholes) which from now on we will consider as real ones (as if we were obtaining their thermal conductivities from in situ measurements).

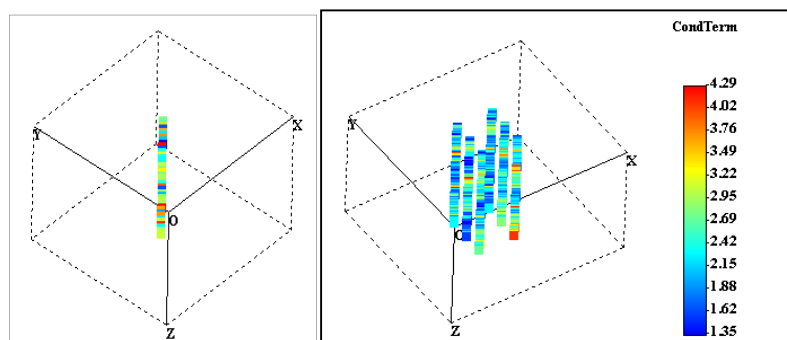


Figure 46 a) Fictitious borehole b) n boreholes extracted from the simulation.

3. We feed our dynamic simulator (FEFLOW) with this “real” data from our n boreholes and with the “real” lithology of the field. For each borehole we obtain a response, which is an evolution of temperature along time (and an evolution of temperature along the length of the borehole for both the circulating fluid and the cement).

-
4. From the same simulation of which at 1) we extract n different boreholes in other locations. Exploiting these data we build up different realizations of thermal conductivity with the same characteristics as the first n boreholes
 5. Now we feed FEFLOW with these different realizations of thermal conductivity, but imposing the locations of boreholes as the real ones (see point 2). We will obtain a response for each borehole and for each realization.
 6. We compare these responses with the real ones and we select best responses according an objective function and compose a secondary image for the next step of the iterative process (co-simulation process).
 7. We repeat the process from the beginning until we reach a robust congruence between real and simulated curve.

Concerning the objective function, we are going to make a comparison between two curves: the real curve of temperature evolution and the simulated one. We have to choose the best minimization function in order not to have errors in the evaluation of the simulations. We first tried the χ^2 test in order to evaluate the efficiency of our simulations.

6.1 Results from few synthetic models

The first case study run was a simple one, same geology in all the domain (sandstone) divided into 20 layers created through a geostatistical simulation. Simulated area was, as written above, $60 \times 60 \times 125 \text{ m}^3$, the borehole was reaching 100 meters of depth and the power injected was equal to $4.2 \cdot 10^8 \text{ J/g}$. Boundary and initial conditions are the one explained in the previous paragraph.

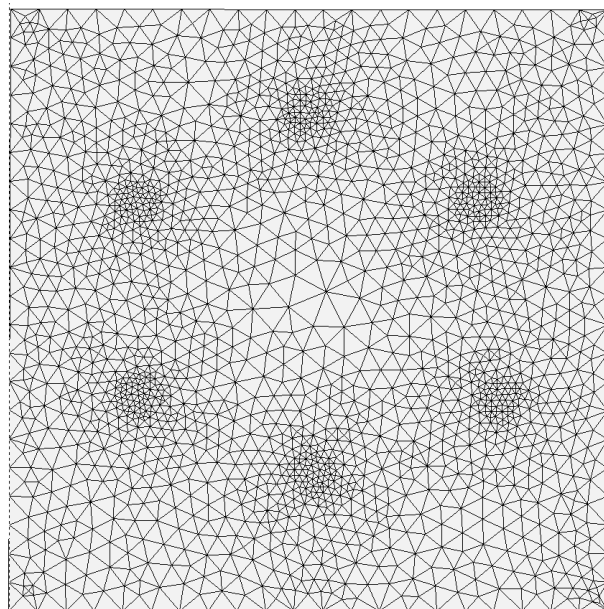


Figure 47 Mesh used in the synthetic case: refined mesh near the six boreholes.

The mesh that has been used is refined near the boreholes, while it much coarser far from them; it was realized by using the Delaunay triangulation. Vertically, there are 11 layers, the first 10 are 10 meters thick each while the last one has a thickness of 25 meters; they are all made by sandstone.

50 simulations were run as a first step, all using the numerical option and all for the same time as a Thermal Response Test (around 3 days). There was indeed something clear right after the first simulations: the curve was increasing slightly rapid after the first calculation step (jumping directly from the ground temperature to the reference one) and the differences between the curves obtained and between them and the real one were almost not visible (same trend, almost the same temperature values along time).

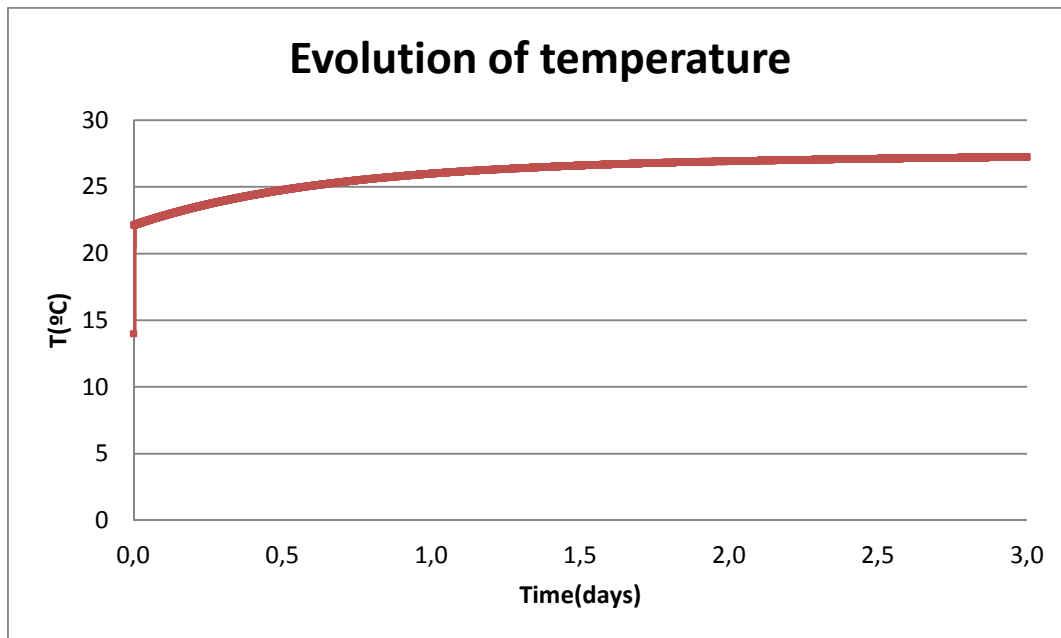


Figure 48 Evolution of outlet temperature of one of the six boreholes, subjected to the constant rate of injection of $4.2 \cdot 10^8$ J/d for 3 days.

We applied the inverse problem to this case and it was very simple to reach the minimum of our minimization function because the responses of the terrain were very similar from case to case.

In order to complicate a bit the conditions and add a source of variability, we decided to put at least different materials in the layers:

- 1) 3 layers of sandstone
- 2) 6 layers of limestone
- 3) 3 layers of dry clay
- 4) 5 layers of sandstone
- 5) 2 layers of dry clay.

But also in this case the results are similar to the other one and we reach easily after the first step the minimum of our minimization function.

7. RECONSTRUCTION OF A REAL TRT WITH THE NUMERICAL MODEL OF FEFLOW

7.1 Reconstruction of a TRT by using FEFLOW model for BHE

It was realized a FEFLOW model of a real case of TRT run in Montegridolfo, a place in Emilia Romagna region, not far from Rimini. Test has been realized on a 100 m length well, with a 0,127 m diameter and an external collector diameter of 0,032 m. Collectors disposition is a double-U.

First it was run a test for verifying the undisturbed ground temperature, that was 14,6°C. After, a real thermal response test has been run: average input temperature is 30.82°C while the average output one is 27.2°C. As a reference temperature for the heat pump we can consider 30°C and an average power of 6000 W (that implies 1500 l/h of circulating water).

From the stratigraphic point of view, this is the series:

- 0 – 1,5 m dry clay with a thermal capacity of 1,6 MJ/m³K
- 1,5-100 m marl with a thermal capacity of 2,25 MJ/m³K (there are some small infiltrations of water between 60 and 65 m of depth).

Concerning FEFLOW model, it has been chosen an area of 60 m x 60 m and a depth of 110 m. Two different models were implemented, one with 11 layers on the vertical and the other with 6 layers. In both cases, for each layer it has been inserted the corresponding volumetric thermal capacity and a file of thermal conductivities geostatistically simulated. Actually I assumed that all the soil was marl with an average thermal conductivity of 1.7 W/m·K, neglecting the 1,5 m of clay.

Soil temperature was calculated following Al-Khoury suggestions: first bottom and top of the model were set to 14,6°C, as the undisturbed ground temperature. Then it was run another simulation with the average outside temperature above 1 year (12,5 °C), in order to obtain the real gradient of temperature in the first 10-15 meters of ground. There is no groundwater. Borehole heat exchanger is located in the middle of the considered volume and the injected power is variable.

Concerning the BHE, we needed to enter also grout's characteristics that in this case are the one of a bentonitic mortar:

Density (kg/m ³)	Thermal conductivity (W/m·K)	Thermal resistance (m ² ·K/W)	Volumetric thermal capacity (J/m ³ ·K)
1420	0,347-0,386	0,018-0,02	1,704·10 ⁶

Table 8 Grout characteristics

Resolution method of geothermal exchange equations was chosen alternatively as analytical or numerical. Choice of reference temperature was varied as a function of average temperature curve obtained post simulation, in order to calibrate our model on the real response.

Different were the cases simulated: in the following table there is a resume of the characteristics.

	Reference temperature (°C)	Ground temperature (°C)	Injected power	Type of solution
Simulation 1	30	Cost	Cost	Analytical
Simulation 2	28	Cost	Cost	Analytical
Simulation 3	28	Cost	Cost	Numerical
Simulation 4	28	Cost	Var	Numerical
Simulation 5	30	Cost	Var	Numerical
Simulation 6	29	Cost	Var	Numerical
Simulation 7	29	Var	Var	Numerical
Simulation 8	27.5	Cost	Var	Numerical
Simulation 9	30	Cost	Var	Analytical

Table 9 Simulation characteristics

The results of the simulations compared to real case (dark purple) are shown in the following graph.

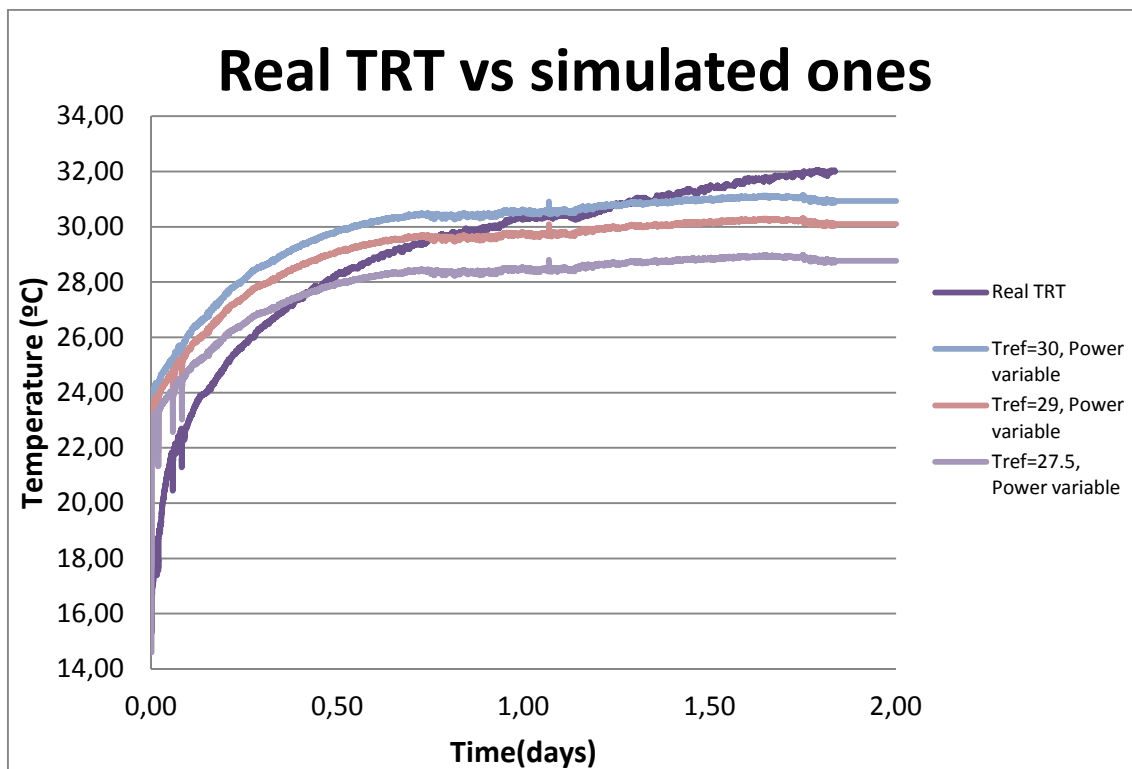


Figure 49 Real thermal response test results compared with the simulated ones.

As it is visible from this graph, simulated temperature reach faster stationarity than real temperatures (see the purple curve which is the one measured in a real BHE). For this reason I think it is necessary to impose another condition relating to the stationarity in the flux simulator.

The part of the curve that never fits the real one is the initial part, independently from the resolution scheme and from the cement conductivity (in the articles I found the numerical model didn't run well with cement conductivity values lower than 1 W/mK).

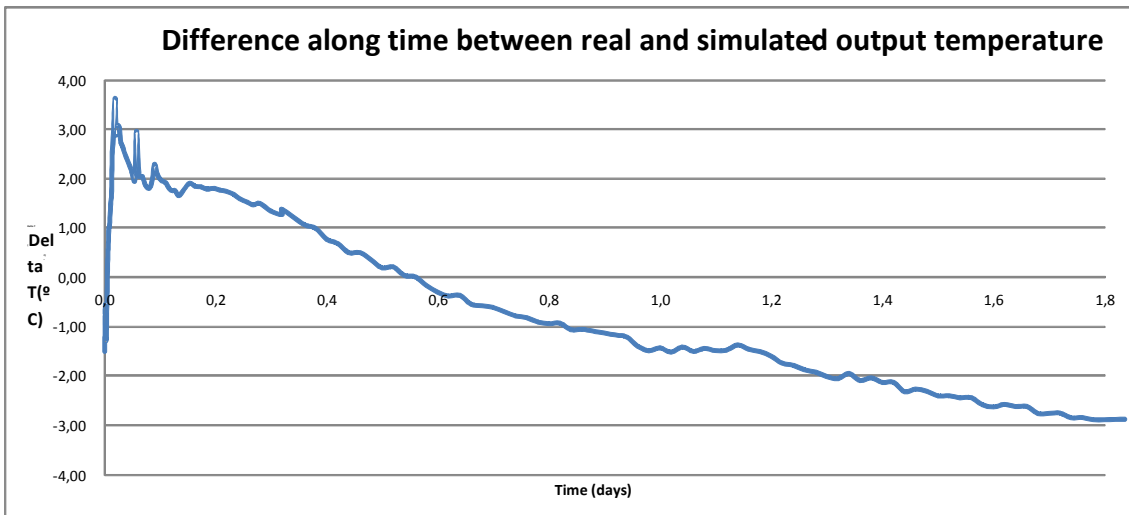


Figure 50 Evolution of the difference of temperature between simulated and real thermal response test results.

In Fig.48 are represented the differences between TRT real curve and one of the simulated: as it is visible from the graph, the initial difference is higher because the simulated curve sketches immediately to steady state, while the real one keeps lower values increasing more slowly and reaching after steady state.

After these first simulations, we started working joint with Prof. Rafid Al-Khoury from Delft University, who is the main developer of the numerical model of BHE implemented in FEFLOW. Several were the analysis we run on FEFLOW simulations and various were the changing that we applied to the way of simulating. In the following paragraph we will go through this analysis.

7.2 Is it possible to have a consistent reproduction of reality by using the numerical model implemented on FEFLOW?

First of all it was necessary to recreate a mesh for our simulation, a coarser one in order to get results faster than with a fine mesh. Moreover, this particular numerical model, in fact, has the advantage of not having convergence problem even if working with coarse mesh and in this way the resolution is much faster. As it was described in Al Khoury's article (Al-Khoury, et al., 2010), numerical model implemented in FEFLOW is better performing when the grid is coarser and the results are not differing from the results obtained with a finer grid. Therefore it has been implemented a coarser grid with around 1000 blocks totally (1500 nodes) and 11 layers on the vertical axe.

With this expedient, we will manage to run a much higher number of simulations and therefore to compare much more results in order to get an idea of the reason of such differences between the output of the numerical model on FEFLOW and the real evolution of output temperature.

This was the mesh used now on for the simulations:

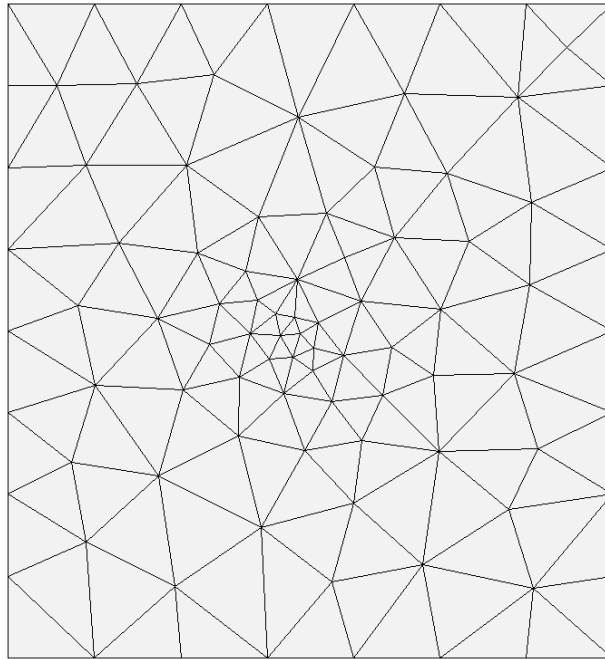


Figure 51 Coarse mesh used for the model.

Then, it was followed the procedure explained in Al Khoury article (Al-Khoury, et al., 2010) in order to simulate the initial conditions of the investigated volume, as far as it's not available a measure of temperature along the borehole, but just an average temperature of the soil. As a first phase it was put as a boundary condition to have undisturbed ground temperature (in this case 14.6°C) both at top and bottom of our system and the simulation was run for one year with time step 1 day. Then it was run a transient condition starting from the condition simulated in the first phase. In this case the bottom was kept at the undisturbed ground temperature, while the top was set as the average air temperature all over the year (12°C). In this way it was reproduced the real condition of the first 10-15 meters of soil that are normally influenced by air temperature. In fact it was verified that the influenced depth corresponds to about 15 meters (see fig...).

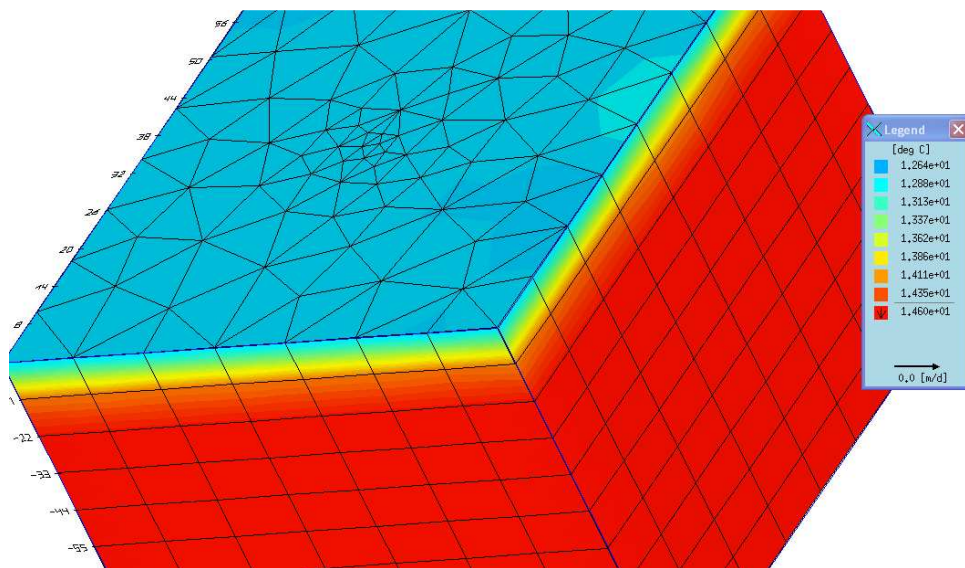


Figure 52 Temperature on the investigated volume.

Now initial conditions are defined and we can run a simulation of the BHE: as thermal conductivity it was used the same one obtained through geostatistical simulations even if on a finer grid, FEFLOW will apply Akima interpolation in order to upscale the conductivity on the grid. The borehole was put in the central part of the grid; it was a double U tube with a variable injected power (input on time varying function). Characteristics of the borehole heat exchanger are summarized in the next table.

	Simulation 1	Simulation 2	Simulation 3	Simulation 4
Power	Variable	Variable	Variable	Variable
Depth of the BHE	100	100	100	100
Reference temperature T_0 (°C)	29	29	28	28
Grout thermal conductivity (W/K m)	0.35	0.35	0.8	0.8
Grout volumetric heat capacity (10^6 MJ/K m)	1.7	1.7	2.3	2.3
Flow rate (m^3/day)	36	36	36	36
Refrigerant dynamic viscosity (10^{-3} kg/m s)	0.52	0.52	0.52	5.2
Number of time steps	900	9000	9000	9000
Time step (day)	0.0028	0.00028	0.00028	0.00028

Table 10 Parameters set per each different simulations run.

Concerning the time step, even using more steps with a smaller dimension, the results are the same; therefore for the next simulation it can be kept a time step of 0.0028 days as far as the differences in the results are negligible, while the difference in the computational time are high (to run a simulation with 900 steps it takes less than 3 minutes, while for a 9000 steps it takes up to 30 minutes).

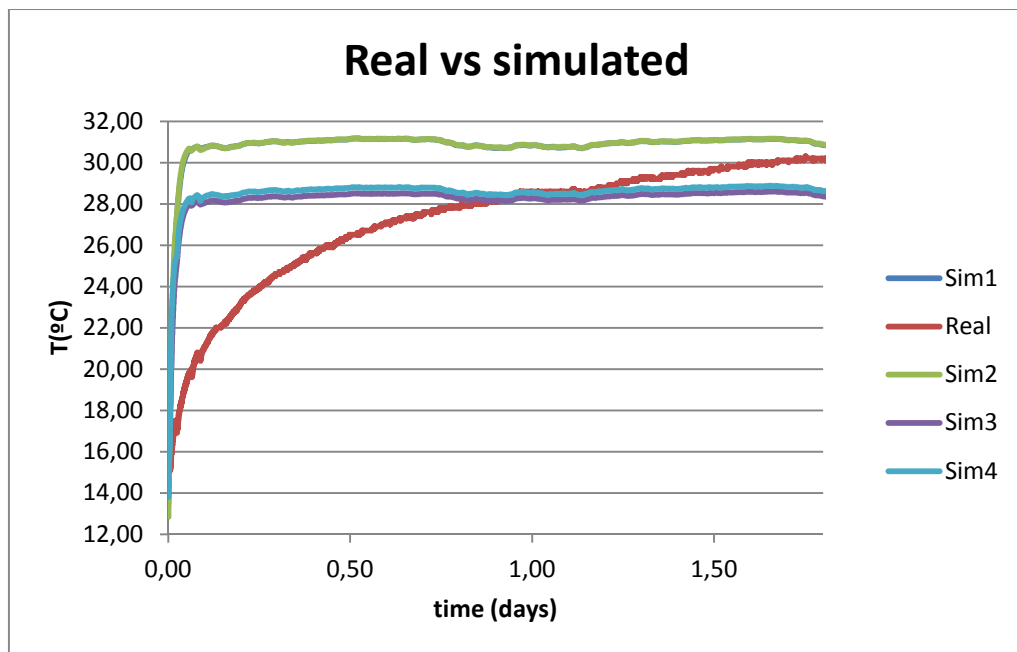


Figure 53 Comparison between the real outlet temperature and the simulated ones.

As it is clear from the results, nothing has changed in the long term simulation. Still our simulated values seem to follow a steady state condition. (Sim 2 is superposed to Sim 1, even changing the number of time steps the results are the same).

The main difference between the couples of curves (sim1-2 vs sim 3-4) is the reference temperature T_0 which corresponds to the following:

$$T_{in} = P / (c_g * q) + T_0$$

Equation 60

Where P is the heat input rate, c_g is the volumetric heat capacity and q is the refrigerant flow discharge.

The main problem seems to be the reference temperature: in fact this formulation

$$T_{in} = P / (c_g * q) + T_0$$

Equation 61

has to be used just for the first time step. Therefore reference temperature corresponds to the inlet temperature at $t=0$. Then, for all the successive steps, another formulation has to be used:

$$T_{in} = P / (c_g * q) + T_{out}$$

Equation 62

where T_{out} changes at every temporal step.

As far as the curve was reaching a stationary condition really fast, we realized that probably there was also a problem in coupling power values to the BHE. In fact, BHE as it is implemented in FEFLOW assumes that the refrigerant enters the inlet pipe at a certain temperature. The refrigerant then flows down the inlet pipe, and up again through the outlet pipe. On its way it exchanges heat with the grout material (which again exchanges heat with the porous medium), therefore the temperature changes with depth. This temperature change can be seen in the temperature profile diagram during the simulation run. Finally, the refrigerant leaves the outlet pipe at a certain temperature. This outlet-temperature is not coupled to inlet-temperature unless we use a specific plug-in: BHE loop.

After each time-step, the plug-in gets the outlet-temperature, adds a certain temperature difference, and applies it as a new inlet temperature of the BHE. This inlet temperature is defined through the heat input rate: the heat input rate Q_h calculates by the refrigerants flow discharge Q_f , the volumetric heat capacity of the refrigerant c , and the difference between inlet temperature T_i and reference temperature T_{ref} (which is kept constant along the simulation): $T_i = Q_h / (c * Q_f) + T_{ref}$.

By using this plug in we managed to obtain curve more similar to the real one, at least not reaching the steady state as fast as the one in Fig. 51.

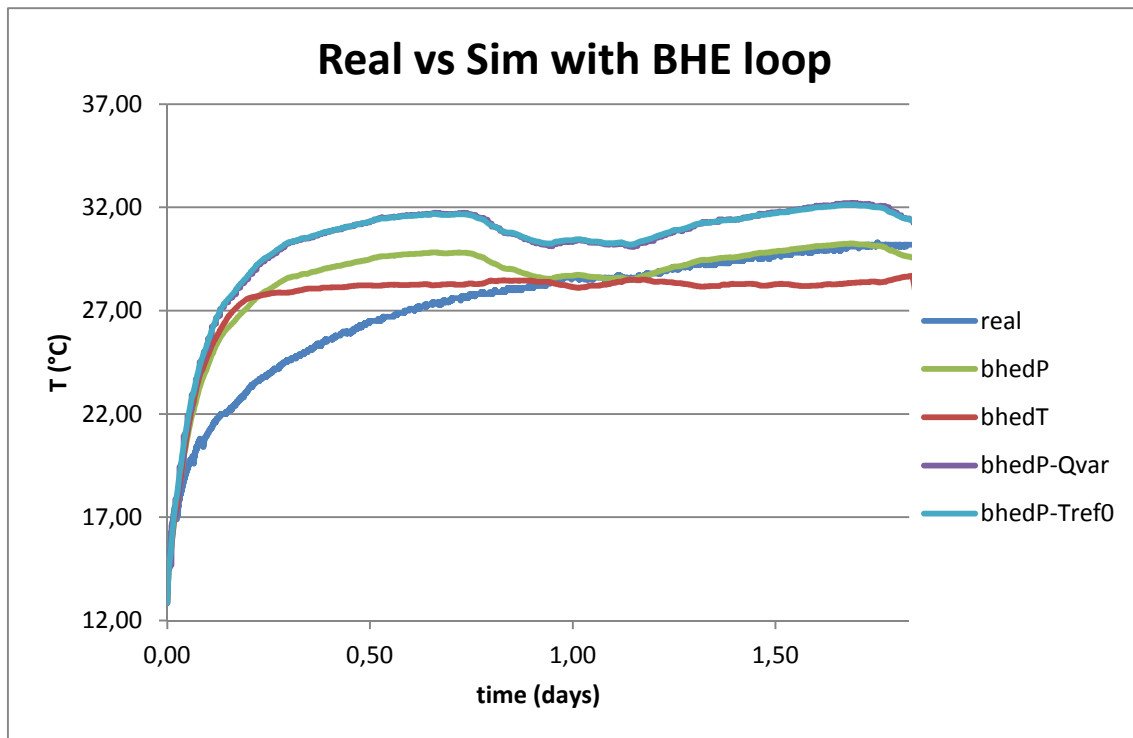


Figure 54 Comparison between the real outlet temperature and the simulated ones through BHE loop module.

	BHE-dP	BHE-dT	BHE-dP Qvar	BHE-dP Tref0
Power	Variable	Variable	Variable	Variable
Depth of the BHE	100	100	100	100
Reference temperature T_0 (°C)	16.7	16.7	16.7	0
Grout thermal conductivity (W/K m)	0.35	0.35	0.8	0.8
Grout volumetric heat capacity (10^6 MJ/K m)	2.3	2.3	2.3	2.3
Flow rate (m^3/day)	36	36	variable	36
Refrigerant dynamic viscosity (10^{-3} kg/m s)	5.2	5.2	5.2	5.2
Number of time steps	700	700	700	700
Time step (day)	0.0028	0.0028	0.0028	0.0028

Table 11 Parameters set per each different simulations run.

As it can be seen from the graph, neglecting the case in which we are entering as an input for the BHE-loop the difference of temperature between inlet and outlet, the other curves follow the same shape, which is different indeed from the real one.

The problem is always the same; it increases too fast at the beginning, reaching the almost steady state temperature. The other curves, reaching a higher temperature, have a different grout thermal conductivity (a higher one).

As far as results were still different from the real ones, we decided not to run the simulation with a constant time step imposed by the user, but to let the software calculate the step, in

order to understand if there were problems of convergence somehow happening during the simulation.

Different are the choices that we can make with an automatic time stepping control. If you decide to work on a predictor corrector scheme (concerning the time discretization), then you can choose between:

- Forward Euler-Backward Euler integrative scheme, 1st order in time, normally used for density dependent problems or for unsaturated problems.
- Forward Adams-Bashfort – Backward trapezoid, 2nd order in time.

Otherwise we can decide to work with an aggressive target based time-marching scheme (concerning time discretization) and we can then choose between:

- a) Fully implicit (Backward Euler integrative scheme)
- b) Semi implicit method (trapezoid rule).

There are also some options for the error and convergence criteria:

- Error tolerance used for nonlinear problems, the smaller it is the higher will be the calculation efforts.
- Error norm can be chosen between Euclidean L2 integral root mean square, Absolute L1 Integral and L^∞ maximum which is useful for finding the maximum error while looking for the solution.
- Maximum number of iterations per time steps can be modified (default value is 12).

We can finally decide if we want to stabilize our numerical result in one of these ways (related to the spatial discretization):

- No upwinding (Galerkin FEM approach), with a high accuracy but it can oscillate in case of coarse mesh and convective processes
- Streamline upwinding, used when we obtain oscillating results.
- Full upwinding, last choice that we can make to stabilize the results. It can lead us to numerical dispersion.
- Shock capturing, it dampens the oscillation by using a nonlinear anisotropy factor, dispersion is not so high.
- Least squares upwinding, to solve transient advection-dispersion transport problems creating a symmetrical matrix.

We tried to run the simulation with different choices; if we use a predictor corrector scheme, we always have problem in the convergence of the resolution. In fact the time step is decreasing so much in the first temporal steps that it reaches 10^{-18} at a simulated time of 0.01782 days. In order not to get this unstable result, we choose the aggressive target based-time marching scheme and, by coupling it with other specific choices, we managed to obtain the curve of the evolution of temperature in an easy way and completely identical to the one obtained by a constant step simulation. The choice made were: fully implicit (backward Euler scheme), initial time step equal to 0.005 days, ending time equal to 1.96 days, error tolerance

equal to $0.01 * 10^{-3}$ applied to Euclidean L2 integral root mean square, maximum iterations per time step equal to 5, full upwinding.

7.3 Comparisons with other solutions

As far as we were not getting realistic results from the simulations, Prof. Al-Khoury decided to run my model on another finite volume implementation of its numerical model, made by Mohamed Nabi, a PhD student in Delft University. In this code they can enter or the varying power or the inlet temperature as an input; what they did obtain is the following:

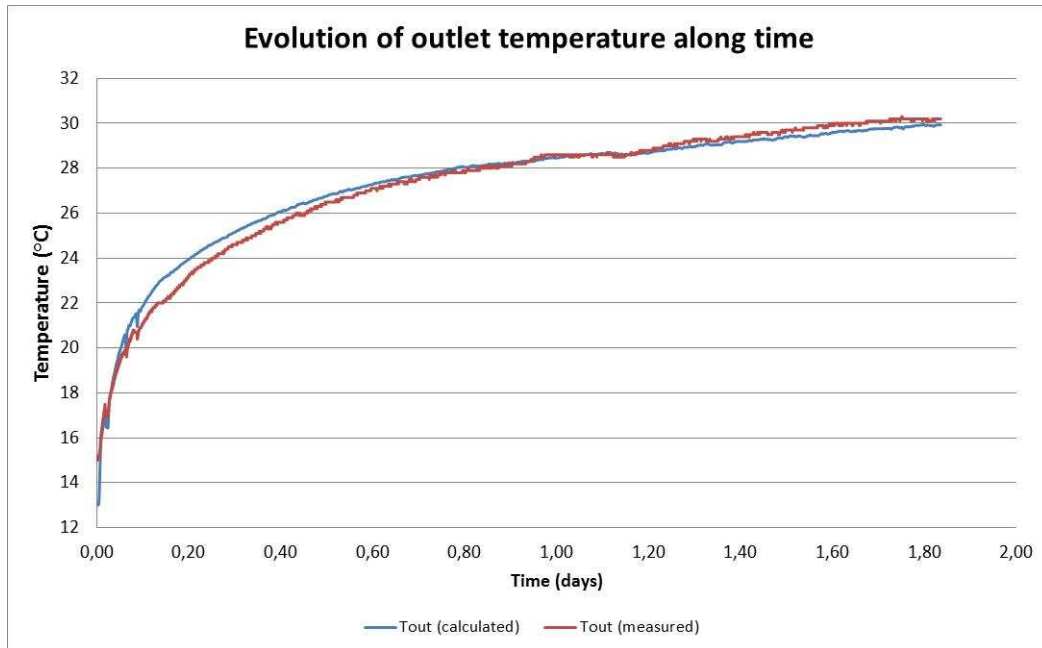
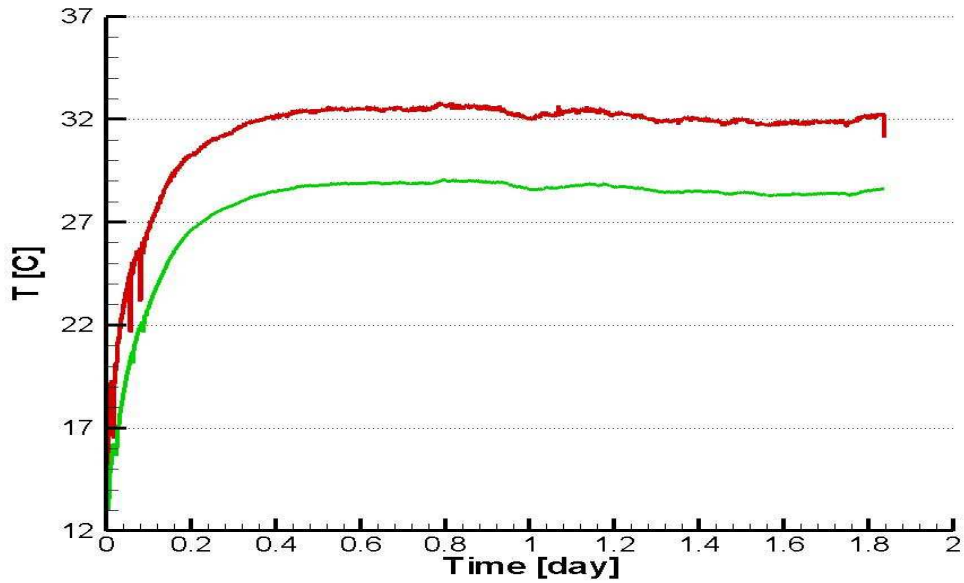


Figure 55 a) this is the evolution of inlet and outlet temperature simulated with the power as input. B) this is the evolution of outlet temperature real and simulated in the case of inlet temperature as input.

In the first of the above figures it is shown the result by applying a varying power, while in the second one the input is the varying inlet temperature. As it can be seen, while the first one reaches the stationary level easily, the second doesn't. In the second graph is clear that the simulated curve is much closer to the real one compared to all the simulations run so far. That's why we had therefore thought that the problem stays in the power, because it is not directly measured during a TRT but calculated through inlet and outlet temperatures.

We tried therefore to contact the developer of FEFLOW, Prof. Hans Diersch, in order to get implemented the option to enter the inlet temperature as an input, because otherwise it would be almost impossible to recreate a TRT by using the data measured in the real one. After contacting him, collaboration has started with Alexander Renz, a modeler of FEFLOW, who tried to help us out with the modeling of a thermal response test. First of all he explained us that FEFLOW BHE loop module has not been tested yet with a predefined time stepping; therefore it has to be used always with an automatic time stepping. Moreover the model has to be run on a refined grid around the borehole, because Al-Khoury model has been implemented in a different way from the one suggested by Al-Khoury. The mesh used now on is the following.

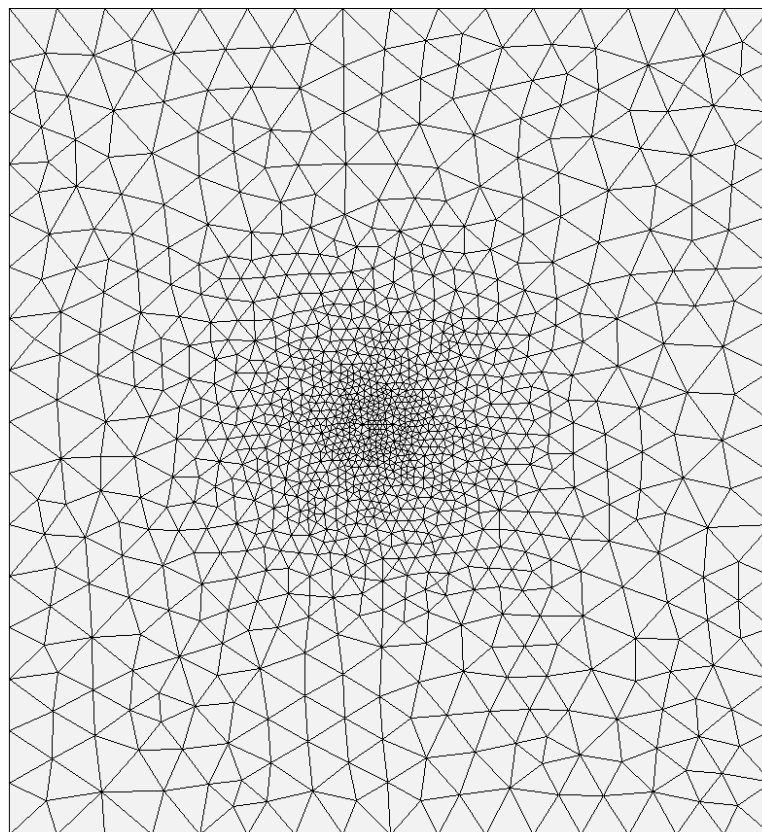


Figure 56 Mesh used in the new numerical model run in FEFLOW. The number of layers is 20.

The simulation has been run with automatic time step control until the end of our test (around 2 days of simulation). The results obtained are shown in the next figure: as it is visible, there are still problems and, even changing the average thermal conductivity, the curve still maintains its behavior. Moreover the computational time now has increased and we needed almost 48 hours to run the model.

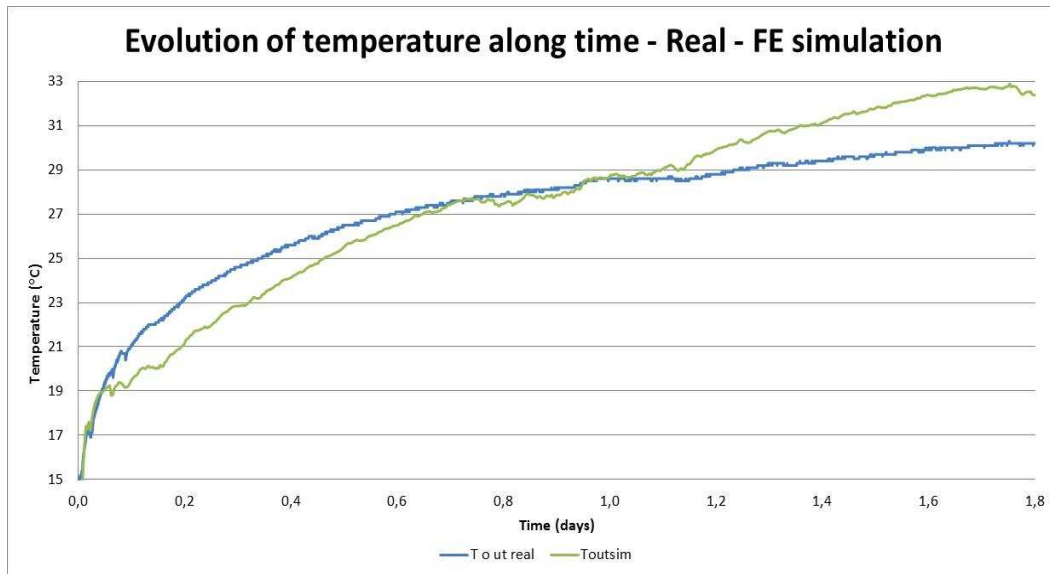


Figure 57 Simulation of thermal response test curve with the new input file as suggested by Alexander Renz, there are still problems in reconstructing the curve.

We are still in contact with Alexander Renz, even though so far his help is not going to be of any need for this work. We hope that or they will implement the possibility of putting as input the varying input temperature or they will manage to help us out understanding how to create a consistent model of reality.

8. RECONSTRUCTION OF A REAL TRT WITH OTHER NUMERICAL MODELS

After the close collaboration with Prof. Al-Khoury I was invited to the Technical University of Delft in order to work intensively for one week with Prof. Al-Khoury, developer of the finite element numerical model implemented in FEFLOW for the borehole heat exchanger and of a spectral model (Al-Khoury, 2012) , and with Mohamed Nabi, a PhD student that had developed a finite volume code for simulating borehole heat exchangers (the results of par. 7.3 were obtained with his code). Basically my work there was helping them out in testing the codes and in calibrating them by comparing real curve and simulated ones.

Both models rely on the same model mechanism, proposed by Prof. Al-Khoury: basically a shallow geothermal system is constituted by two thermally interacting components, BHE and soil mass. The geometry of this system can be described by using an axial-symmetric coordinate system, with the symmetry axis coincident with the centerline of the borehole.

BHE is subjected to an inlet temperature coming from a heat pump, to an initial soil temperature and a transient soil temperature. The soil mass, on the other hand, is subjected to initial soil temperature, to air/surface temperature and to a BHE temperature. The system represents therefore a typical non-homogenous Dirichlet problem from the upper side and the side of contact between BHE and the soil mass: to solve this problem, the superposition principle is used (Eskilson, et al., 1988). In this way we decompose the system into two subsystems, each one with homogenous boundary conditions on parallel boundaries. The first sub-system represents a one dimensional heat flow generated by the air/surface temperature, while the second represents an axial-symmetric transient heat flow generated by the BHE.

Unfortunately both codes are not able to input different block values of thermal conductivity, so basically we will not be able to perform a geostatistical inverse model.

8.1 Spectral model

Deepening the spectral model developed by Al-Khoury, in this case we will not anymore work with finite element method: in order to solve our boundary value problem, it is applied a discrete Fourier transform approach. In such technique, the discretization of the function will be in the frequency (and not in time) and in the spatial domains. To discretize in frequency domain, a FFT (Fast Fourier Transform) is going to be used as a way to speed up the calculation of the discrete Fourier transform (the magnitude of calculation time is reduced from N^2 to $N \log N$, where N is the number of discrete values).

By using a spectral model we will manage to solve the systems in less than a second per simulation. The model implemented is capable of simulating fully transient conductive-convective heat transfer processes for a borehole heat exchanger and it combines analytical methods with geometry and boundary conditions of numerical methods. Moreover the boundary conditions can be varying in time both in short and long term.

Equations will be therefore defined for the BHE and for the soil mass; concerning the BHE the heat transfer will be considered only along the axial axis, due to the slenderness of the

borehole. Concerning the soil mass, it has to be decomposed into two subsystems, a one dimensional soil temperature and an axial symmetric soil temperature.

The code needs 4 input files in order to run a simulation:

- 1) .DAT file with all the information about our borehole (diameter, length, number of pipes), grout, fluid, pipes and about the number of samples we will use.

```
sara7.DAT - Notepad
File Edit Format View Help
20 16384
16384 0.2
0. 20.
1
0.01 0.0
0.032 0.127 100.
0.58 1000. 4186. 0.00042
0.8 1420. 1800.
1.7 1680. 400.
1.e1
-1.0 -1. -1.0
150. 10. 10.
2
100 20.
0.001 10.2 0.0029 0.42
2
!!!!!!!!!!!!!!
Sampling dt, sample number (2^2... 2^14)
Sample number , Dummy
Dummy, Dummy
noutp (always 1)
z, r
DiaP, DiaBore, L
Lambda_r, rho_r, c_r, u_r
LambdaG, rhoG, cG
LambdaS, rhoS, cS
Dummy
Dummy
Dummy
Dummy
mdata, Dummy
Viscosity, Pr, Pthick, Lambdap
borehole type
```

- 2) .TAT file with the air temperature at different times.
- 3) .INT file with the initial soil temperature.
- 4) .LOD file with the inlet temperature along time of our real thermal response test.

8.1.1 Reconstruction of a thermal response test

First of all we tried to reconstruct in the best way possible a Thermal Response Test and then we run a sensitivity analysis, in order to understand which are the parameters influencing more the thermal response of the soil. During the reconstruction various parameters were adjusted, mostly because at the beginning it was not sure if the results would have been completely reliable or not: in fact the code has been calibrated on the basis of the evolution of the fitting curve.

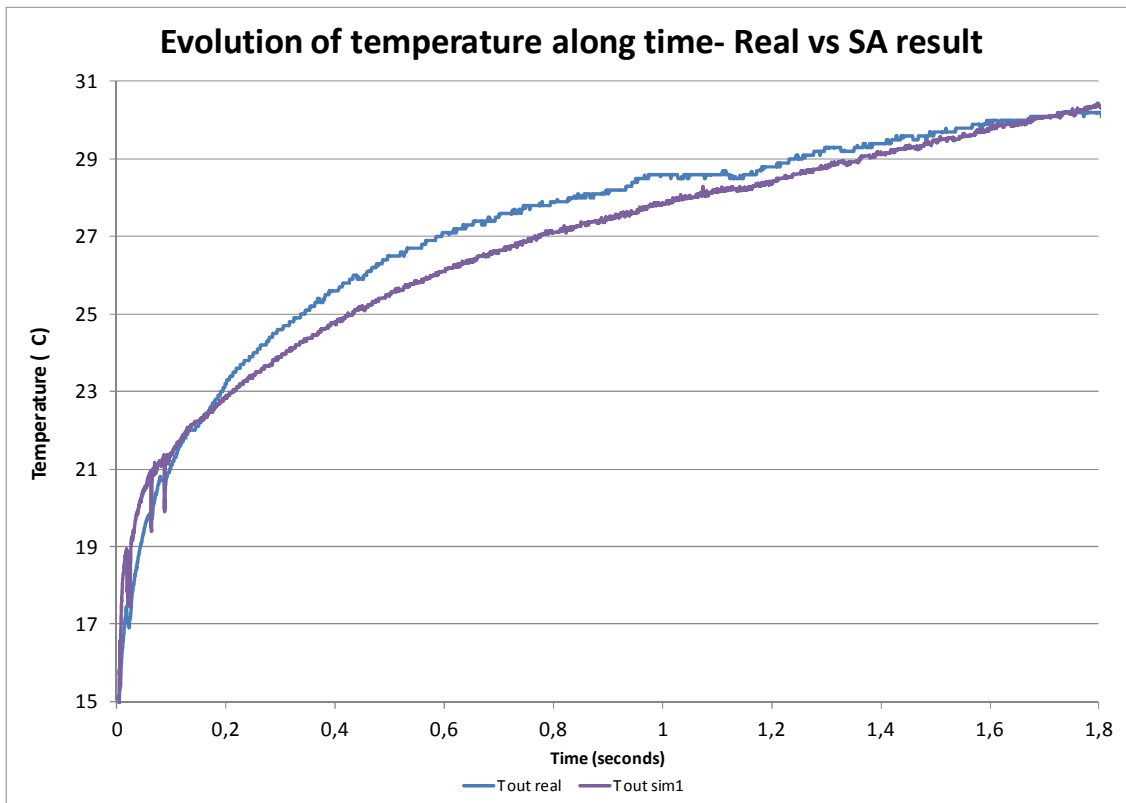


Figure 58 Evolution of temperature along time: real curve and curve obtained by SA-Geotherm run.

The best solution was found with a thermal conductivity equal to 2.15 W/m K while the other parameters were fixed on the real ones of grout and pipes, which are expressed in the following table. The average ground thermal conductivity expressed in the table actually refers to the average calculated by a weighted mean above the different layers (we know the geology by the geological map of the area). By running the forward model various time with different thermal conductivities we find the best thermal conductivity for our case (it is the one that makes the curve fitting better the real response one).

Borehole length	Borehole diameter	Pipe thermal conductivity (PE100)	Pipe external diameter	
100 m	0,127 m	0.38 W/(mK)	0,032 m	
Stratigraphy	Average ground thermal conductivity	Average ground thermal capacity		Average power injected
Marl	1,7 W/(mK)	2.24 MJ/(m ³ K)		6000 W
Grout density	Grout thermal conductivity	Grout volumetric thermal capacity		
1420 kg/m ³	0,37 W/(mK)	1800 MJ/(m ³ K)		

Table 12 Real parameters of the thermal response test.

By knowing which one was the best solution, we kept constant thermal conductivity of the soil and we changed every time one of the other parameters in order to perform a sensitivity analysis and understand better which one is the property more influencing the response test.

Different were the properties we changed in a defined range in order to see their influences on the response.

- Prandtl number

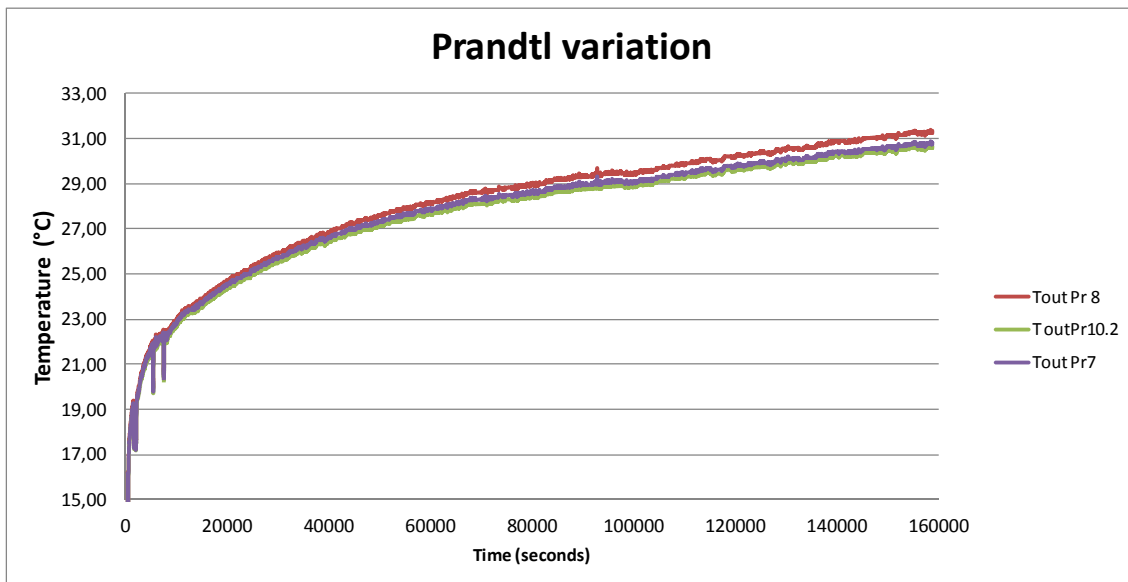


Figure 59 Variations of number of Prandtl in between 7 and 10.2 (Al-Khoury default value)

- Thermal conductivity of the grout

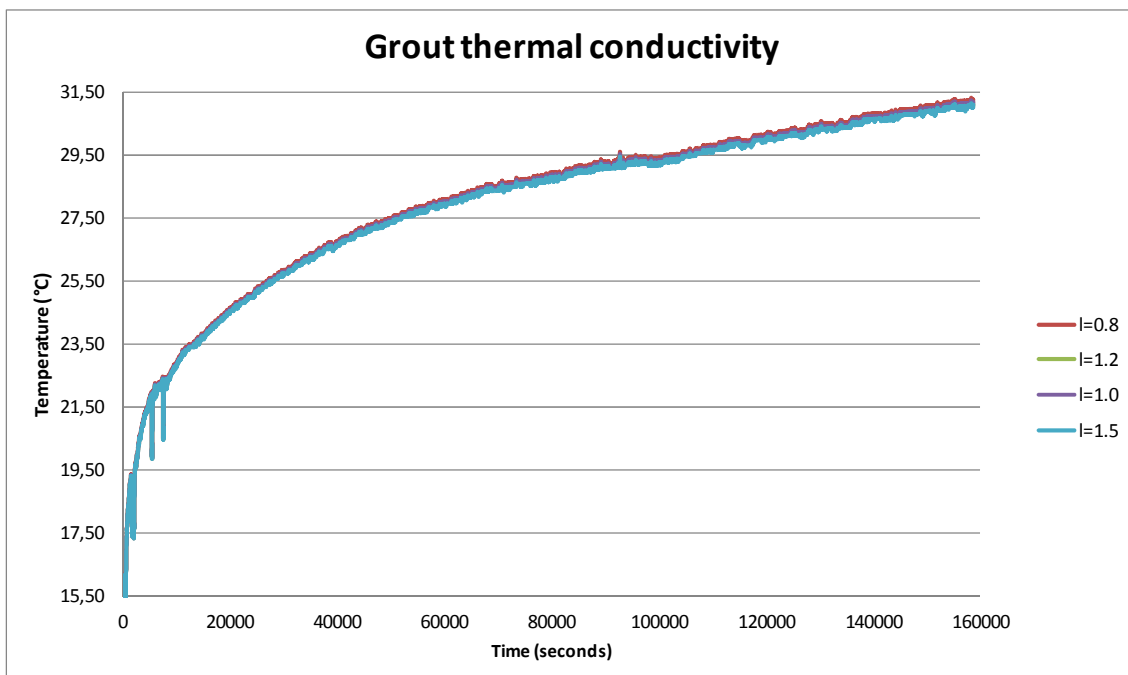


Figure 60 Variations of grout thermal conductivity within 0.8 and 1.5 W/mK.

- Speed of the injected fluid

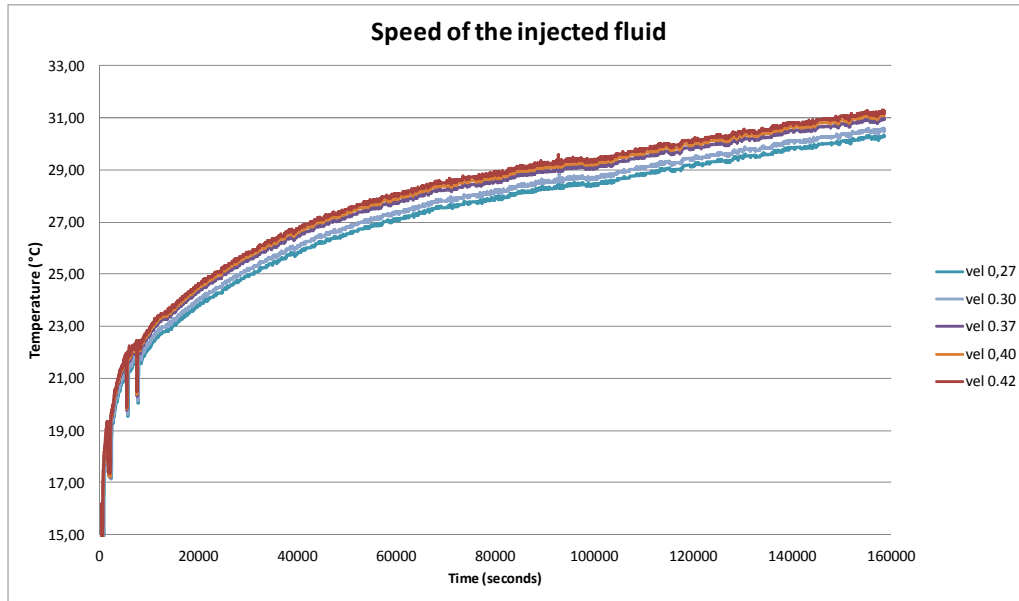


Figure 61 Variation of the speed of the injected fluid within 0.27 and 0.42 m/s.

- Viscosity of the injected fluid

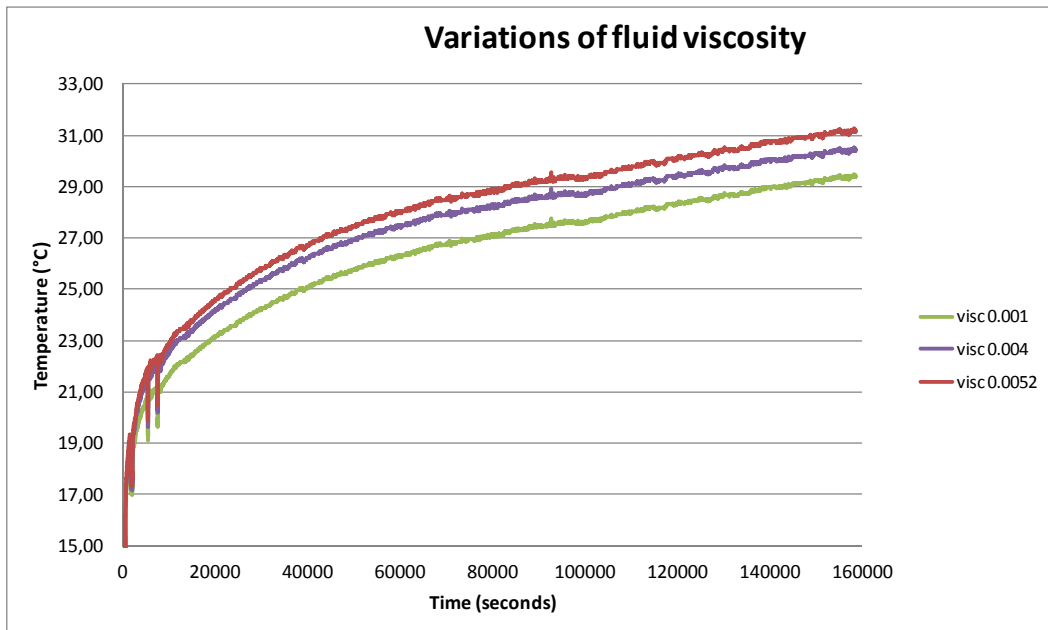


Figure 62 Variations of viscosity of injected fluid within 0.001 (pure water) up to 0.0052 (water + 25% of antifreeze) kg/m s.

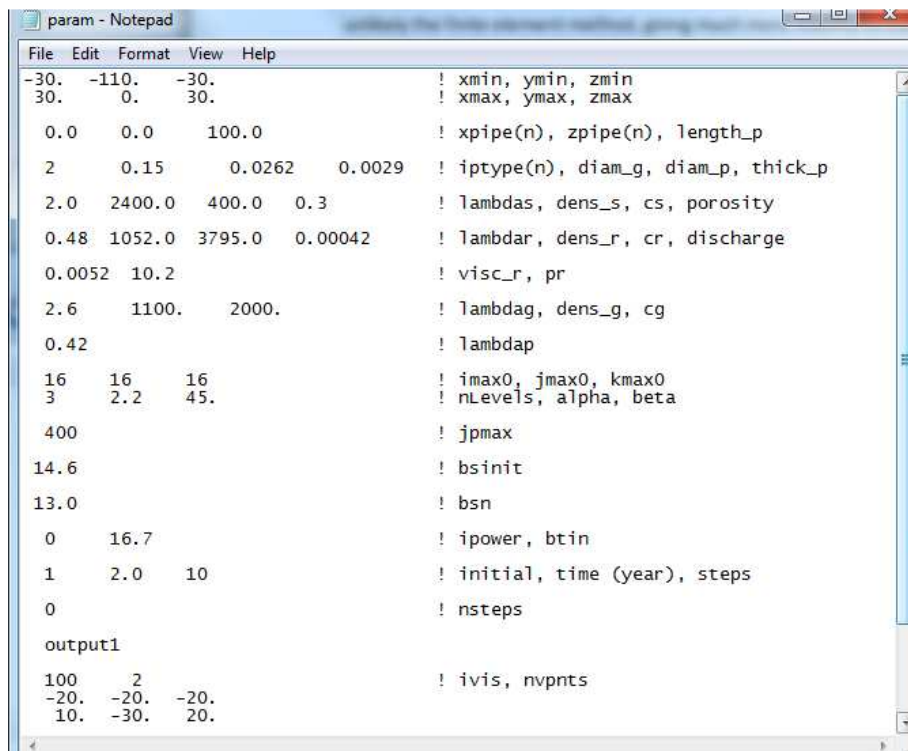
By comparing these results it appears clearly that the most important property changing the test response is the viscosity of the injected fluid. This result will be then confirmed by the runs of the finite volume model.

8.2 Finite volume model

The finite volume method is typically used for solving partial differential equations and compared to the finite element method it has the advantage that it can be implemented in a structured or an unstructured mesh. Moreover the boundary conditions are not invasive, unlikely the finite element method, giving much more stability to the numerical processes.

The discretization of the initial and boundary value problems of the soil mass and borehole heat exchanger results into two sets of coupled algebraic equations; these equations are linear and can be solved using direct or iterative solvers. However the governing equations are non-symmetric so it has to be used a sequential algorithm for the solution.

This model was implemented in Fortran and it has a text files as input: the first one is for the parameters while the second one is for the variable power or variable inlet temperature.



```
param - Notepad
File Edit Format View Help
-30. -110. -30. ! xmin, ymin, zmin
30. 0. 30. ! xmax, ymax, zmax

0.0 0.0 100.0 ! xpipe(n), zpipe(n), length_p
2 0.15 0.0262 0.0029 ! iptype(n), diam_g, diam_p, thick_p
2.0 2400.0 400.0 0.3 ! lambdas, dens_s, cs, porosity
0.48 1052.0 3795.0 0.00042 ! lambdar, dens_r, cr, discharge
0.0052 10.2 ! visc_r, pr
2.6 1100. 2000. ! lambdag, dens_g, cg
0.42 ! lambdap
16 16 16 ! imax0, jmax0, kmax0
3 2.2 45. ! nLevels, alpha, beta
400 ! jpmax
14.6 ! bsinit
13.0 ! bsn
0 16.7 ! ipower, btin
1 2.0 10 ! initial, time (year), steps
0 ! nsteps
output1
100 2 ! ivis, nvpnts
-20. -20. -20.
10. -30. 20.
```

The code is first of all asking for the dimension of the grid, which is the first thing to be done. The first two lines of the code will be used for defining x-y and z extremes of the meshing; then we will define the type of borehole, in detail where the pipe is located (xpipe and zpipe), which is the pipe length (length_p in meters), the type of pipe (iptype, if it is 1 is a single U-tube, 2 is a double one) and all its measures (grout diameter diam_g, internal pipe diameter diam_p and pipe thickness thick_p). Next, all the properties of soil s, refrigerant r, grout g and pipe p are defined (lambda is the thermal conductivity in W/mK, dens is the density in kg/m³, c is the thermal capacity (J/m³K), visc is the viscosity and Pr is the Prandtl number (if it is equal to 0 then the code will calculate it, otherwise it will use the written value).

Subsequently, we will have to decide how coarse is our mesh and how many refinement we want: imax, jmax and kmax are respectively the number of grid cells of the first level of meshing (so called level 0) and they can be only multiples of 16. It has to be defined as well the

number of levels that I want for the refining (nlevels) and alpha and beta are grid control parameters. As far as the effect of pipe and soil are calculated separately, the number of cells in the pipe can be different from the grid refinement: it is indeed specified in jpmx which is the number of cells of the pipe (considered as mono dimensional).

We have to define initial ground temperature (bsinit), surface-air temperature (bsn) and first inlet temperature (btin) as well as which kind of input file we will use (ipower equal to 0, input file is made of inlet temperature, while if it is equal to 1 is made of power). We can also decide how many steps we want the code to calculate: if nsteps is equal to 0, the code will solve the equations for every step of the input, while if it is equal to a particular number it will stop at that defined step number.

The results will be put, joint with a copy of the input, inside a new folder called "output-03red) in this case. The output files will be the input and output temperatures of the pipe, a predefined number of results printed for the pipe along its length (ivis) and a number of soil temperatures along the length for points that we choose (nvpnts).

The line with initial, time (years) and steps will be used in case we want to run the code first without the pipes in order to obtain the real ground temperature. If we put initial equal to 1 the code will simulate for the time (in years) and in the number of steps defined by the user, the initial temperature of the ground knowing its surface temperature and its bottom average initial temperature (e. g. the average temperature of the soil measured before running the thermal response test).

8.2.1 Reconstruction of a thermal response test

We run our simulations with the same initial condition used for the SA-Geotherm code and the result is shown in the following figure.

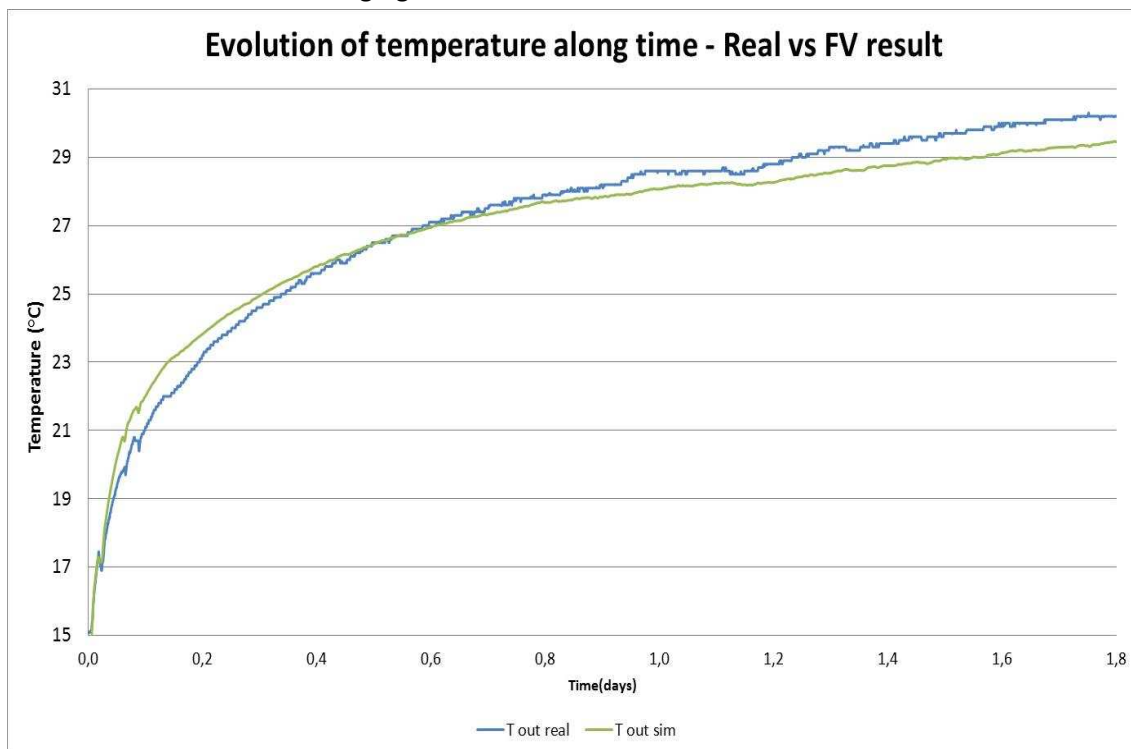


Figure 63 Evolution of temperature along time: real curve and finite volume model curve.

As it is visible from the curve, also the finite volume code lets us to reconstruct in a realistic way the thermal response test. In this case as well it was performed a sensitivity analysis for testing which one was the most influencing property; the curves obtained showed the same result as the one of SA-Geotherm, viscosity is the most influencing one.

CONCLUSION

The research developed in this thesis has been addressed to a detailed study of the characterization of thermal parameters in a low enthalpy geothermal reservoir, with particular reference to thermal conductivity and thermal capacity measured by laboratory tests, in situ tests and numerical models.

Bibliographical, laboratory and on field work demonstrated the inadequacy of technologies and methodologies used for investigating thermal parameters and for furnishing useful information for shallow geothermal reservoir characterization. Particularly it has shown that there is a lack of direct or indirect measuring devices able to allow the reconstruction of the time and space variability of these properties in an operative, cheap and reliable way.

The work was therefore concentrated on the development of an original methodology for defining the spatial distribution of thermal parameters based on the application of the so-called “inverse problem”. This type of technique is normally applied to the oil case, but it can be applied also in the geothermal case as far as we can interpret as hard data the ones obtained from the thermal response test. It has to be underlined that in this particular case the simulator to be chosen isn't only a flow simulator, but moreover a heat flow simulator.

The methodology of inverse problem applied to geothermal reservoir used synthetic numerical model of spatial distribution of reservoir properties, coupled to the results of the real “production test” of shallow geothermal reservoirs. While the research has validated the results of the numerical modeling with the theoretical ones in a stationary condition, on the other side it has shown the non-perfect adequacy of the numerical model implemented on FEFLOW concerning the reconstruction of the transient phases of thermal response test.

Thanks to the contact with international researchers as Prof. Rafid Al-Khoury, it has been revealed the existence of a problem in the implementation of its numerical model in FEFLOW and it has been proposed a way to solve it (adding a module for entering the inlet temperature as input, instead of the heat input rate).

After this discovery, other two codes have been used: both of them were developed in Delft and they implement the model of Al-Khoury: one as a spectral analysis and the other as finite volume model.

While FEFLOW lets the user define a very specific input file, with different thermal conductivity per each block, SA-Geotherm and FV-Geotherm have, on the contrary, a very simplified input file and they don't let the user introduce different conductivities per each block. Their main advantage is the reduced computational time (few seconds for the SA, 10-15 minutes for the FV in case of a 10000 blocks input) and therefore the possibility of running a lots of simulations performing a sensitivity analysis. Both the curves obtained are much closer to the real thermal response test compared to the one obtained by using FEFLOW. Concerning the sensitivity analysis, runs with different grout, circulating fluid properties, ground characteristics, etc. were made. It was found out that the most influencing parameter in the short term effect of a thermal response test is the fluid viscosity, the curve changes significantly when changing the viscosity from water properties to water & antifreeze properties. On the contrary, by changing the thermal conductivity we don't have such big differences in the curve, but we can still adjust the model by varying the thermal conductivity.

WHAT'S NEXT?

The medium term conditions and the geothermal system monitoring (GSM)

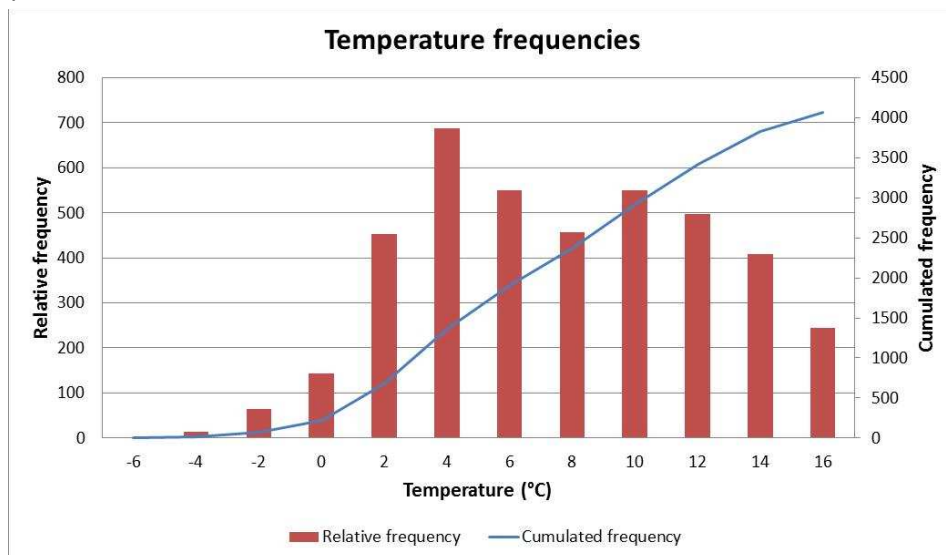
The application of the inverse problem can be enlarged on the temporal point of view: in fact we can decide to apply it for a longer period (not only 72 hours), namely a winter period or a summer one. In this case we will have to arrange a power input file related to the effective consumption of a building, so it is important to have knowledge of the heating and cooling options for a private building.

In fact we can clearly see a parallelism between a thermal response test, which is basically a monitoring 72 hours long of a functioning system, and a monitoring system, that can record all the power injected/extracted from the borehole in a working geothermal system. A monitoring system, actually, acts as a thermal response test because it records power evolution of our system; this system can be useful in order to control and vary the used power by relating it to underground thermal evolution or to external/internal temperature evolution.

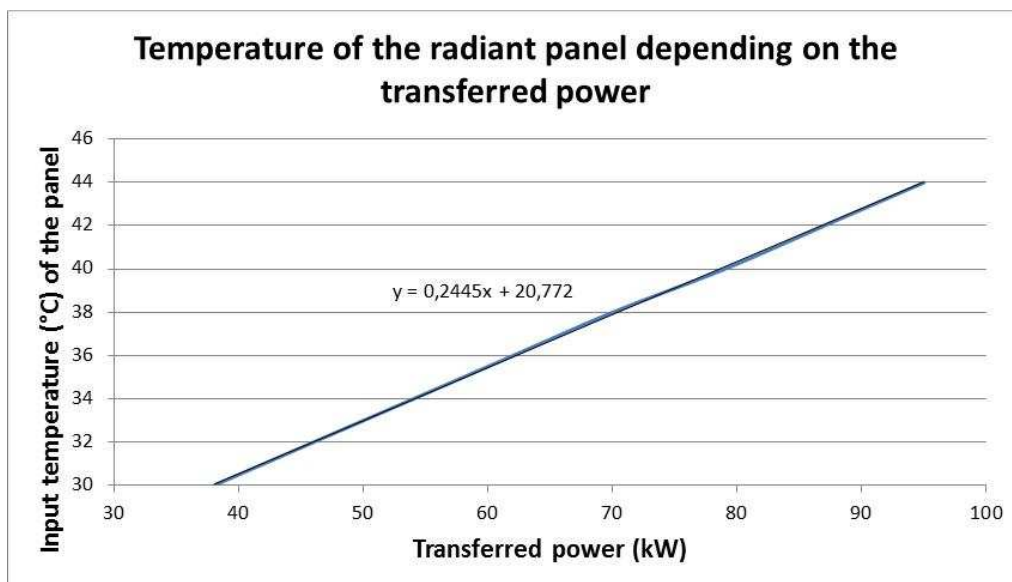
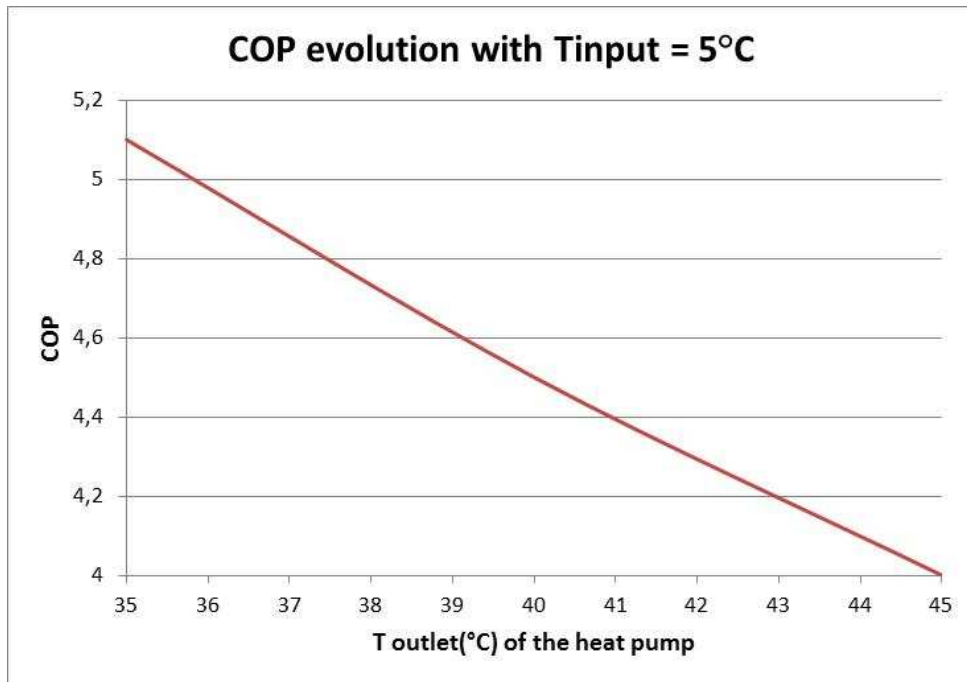
Deepening our application, we will be working in a synthetic case because we don't have any real case to monitor. We will therefore build up a hypothetical input file for FEFLOW, representing an evolution of power in time.

The procedure developed to create it can be divided in the following steps:

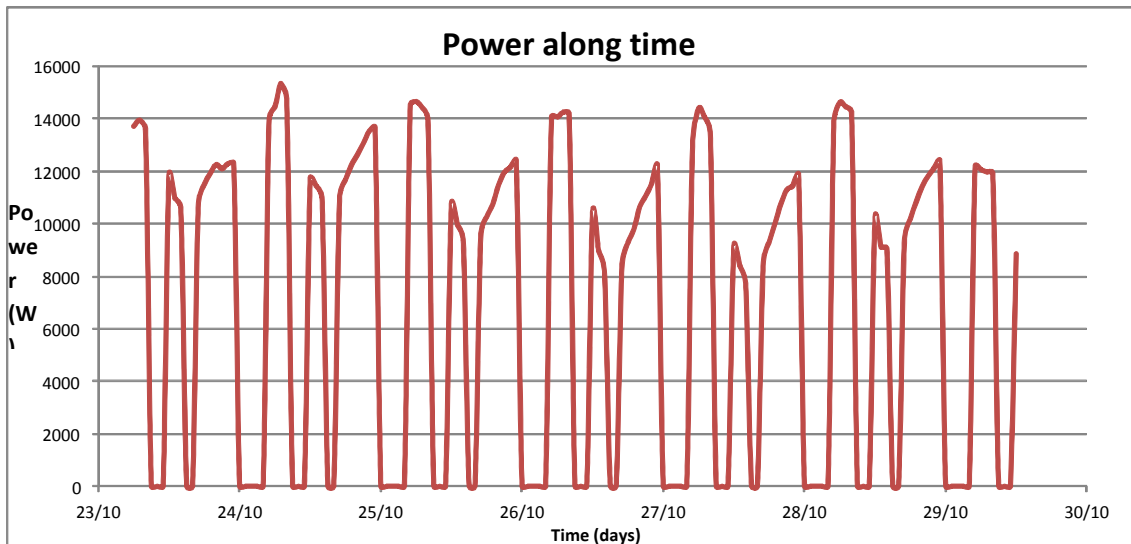
- 1) Climate analysis of the area involved: average of hour-temperature above ten years
- 2) Definition of temperature classes created knowing minimum and maximum of ten years evolution



- 3) Analysis of the considered building: its external area, surface, insulation characteristics and its thermal transmittance
- 4) Definition of the maximum power requested from the house considering peak temperatures (one for winter and one for summer)
- 5) Definition of load factor for the different temperature classes
- 6) Definition of the COP (coefficient of performance) or EER (energy efficiency ratio) for each class



- 7) By knowing the COP and peak load (\rightarrow power) we choose a heat pump
- 8) We can calculate hourly the power requested from the house and therefore how much power I should extract from the ground (in winter case) or inject (in summer). It will be then created an input file to feed our dynamic simulator FEFLOW.



Analyzing every step of the procedure, first of all we used data of hour temperature taken from ARPA database, from 2001 to 2011; we performed a statistical analysis obtaining then the average of temperatures for every hour of the ten years period.

Temperature classes are defined by knowing the minimum and the maximum of the 2 different period of use of our systems: heating (mid-October to mid-April) and cooling (mid-April to mid-October).

Knowing these temperatures it is therefore possible to understand how much is the power needed in order to maintain a certain room temperature in the house; in particular, we have considered as medium room temperature optimal for the house 20°C. Given the dimension of the house, its external and internal surface, what we need to calculate the power is the thermal load of the house, related to the gain and loads of the house.

The thermal load calculation process (Sanner, et al., 2011) has two principal stages:

- 1) Heat gains calculation (instantaneous heat flow from the outside to the inside)
- 2) Thermal load calculation.

Concerning the heat gains calculation, it is better to divide heat flow in two groups: external and internal gains, where the external ones are basically radiation from windows, skylights and conduction through walls, floors, windows in contact with a different temperature environment, while the internal ones are due to people, lighting and equipment.

Heat gains calculation

Different are the mathematical models for calculating the heat gains and various are the software in which these models are implemented. In this section we will go rapidly through them just to have a basic idea about how they work (Sanner, et al., 2011).

- a) *External walls*: Mitlas transfer relationships are normally used for their modeling. The heat conduction at the inside surface at a time n is:

$$\dot{Q}(n) = \sum_{i=0} a_i E(n-i) - \sum_{i=0} b_i Q(n-i)$$

Equation 63

Where a and b are z-transfer function coefficients, E is the outside surface temperature and n is the number of steps (related to the thermal behavior of the wall).

- b) *Internal walls*: we assume that these walls have low thermal mass and constant boundary conditions. This is the equation to use for calculating the heat flow:

$$\dot{Q} = \frac{\Delta T}{\frac{1}{h_1} + \sum_n \frac{\Delta x_i}{K_i} + \frac{1}{h_2}}$$

Equation 64

Where h is the convective heat transfer coefficient at surface (W/m²°C), ΔT is the temperature gradient through the wall (°C), x is the thickness of the layer i (m) and K is the thermal conductivity of the layer i (W/m°C).

- c) *Windows*: the heat transfer in this case is due to temperature gradient between the two glasses surfaces (conduction heat transfer) and due to the incident solar radiation (radiant transmission). For the conductive part this is the equation used: $\dot{Q} = U \cdot \Delta T$. For the effect of solar radiation, it will be defined a solar factor (SF) as a ratio between the total energy that enters through the glazing and the amount that strikes the surface outside the glass:

$$SF = \tau_D I_D + \tau_d I_d + h_i \frac{\alpha_D I_D + \alpha_d I_d}{h_e + h_i}$$

Equation 65

Where α and τ are absorption and transmittance coefficients, h is the convective heat transfer coefficient at internal (i) or external (e) window surface (W/m²°C), I_D is the direct solar radiation (W/m²) and I_d is the diffuse solar radiation (W/m²).

- d) *Infiltration and ventilation*: the heat transfer can be considered as purely convective and in both cases the heat gain is calculated through an energy balance performed on the outside air volume:

$$\begin{aligned}\dot{Q}_{inf} &= \dot{m}_{inf} \rho C_p (T_{out} - T_{in}) \\ \dot{Q}_{vent} &= \dot{m}_{vent} \rho C_p (T_{vent} - T_{in})\end{aligned}$$

Equation 66

Where ρ is the air density (kg/m³), C_p is the air specific heat capacity (J/kg°C), m_{inf} is the mass flow rate (m³/s) estimated by empirical methods, m_{vent} and T_{vent} are defined by law.

- e) *Internal heat*: the instantaneous heat gain can be expressed as follows:

$$\dot{Q} = n \dot{Q}_0 f$$

Equation 67

Where f is the schedule while for people Q depends on the number n and Q₀ on the degree of activity, clothing; for artificial lighting Q depends on the number n, Q₀ on the type of lamp; for equipment Q depends on the number n and Q₀ on the installed power.

Concerning the European standards to which we have to refer to in order to model thermal performances of the buildings, EN ISO 13790:2008 gives calculation methods for assessment of the annual energy use for building heating and cooling. This method includes the calculation of:

- a) Heat transfer by transmission and ventilation of the building zone when heated or cooled to constant internal temperature
- b) Contribution of solar and internal heat gains
- c) Annual energy need for heating and cooling to maintain a specific temperature
- d) Annual energy use for heating and cooling of the building.

Another method used is the one defined by the ASHRAE standards, which is named TFM-Transfer Function Method. The last one is the method based on the Cooling or Heating Degree Day (CDD, HDD); those are indices designed to reflect the demand for energy needed to cool or heat a building, derived from daily temperature observations. It has to be defined a base temperature to calculate the degrees: this base temperature is the outside temperature above which a building needs no heating.

Normally buildings are heated up through a boiler, which produces hot water that passes into the radiators with a temperature of 60-70°C. By using a geothermal system we obtain hot water coupling the borehole heat exchanger and the heat pump: this water is therefore pumped into the heating system. In this case, the water has a lower temperature compared to the boiler case. In fact, normally in the geothermal systems temperatures are in the range of 30°C to 45°C: the heating systems used in this case are different. We use radiant panels (under floor heating systems) and/or fan coils.

In the same way, for cooling a building air heat pumps are normally used; in the case of geothermal systems, cooled water coming from the coupling borehole heat exchanger and heat pump is used in the system and every type of distribution system is suitable for it.

Inversion model applied to the medium term calculation

By creating this kind of input, we want to check how the system works in a medium term condition. In fact the solicitation to which the ground is subject are different in a simple thermal response test and in a 6 months functioning period. That's why could be interesting to simulate a medium term condition and perform the inverse modeling (in this case everything is synthetic, but if in the future we will have the possibility to study and monitor a real system, we could therefore be able to check it in the reality and calibrate then the powers used).

Bibliography

- Abu-Hamdeh N. H.** Thermal Properties of Soil as affected by Density and Water Content [Journal]. - [s.l.] : Biosystems Engineering, 2003. - 1 : Vol. LXXXVI.
- Abu-Hamdeh N.H.** Soil and water: measurement of the thermal conductivity of sandy loam and clay loam soils using single and dual probes [Journal]. - [s.l.] : Journal of Agricultural Engineering Research, 2001. - 2 : Vol. LXXX.
- Akima H.** A New Method of Interpolation and Smooth Curve Fitting Based on Local Procedures [Journal]. - [s.l.] : Journal of the Association for Computing Machinery, 1970. - 4 : Vol. XVII.
- Al-Khoury R. and Bonnier P.G.** Efficient finite element formulation for geothermal heating systems. Part II: transient [Journal]. - [s.l.] : International Journal for Numerical Methods in Engineering, 2006. - Vol. LXVII.
- Al-Khoury R., Bonnier P. G. and Brinkgreve R. B. J.** Efficient finite element formulation for geothermal heating systems. Part I: Steady state [Journal]. - [s.l.] : International Journal for Numerical Methods in Engineering, 2005. - Vol. LXIII.
- Al-Khoury R., Kölbl T. and Schramedei R.** Efficient numerical modeling of borehole heat exchangers [Journal]. - [s.l.] : Computers & Geosciences, 2010. - 10 : Vol. XXXVI.
- ANTER Corporation** Principal methods of thermal conductivity measurements // Technical Note #67.
- Antonopoulos V.Z. and Wyseure G.C.L.** [Journal]. - Modeling of Water and Nitrogen Dynamics on an Undisturbed Soil and a Restored Soil After Open-Cast Mining : Agricultural Water Management, 1998. - Vol. XXXVII.
- Antriasian A. M.** The Portable Electronic Divided Bar (PEDB): a Tool for Measuring Thermal Conductivity of Rock Samples [Conference] // Proceedings World Geothermal Congress. - 2010.
- ASCE** The ASCE Task Committee on Definition of Criteria for Evaluation of Watershed Models of the Watershed Management Committee. Irrigation and Drainage Division, Criteria for evaluation of watershed models [Journal]. - [s.l.] : Journal of Irrigation and Drainage Engineering, 1993. - 3 : Vol. CXIX.
- Authors Various** FEFLOW- White Papers Vol. V [Book]. - Berlin : DHI-WASY GmbH, 2010.
- Bandos Tatyana V. [et al.]** Finite line-source model for borehole heat exchangers: effect of vertical temperature variations [Journal]. - [s.l.] : Geothermics, 2009. - Vol. XXXVIII.
- Barringer J.R. and Lilburne L.** An Evaluation of Digital Elevation Models for Upgrading New Zealand Land Resource Inventory Slope Data [Conference] // GeoComputation '97 & SIRC '97. - Otago, NZ : [s.n.], 1997.
- Basta S. and Minchio F.** Geotermia e pompe di calore [Book]. - Verona : S. Basta, 2007.

Boken V.K. [et al.] Agricultural Water Use Estimation Using Geospatial Modelling and a Geographic Information System [Journal]. - [s.l.] : Agricultural Water Management, 2004. - 3 : Vol. LXVII.

Brailsford A. D. and Major K. G. The thermal conductivity of aggregates of several phases, including porous materials [Journal]. - [s.l.] : Journal of Applied Physics, 1964. - 3 : Vol. XV.

Carlsaw H. and Jaeger J. Conduction of Heat in Solids [Book]. - [s.l.] : Oxford, 1947.

Castano E.T. [et al.] Statistical Functional Modeling of Quality Changes of Garlic under Different Storage Regimes. [Journal]. - [s.l.] : Journal of Data Science, 2006. - 2 : Vol. IV.

Chanasyk D.S., Mapfumo E. and Willms W. Quantification and Simulation of Surface Runoff from Fescue Grassland Watersheds [Journal]. - [s.l.] : Agricultural Water Management, 2003. - 2 : Vol. LIX.

Change Committee on Climate The renewable energy review [Report]. - 2011.

Clauser C. and Huenges E. Thermal conductivity of rocks and minerals [Book Section] // Rock physics and phase relations: a handbook of physical constants / book auth. Ahrens T. J.. - 1995.

Cosenza P., Guérin R. and Tabbagh A. Relationship between thermal conductivity and water content of soils using numerical modelling [Journal]. - [s.l.] : European Journal of Soil Science, 2003. - Vol. LIV.

Côté J. and Konrad J.M. Thermal conductivity of base-course materials [Journal]. - [s.l.] : Canadian Geotechnical Journal, 2005. - Vol. XLII.

Cui P. [et al.] Heat transfer analysis of pile geothermal heat exchangers with spiral coils [Journal]. - [s.l.] : Applied Energy, 2011.

Daw J. [et al.] Hot wire needle probe for In-pile thermal conductivity detection [Report]. - [s.l.] : Idaho National Laboratory, 2010.

De Lucia M. Influenza della variabilità spaziale sul trasporto reattivo. - [s.l.] : Department of Chemical, Mining Engineering and Environmental Technologies. University of Bologna, 2008.

Delhomme J.P. and de Marsily Ghislain Flow in porous media: An attempt to outline Georges Matheron's contributions [Journal]. - [s.l.] : Lecture Notes in Statistics, 2005. - Vol. CLXXXIII.

Demirci A., Görgülü K. and Durutürk Y.S. Thermal conductivity of rocks and its variation with uniaxial and triaxial stress [Journal]. - [s.l.] : International Journal of Rock Mechanics & Mining Sciences, 2004. - Vol. XLI.

Diao N., Li Q. and Fang Z. Heat transfer in ground heat exchangers with groundwater advection [Journal]. - [s.l.] : International Journal of Thermal Sciences, 2004. - Vol. XLIII.

Diersch H. J. G. [et al.] Numerical Modelling of Solar Heat Storage Using Large Arrays of Borehole Heat Exchangers [Conference] // Proceedings World Geothermal Congress 2012. - Bali : [s.n.], 2010.

Eching S.O. and Hopmans J.W. Optimization of Hydraulic Functions from Transient Outflow and Soil Water Pressure Data. [Journal]. - [s.l.] : Soil Science Society of America Journal, 1993. - Vol. LVII.

Eklöf C. and Gehlin S. TED. A mobile equipment for thermal response test [Report]. - Luleå : University of Luleå, 1996.

Eskilson P. and Claesson J. Simulation model for thermally interacting heat extraction boreholes [Journal]. - [s.l.] : Numerical Heat Transfer , 1988. - 2 : Vol. XIII.

Eskilson P. Thermal analysis of heat extraction boreholes. - Lund : Department of Technical Physics-University of Lund, Sweden, 1987.

Fujii H. [et al.] An improved thermal response test for U-tube ground heat exchanger based on optical fiber thermometers [Journal]. - [s.l.] : Geothermics, 2009. - 4 : Vol. XXXVIII.

Fujii H. [et al.] Optimizing the design of large-scale ground-coupled heat pump systems using groundwater and heat transport modeling [Journal]. - [s.l.] : Geothermics, 2005. - Vol. XXXIV.

Fujii H., Okubo H. and Itoi R. Thermal response tests using optical fibre thermometers [Conference] // Geothermal Resources Council Transactions. - 2006. - Vol. XXX.

Fujimitsu Y. [et al.] Evaluation of Subsurface Thermal Environmental Change Caused by a Ground-coupled Heat Pump System [Journal]. - [s.l.] : Current Applied Physics, 2009.

Gehlin S. Thermal Response Test - In Situ Measurements of Thermal Properties in Hard Rock. [Report]. - [s.l.] : Luleå University, 1998.

Gehlin S. Thermal response test. Method, development and evaluation [Report]. - Luleå : University of Luleå, 2002.

Gomez-Hernández J.J., Sahuquillo A. and Capillar J.E. Stochastic Simulation of Transmissivity Fields Conditional to Both Transmissivity and Piezometric Data – I.Theory [Journal]. - [s.l.] : Journal of Hydrology, 1997. - 1-4 : Vol. CCIII.

Goovaerts P. Geostatistical Approaches for Incorporating Elevation into the Spatial Interpolation of Rainfall. [Journal]. - [s.l.] : Journal of Hydrology, 2000. - 1-2 : Vol. CCIIVIII.

Gustafsson A. M., Nordell B. and Tuomas G. Thermal response test integrated to drilling [Conference] // Futurestock. 9th international conference on thermal energy system. - Warsaw : [s.n.], 2003.

Gustafsson A. M., Nordell B. and Tuomas G. Thermal response test integrated to drilling [Conference] // Futurestock. 9th international conference on thermal energy system. - Warsaw : [s.n.], 2003.

Gustafsson Anna-Maria Thermal Response Test - Numerical simulations and analyses. - Luleå : Luleå University of Technology, 2006.

-
- He M., Rees S. and Shao L.** Dynamic Response Simulations of Circulating Fluid and a Borehole Heat Exchanger [Conference] // Proceedings World Geothermal Congress. - 2010.
- He M., Rees S. and Shao L.** Dynamic Response Simulations of Circulating Fluid and a Borehole Heat Exchanger [Conference] // Proceedings World Geothermal Congress 2010. - Bali : [s.n.], 2010.
- Hu L. and Ravalec-Dupin M.** An Improved Gradual Deformation Method for Reconciling Random and Gradient Searches in Stochastic Optimizations [Journal]. - [s.l.] : Mathematical Geology, 2004. - 6 : Vol. XXXVI.
- Hu L.** Combination of dependent realization within the gradual deformation methods [Journal] // Mathematical Geology. - 2002. - pp. 953–963.
- Hu L., Blanc G. and Noetinger B.** Gradual deformation and iterative calibration of sequential simulations [Journal] // Mathematical Geology. - 2001. - pp. 475–489.
- Hvilshoj S.** Estimation for Ground Water Hydraulic Parameters.. - [s.l.] : Technical University of Denmark, 1998.
- Ingenieure Verein Deutscher** Utilization of the subsurface for thermal purposes - Underground thermal energy storage. - Düsseldorf : [s.n.], 2001. - Vol. III.
- Ingenieure Vereine Deutscher** Thermal use of the underground - Direct uses. - Düsseldorf : [s.n.], 2004. - Vol. IV.
- Ingersoll L. R. and Plass H. J.** Theory of the ground pipe heat source for the heat pump. - [s.l.] : ASHVE Transactions, 1948. - Vol. XLVII.
- Ingersoll L.R., Zobel O. J. and Ingersoll A.C.** Heat conduction with engineering, geological and other applications. [Book]. - New York : McGraw-Hill, 1954.
- Javed S., Fahlén P. and Claesson J.** Vertical ground heat exchangers: a review of heat flow models [Report]. - Göteborg, Sweden : Chalmers University of Technology, 2009.
- Kim S.K. [et al.]** A Parallelized Model For Simulating A Vertical Closed-Loop Geothermal Heat Pump System [Conference] // Proceedings World Geothermal Congress 2010. - Bali : [s.n.], 2010.
- Kim S.K. [et al.]** Model Development to Simulate Geothermal Heat Transport and Sensitivity Analyses on the Design Parameters of Closed-loop Geothermal Heat Pump System [Journal]. - [s.l.] : Korean Society for Geosystem Engineering, 2008. - Vol. XLV.
- Klein S.A. et al.** TRNSYS 17. A Transient System Simulation Program [Book]. - [s.l.] : Solar Energy Laboratory, University of Wisconsin-Madison, 2010.
- Kohl T. [et al.]** Coupled hydraulic, thermal and mechanical considerations for the simulation of hot dry rock reservoirs [Journal]. - [s.l.] : Geothermics, 1995. - 3 : Vol. XXIV.

-
- Kohl T. and Hopkirk R. J.** A simulation code for forced fluid flow and transport in fractured, porous rock [Journal]. - [s.l.] : Geothermics, 1995. - 3 : Vol. XXIV.
- Lamarche Louis and Beauchamp Benoit** A new contribution to the finite line-source model for geothermal boreholes [Journal]. - [s.l.] : Energy and Buildings, 2007. - Vol. XXXIX.
- Lamarche Louis and Beauchamp Benoit** New solutions for the short-time analysis of geothermal vertical boreholes [Journal]. - [s.l.] : International Journal of Heat and Mass Transfer, 2007. - Vol. L.
- Landa J.L.** Reservoir Parameter Estimation Constrained to Pressure Transients, Performance History and Distributed Saturation Data.. - [s.l.] : Department of Petroleum Engineering, Stanford University, California, 1997.
- Lee C.K. and Lam H.N.** Computer simulation of borehole ground heat exchangers for geothermal heat pump systems [Journal]. - [s.l.] : Renewable Energy. - 6 : Vol. XXXIII.
- Lee C.K. and Lam H.N.** Computer simulation of borehole ground heat exchangers for geothermal heat pump systems [Journal]. - [s.l.] : Renewable Energy, 2008. - 6 : Vol. XXXIII.
- Li Z.** On the Measure of Digital Terrain Model Accuracy [Journal]. - [s.l.] : Photogrammetric Record, 1988. - 12 : Vol. LXXII.
- Loague K. and Green R. E.** Statistical and Graphical Methods for Evaluating Solute Transport Models: overview and application. [Journal]. - [s.l.] : Journal of Contaminant Hydrology, 1991. - 1-2 : Vol. VII.
- Lu S. [et al.]** An Improved Model for Predicting Soil Thermal Conductivity from Water Content at Room Temperature [Journal]. - [s.l.] : Soil Science Society of America Journal, 2007. - Vol. LXXI.
- Lund J.W., Freeston D.H. and Boyd T.L.** Direct utilization of geothermal energy 2010 worldwide review [Conference] // World geothermal congress. - Bali, Indonesia : [s.n.], 2010.
- Magraner T. [et al.]** Comparison Between Simulation and Experimental Results for a Monitored Ground Coupled Heat Pump System [Conference] // Proceedings World Geothermal Congress 2010. - Bali : [s.n.], 2010 .
- Manohar K., Yarbrough D.W. and Booth J.R.** Measurement of apparent thermal conductivity by the thermal probe method [Journal]. - [s.l.] : Journal of Testing and Evaluation, 2000. - 5 : Vol. XXVIII.
- Marcotte D. and Pasquier P.** On the estimation of thermal resistance in borehole thermal conductivity test [Journal]. - [s.l.] : Renewable Energy, 2008. - 11 : Vol. XXXIII.
- Maritan D. and Panizzolo R.** Ground source heat pumps applications in Italy [Conference] // Thirty-Third Workshop on Geothermal Reservoir Engineering. - Stanford, California : [s.n.], 2008.

-
- Martelli L. and Molinari F. C.** Il quadro della risorsa geotermica in Emilia-Romagna, nuovi scenari [Conference] // Geotherm Expo 2011. - Ferrara : [s.n.], 2011.
- Mata-Lima Herlander** Modelação Inversa de Reservatórios Petrolíferos-Integração de Dados da Dinâmica de Flúidos na Parametrização e Upscaling. - Lisbon : IST, January 2006.
- Mata-Lima Herlander** Reservoir characterization with iterative direct sequential co-simulation: Integrating fluid dynamic data into stochastic model [Journal] // Journal of Petroleum Science and Engineering. - [s.l.] : Journal of Petroleum Science and Engineering, 2008. - 3-4 : Vol. 62. - pp. 59-72 .
- Matheron G.** Eléments Pour Une Théorie des Milieux Poreux [Book]. - Paris : Masson et Cie, 1967.
- Matheron G.** L'emergence de la loi de Darcy [Book Section]. - [s.l.] : Paris School of Mines, 1983. - Vols. N-592.
- Matheron G.** The theory of regionalized variables and its applications [Book]. - [s.l.] : École Nationale Supérieure des Mines de Paris, 1971.
- Matthias A.D. [et al.]** Surface Roughness Effects on Soil Albedo. [Journal]. - [s.l.] : Soil Science Society of America Journal, 2000. - Vol. LXIV.
- Mohanty S.** Effect of multiphase fluid saturation on the thermal conductivity of geologic media [Journal]. - [s.l.] : Journal of Physics D:Applied Physics, 1997. - 24 : Vol. XXX.
- Mottaghy D., Vosteen H.D. and Schellschmidt R.** Temperature dependence of the relationship of thermal diffusivity versus thermal conductivity for crystalline rocks [Journal]. - [s.l.] : International Journal of Earth Sciences, 2007. - 2 : Vol. XCVII.
- Munoz J.J.** Thermo-hydro-mechanical analysis of soft rock - Application to a large scale heating test and a large scale ventilation test. - Barcelona : Department of Geotechnical Engineering and Geosciences of Technical University of Catalunya, 2006.
- Munoz J.J., Alonso E.E. and Lloret A.** A laboratory heating test for thermo-hydraulic identification of rocks. - Paris : Department of Geotechnical Engineering and Geosciences of Technical University of Catalunya, 2005.
- Nagano K., Katsura T. and Takeda S.** Development of a design and performance prediction tool for the ground source heat pump system [Journal]. - [s.l.] : Applied Thermal Engineering, 2006. - 14-15 : Vol. XXVI.
- Nam Y. and Ooka R.** Numerical simulation of ground heat and water transfer for groundwater heat pump system based on real-scale experiment [Journal]. - [s.l.] : Energy and Buildings, 2010. - 1 : Vol. XLII.
- Nam Y., Ooka R. and Hwang S.** Development of a numerical model to predict heat exchange rates for a ground-source heat pump system [Journal]. - [s.l.] : Energy and Building, 2008. - 12 : Vol. XL.

Narasimhan T.N. and Witherspoon P.A. An Integrated Finite Difference Method for Analyzing Fluid Flow in Porous Media [Journal]. - [s.l.] : Water Resour. Res., 1976. - Vol. XII.

Nash J.E. and Sutcliffe River Flow Forecasting Through Conceptual Models. Part I: a discussion of principles [Journal]. - [s.l.] : Journal of Hydrology, 1970. - 3 : Vol. X.

Netzsch Heat Flow Meter- Method, Technique, Application.

Noetinger B. The effective permeability of a heterogeneous porous medium [Journal]. - [s.l.] : Transport in Porous Media, 1994. - Vol. XV.

Oliver D.S., Reynolds A.C. and Liu N. Inverse theory for petroleum reservoir characterization and history matching [Book]. - [s.l.] : Cambridge University Press, 2008.

Özkahraman H.T., Selver R. and Isik E.C. Determination of the thermal conductivity of rock from P-wave velocity [Journal]. - [s.l.] : International Journal of Rock Mechanics & Mining Sciences, 2004. - Vol. XLI.

Pandey G.R. and Nguyen V. A Comparative Study of Regression Based Methods in Regional Flood Frequency Analysis [Journal]. - [s.l.] : Journal of Hydrology, 1999. - 1-2 : Vol. CCXXV.

Panigrahi B. and Panda S.N. Field Test of a Soil Water Balance Simulation Model. [Journal]. - [s.l.] : Agricultural Water Management, 2003. - Vol. LVIII.

Pearson K. On the criterion that a given system of deviations from the probable in the case of a correlated system of variables is such that it can be reasonably supposed to have arisen from random sampling [Journal]. - [s.l.] : Philosophical Magazine, 1900. - 302 : Vol. L.

Pruess K., Oldenburg C. and Moridis G. TOUGH2 User's Guide, V2.0 [Book]. - Berkeley, CA : Lawrence Berkeley National Laboratory Report, 1999.

Rohner E. [et al.] New measurement techniques for geothermal heat pump- borehole heat exchanger quality control [Conference] // 9th IEA International Heat Pump Conference. - Zurich : [s.n.], 2008.

Rohner E., Rybach L. and Schärli U. A new, small, wireless instrument to determine ground thermal conductivity in situ for borehole heat exchanger design [Conference] // Proceedings of the World Geothermal Congress . - Antalya : [s.n.], 2005.

Rybach L., Rohner E. and Scharli U. A new, small, wireless instrument to determine ground thermal conductivity in-situ for borehole heat exchanger design [Conference] // Proceedings World Geothermal Congress. - Antalya : [s.n.], 2005.

Sanner B. [et al.] Current status of ground source heat pumps and underground thermal energy storage in Europe [Journal]. - [s.l.] : Geothermics, 2003. - Vol. XXXII.

Sanner B. [et al.] Geotrainet training manual for designers of shallow geothermal systems [Book]. - Brussels : GEOTRAINET, EFG, 2011.

-
- Schonder J.A. and Beck J.V.** A New Method to Determine the Thermal Properties of Soil Formations from In Situ Field Tests [Report]. - [s.l.] : U.S. Department of Energy, 1997.
- Sharma V. [et al.]** Neural Networks for Predicting Nitrate-Nitrogen in Drainage Water [Journal]. - [s.l.] : Agricultural Water Management, 2003. - Vol. LVIII.
- Signorelli S. [et al.]** Numerical evaluation of thermal response tests [Journal]. - [s.l.] : Geothermics, 2006. - 2 : Vol. XXXVI.
- Signorelli S.** Numerical evaluation of thermal response tests [Journal]. - [s.l.] : Geothermics, 2007. - Vol. 36.
- Soares A.** Direct Sequential Simulation and Cosimulation [Journal]. - [s.l.] : Mathematical Geology, 2001. - 8 : Vol. XXXIII.
- Soares Amilcar** Direct Sequential Simulation and Cosimulation [Journal]. - [s.l.] : International Association for Mathematical Geology, 2001. - Vol. XXXIII.
- Sundberg J. and Hellström G.** Inverse modelling of thermal conductivity from temperature measurements at the Prototype Repository, Äspö HRL [Journal]. - [s.l.] : International Journal of Rock Mechanics and Mining Sciences, 2009. - 6 : Vol. XLVI.
- Tavman I. H.** Effective thermal conductivity of granular porous materials [Journal]. - [s.l.] : International Communications in Heat and Mass Transfer, 1996. - 2 : Vol. XXIII.
- USACE** Flood-runoff Analysis. - Washington : U.S. Army Corps of Engineers, Hydrologic Engineering Center, 1994.
- USACE** Hydrologic Modelling System HEC-HMS. [Book]. - Washington : US Army Corps of Engineers (USACE), Hydrologic Engineering Center, 2001.
- Usovicz B., Kossowski J. and Branowski P.** Spatial variability of soil thermal properties in cultivated fields [Journal]. - [s.l.] : Soil & Tillage Research, 1996. - Vol. XXXIX.
- Valeo C. and Moin S.M.A.** Variable Source Area Modelling in Urbanizing Watersheds [Journal]. - [s.l.] : Journal of Hydrology, 2000. - 1-2 : Vol. CCXXVIII.
- Various** Dubbel: Handbook for Mechanical Engineers [Book]. - [s.l.] : Springer, 2001.
- Verein Deutscher Ingenieure** VDI 4640 - part 2 // Thermal use of the underground -Ground source heat pump systems. - Düsseldorf : [s.n.], 2001. - Vol. II.
- Vosteen H.D. and Schellschmidt R.** Influence of temperature on thermal conductivity, thermal capacity and thermal diffusivity for different types of rock [Journal]. - [s.l.] : Physics and Chemistry of the Earth, 2003. - Vol. XXVIII.
- Wagner R. and Clauser C.** Evaluating thermal response tests using parameter estimation for thermal conductivity and thermal capacity [Journal]. - [s.l.] : Journal of Geophysical Engineering, 2005. - Vol. 2.

Wang H. [et al.] Thermal performance of borehole heat exchanger under groundwater flow: a case study from Baoding [Journal]. - [s.l.] : Energy and Buildings, 2009. - Vol. XVI.

Wen X. H. and Gómez-Hernández J. J. Upscaling hydraulic conductivities in heterogeneous media: an overview [Journal]. - [s.l.] : Journal of Hydrology, 1996. - Vol. CLXXXIII.

Willmott C.J. Some Comments on the Evaluation of Model Performance. [Journal]. - [s.l.] : Bulletin of American Meteorological Society, 1982. - Vol. LXIII.

Witte H. G. L. Thermal response testing for borehole heat exchangers. Validation of assumptions [Conference] // Symposium 10 years of TRT in Germany. - Gottingen : [s.n.], 2009.

Witte H. J. L. and Van Gelder A.J. Geothermal response tests using controlled multi-power level heating and cooling pulses (MPL-HCP):quantifying ground water effects on heat transport around a borehole heat exchanger [Conference] // 10th International Conference on the Thermal Energy Storage, Ecstock. - [s.l.] : Stockton College New Jersey, 2006.

Woodside W. and Messmer J. H. Thermal Conductivity of Porous Media. II. Consolidated Rocks [Journal]. - [s.l.] : Journal of Applied Physics, 1961. - Vol. XXXII.

Yang C. A linear inverse model for the temperature-dependent thermal conductivity determination in one-dimensional problems [Journal]. - [s.l.] : Applied Mathematical Modelling, 1998. - 1-2 : Vol. XXII.

Yang H., Cui P. and Fang Z. Vertical-borehole ground-coupled heat pumps: a review of models and systems [Journal]. - [s.l.] : Applied Energy, 2010. - Vol. LXXXVII.

Yang W. [et al.] A two-region simulation model of vertical U-tube ground heat exchanger and its experimental verification [Journal]. - [s.l.] : Applied Energy, 2009. - Vol. LXXXVI.

Yavuzturk C., Spitler J.D. and Rees S.J. A transient two-dimensional finite volume model for the simulation of vertical U-tube ground heat exchangers. - [s.l.] : ASHRAE Transactions, 1999. - Vol. CV.

Yavuzturk Cenk Modeling of vertical ground loop heat exchangers for ground source heat pump systems. - [s.l.] : Oklahoma State University, 1999.

Yue S. and Hashino M. Unit Hydrographs to Model Quick and Slow Runoff Components of Streamflow [Journal]. - [s.l.] : Journal of Hydrology, 2000. - 1-4 : Vol. CCXXVII.

Zeng H. Y., Diao N. R. and Fang Z.H. A finite line-source model for boreholes in geothermal heat exchangers [Journal]. - [s.l.] : Heat Transfer—Asian Research, 2002. - 7 : Vol. XXXI.

Annexes – Published articles and conferences’ act

a) “Recent developments of thermal response test”

Geothermal Energy Exhibition – 1st edition, Ferrara 23-25 settembre 2009
Coauthors: Roberto Bruno, Francesco Tinti, Sevinc Mantar

In recent years, for the proper dimensioning of geothermal fields for conditioning of buildings, has been increasing the choice of realizing a Thermal Response Test, carried out on the first vertical borehole heat exchanger, which will be part of the future geothermal field. Basically, the standard test consists on putting a certain amount of heat load in the borehole heat exchanger, and then measuring the change in temperature of the circulating fluid. The temperature changes will depend on the thermal characteristics of the soil, the heat exchanger and the hole.

This poster shows the recent developments of the method of the Thermal Response Test in Italy and abroad, according to the guidelines proposed by the Working Group inside of the IEA-ECES, Annex 21.

b) “La caractérisation d’un réservoir géothermique superficiel ”

Journées de Géostatistique - CG-Fontainebleau (Paris), 24-25 Septembre 2009

Coauthors: Roberto Bruno, Francesco Tinti

Cette contribution s’occupe d’un aspect peu considéré dans l’exploitation de la géothermie a basse (ou très basse) enthalpie pour la climatisation avec pompe à chaleur : la caractérisation spatiale du réservoir géothermique vis aux paramètres utiles, a savoir les caractéristiques thermiques.

La transmission du chaleur au dedans du reservoir est étudié en utilisant des «classiques» simulateurs de flux, basés sur des modèles aux différences finies intégrales ou aux éléments finis. Les deux propriétés thermiques sont deux variables régionalisées, $k(x)$ (conductivité thermique), $cp(x)$ (capacité thermique), interprétées comme réalisations d’une FA vectorielle, $K(x)$ et d’une FA sommable, $Cp(x)$. Dans le suivi l’on fait référence seulement a la conductivité thermique, parce que plus difficile a traiter.

La contribution de la Géostatistique à la modélisation du flux thermique est plus difficile que dans le cas hydrogéologique, parce que la résolution du problème est assez plus compliquée, au moins théoriquement.

Effectivement, la conductivité thermique, outre que à la nature du matériel de la matrice solide, est potentiellement influencée, donc corrélée, à facteurs qui changent (état tensorielle, température du milieu, saturation, etc.).

En pratique on doit considérer, aux mêmes temps, conductivité, perméabilité, saturation, vitesse de l’eau, module d’élasticité, les trois tensions et la pression interstitielle, c’est-à-dire variables sommables et non sommables, liés par différents équations différentielles. Il est clair que si les intervalles de la variabilité sont réduits, plusieurs simplifications sont possibles.

Plusieurs problèmes restant:

- le problème de la corrélation après upscaling.
- La variabilité espace-temporelle des paramètres dérive du fait que pendant le fonctionnement du système il y a des paramètres qui changent.
- L’absence de données est un problème pratique plutôt que théorique, mais courant et, jusque aujourd’hui, sans une solution générale et acceptée.

L’analyse suggère une variabilité anisotrope et non-stationnarité (spatialement) dans la verticale, au moins du a l’accroissement de la charge litho-statique. En outre, la variabilité espace-temporelle de paramètres comme la saturation ou la vitesse de l’eau affectent la conductivité d’un ordre de grandeur plus importante que la variabilité spatiale en conditions hydrodynamiques stationnaires.

c) “Geostatistical modeling of shallow geothermal reservoir ”

Oral presentation & poster at the 1st Geothermal PhD day, Potsdam - 12 february 2010

Coauthors: Roberto Bruno, Francesco Tinti

The design of shallow geothermal fields for air conditioning today has achieved good levels of detail, because the fundamental properties of a reservoir (geological variations, hydrogeological and thermal properties) are no longer considered as constant in space and time inside the geothermal field. In fact the actual simulators (ex. FEFLOW, a finite elements flow and heat simulator) can take into account:

- underground stratification along the borehole heat exchanger
- influence of groundwater flow which, moving in a direction determined by potential difference, makes dynamic the heat flux
- thermal interference between various borehole heat exchangers in a geothermal field.

But even this approach has some limits: it doesn't consider the spatial anisotropy of some variables and the tensorial nature of some other (thermal conductivity and permeability). As a first approximation, these are spatial regionalized vectorial variables, changing in each point, for each direction and for the elementary volume at hand, also for a single type of material and, over all, they are non-additive.

This makes fundamental a geostatistical approach in order to better modeling reservoir's thermal conductivity, which is characterized by its covariance and variogram. By this knowledge we can obtain geostatistical simulations of thermal conductivity and, after an upscaling, we can use them as input for heat flow simulators.

d) “Thermal Response Test: un approccio geostatistico”

Poster at Geotherm Expo 2nd edition- Ferrara, 21-23 september 2010

Coauthors: Roberto Bruno, Francesco Tinti

Il Thermal Response Test (TRT) è un test in situ utilizzato per ottenere il valore di conduttività termica dei terreni adibiti all’installazione degli impianti geotermici a bassa entalpia. I risultati del test sono influenzati da fattori statici, come le caratteristiche termiche del foro, o dinamici, come le fluttuazioni della potenza iniettata e della temperatura esterna.

Nell’ambito della ricerca del DICAM sulla geotermia a bassa entalpia, è stato sviluppato un approccio probabilistico per la valutazione della conduttività termica. Tale approccio permette di caratterizzare e modellizzare la variabilità dell’informazione restituita dal test, filtrando opportunamente i fattori esterni che influenzano i dati registrati e che possono rendere problematica la definizione quantitativa delle proprietà termiche dei terreni. In particolare, la metodologia si basa sulla modellizzazione geostatistica delle variabili registrate durante il test.

Tutta l’analisi dati è stata condotta su test realmente eseguiti, forniti dall’azienda GEO-NET e dal sotto-comitato dell’Agenzia Internazionale dell’Energia incaricato dello sviluppo del TRT, al quale il DICAM partecipa. Infine, nell’ambito di tale Comitato, è stato progettato un sistema innovativo di TRT, che sarà messo a punto e sperimentato sul futuro campo sonde di prova della Facoltà di Ingegneria di Bologna.

e) “Analysis of Thermal Response Test data”

Oral presentation & poster at the 2° European Geothermal PhD day – Reykjavik, 1-2 march 2011

Coauthors: Roberto Bruno, Francesco Tinti

Thermal Response Test (TRT) is an onsite test used to characterize the thermal properties of shallow underground and of the borehole used to extract / inject heat.

The consolidated deterministic methodology based on the “Infinite Linear Source” (ILS) theory is reviewed and a nested probabilistic approach for TRT output interpretation is proposed. 5 key parameters are required for applying the theory and must be deduced by the test records.

3 of them are the target (ground thermal conductivity- λ , ground volumetric heat capacity ρC and borehole thermal resistance- R_b), 2 of them (initial time- t_i and final time- t_f) are necessary for applying the classical computing procedure based on a linear regression and guess values. The probabilistic approach calls for a nested sequential procedure. Based on a geostatistical residual model in the time-logarithm, the drift analysis of temperature records allows for robust ground thermal conductivity (λ) identification. The modeling of log-time residual variogram allows for the computation of the estimation variance for different regression conditions. Consequently, the initial time is defined as the time at which the ILS theory hypothesis is not verified by the TRT results and the final time is simply identified, in advance and during the test, by the minimum time able to guarantee the required confidence for the regression analysis results. Afterwards, based on λ , t_i and t_f estimates, a new univariate regression on the original data allows for the identification of the theoretical hyperbolic relationship between ρC and R_b . Then, the methodology requires the user to propose a guess probability distribution function for both variables. Once available, the identification of the joint conditional probability distribution function to the ρC - R_b relationship is found. And finally the conditional expectation allows for identifying the correct and optimal couple of the ρC - R_b estimated values.

f) Annex 21 Thermal Response Test Final Report

Final project document of the International Energy Agency (IEA) – In print.

Coauthors (in alphabetical order): J. Bereton, R. Bruno, F. Cruickshanks, H. Elviya, H. Fujii, S. Gehlin, G. Hellstrom, J. Kallio, M.Kharseh, N.Leppärharju, B. Nordell, D. Marcotte, I. Martinkauppi, A.Montero, K. Nagano, R. Nederbruecker, H. Paksoy, M. Proell, M. Reuss, B. Shim, H. Steger, F. Tinti, H.Witte ,R. Zorn, e altri.

The overall objectives of Annex 21 are to compile TRT experiences worldwide in order to identify problems, carry out further development, disseminate gained knowledge, and promote the technology. Based on this overview, a TRT state-of-the-art, new developments and further work are studied.

The Specific Objectives of Annex 21 are:

Overview

- Worldwide use of TRT (country, type, number)
- Purpose of test (design values, research & development, quality control / failure analysis).
- Applications (BHE, energy piles, heat pipe BHE's, etc.)
- TRT method (heating and / or cooling)
- Experimental setup (monitoring accuracy, etc.)
- Test procedure
- Evaluation models

New Developments and Further work

- Method to determine undisturbed ground temperature
- Swiss method for detailed logging of borehole temperature – swimming data acquisition 'Fisch', etc.
- Groundwater influence
- TRT while drilling
- Software for automatic evaluations
- Comparison of equipment and evaluation
- Initiate a common quality standard of TRT worldwide
- Invitation to "new" countries – workshop and courses on how to use TRT

g) Test di Risposta Termica per la geotermia superficiale: un approccio geostatistico

Acque sotterranee, 122 (dicembre 2010): 37 – 41

Coauthors: Roberto Bruno, Francesco Tinti

Negli ultimi anni, si è evidenziato un crescente interesse per sistemi di condizionamento a pompa di calore accoppiati a reservoir geotermici superficiali. Il sottosuolo, installando opportuni geo-scambiatori, viene sempre di più usato come stoccaggio stagionale di energia termica, dal quale è possibile estrarre calore in inverno ed immetterlo in estate.

I geo-scambiatori, di diverso tipo e dimensione, sono prevalentemente a circuito chiuso, dentro i quali circola il fluido termovettore; questo fluido scambia energia termica, principalmente per conduzione, con i materiali naturali incontrati lungo il ciclo.

La variabilità delle condizioni geologiche ed idrogeologiche per ogni installazione dà luogo a diverse potenze termiche supportabili da ogni geo-scambiatore, e conseguentemente a diversa energia estraibile dal terreno.

Per questa ragione, un punto critico di ogni buon progetto è la conoscenza, più dettagliata possibile, delle proprietà termiche del sottosuolo.

Allo stato attuale della tecnologia, il test esistente con il più alto grado di accuratezza per la caratterizzazione del reservoir geotermico superficiale è il Test di Risposta Termica (TRT), che consiste in una simulazione del funzionamento del sistema per un periodo limitato di tempo, attraverso l'iniezione/estrazione di calore a potenza costante all'interno del geo-scambiatore.

Dall'analisi della variazione delle temperature del fluido circolante all'interno del circuito, è possibile avere una stima delle proprietà termiche medie dell'intera porzione del reservoir geotermico considerato.

In questo articolo sono stati proposti due metodi basati sulla caratterizzazione geostatistica del TRT i quali permettono il calcolo di: i) conduttività termica del terreno e ii) capacità termica volumetrica del terreno e resistenza termica del foro.

- i) Il metodo della deriva garantisce una stima migliore della conduttività, comparato con il metodo tradizionale. In termini numerici la precisione è simile per test con migliaia di misure. Cionondimeno è interessante e immediato il raffronto fra i valori ottenuti con i diversi approcci.
- ii) L'approccio condizionante riguardante il calcolo accoppiato di capacità termica volumetrica del terreno e resistenza termica del foro che permette di ottenere una coppia di valori più attendibile e legata al test reale.

h) Geostatistical modeling of a shallow geothermal reservoir for air conditioning of buildings

*Acts of IAMG 2011 Salzburg. Mathematical Geoscience at the crossroad of theory and practice.
(september 2011): 146 – 163*

Coauthors: Roberto Bruno, Francesco Tinti

Shallow geothermal energy, coupled to heat pump systems, is a growing technology to save energy and to store exhausted heat in the ground. Different models and techniques for systems design exist and are well known.

Up to now, in the analysis there is a lack of probabilistic approach and the shallow geothermal reservoir is studied as a simple energy tank, whose parameters are considered constant in time and space.

With this paper we propose to apply a geostatistical approach to reservoir characterization referring to the study of random components in thermal response test procedure and of variability of equivalent thermal conductivity of geothermal reservoir.

Our final aim is to underline the influence of natural variability on the shallow geothermal systems.

i) “Inverse modeling applied to shallow geothermal reservoirs”

To present at the 9th Geostatistical Congress– Oslo, 11-15 June 2012

Coauthors: Roberto Bruno, Amilcar Soares

A shallow geothermal reservoir allows storing and extracting heat in the underground, usually for air conditioning purposes. Reservoir characterization requires modeling of spatial distribution of thermal parameters, linked to petro-physical properties as well as to water content and water flow. Direct small scale data actually are scarce and the main tool to characterize the reservoir is Thermal Response Test (TRT), a sort of production test which allows to estimate underground equivalent values of thermal properties. There are also many space-time components that are never constant during system working time and that influence the equivalent thermal conductivity. Therefore we need a numerical model to simulate the reservoir performance in a complex dynamic framework.

The approach adopted for reservoir characterization is the “inverse problem”, typical of oil&gas field analysis, given the existing similarities.

In fact, normally, inverse method consists on the perturbation of a set fine grid values of hydraulic conductivity and porosity numerical model, in order to feed a process simulator and to match the production real response. Similarly, we create different realizations of thermal properties by direct sequential simulation and we find the best one fitting real production data (fluid temperature along time).

The software used to develop heat production simulation is FEFLOW 5.4 (Finite Element subsurface FLOW system). In this first study, a geostatistical reservoir model has been set up based on literature thermal properties data and spatial variability hypotheses, and a real TRT has been tested. To compare simulation results with classical results obtained by ILS (Infinite Line Source) theory, we set up an upscaling procedure of vector properties (thermal and hydraulic conductivity). The whole procedure adopted is presented and commented. The main conclusion is the positive evaluation of this first attempt of shallow geothermal reservoir characterization by inverse problem solution.

I) Thermal Response Test for shallow geothermal applications: a geostatistical approach & the DCE Analysis Method. Part I and II

Papers submitted to the Mathematical Geosciences Journal.

Coauthors: Roberto Bruno, Francesco Tinti

Thermal Response Test (TRT) is an onsite test used to characterize the thermal properties of shallow underground and of the borehole heat exchanger used to extract / inject heat. The consolidated deterministic methodology based on the “Infinite Line Source” (ILS) theory is reviewed and a nested probabilistic approach for TRT output interpretation is proposed. Five key parameters are required for applying the ILS theory and must be deduced by the test records. Three of them are the target (ground thermal conductivity λ_g , ground volumetric heat capacity c_g and borehole thermal resistance R_b); two of them (initial time t_0 and final time t_f) are necessary for applying the classical computing procedure based on a linear regression in the time-logarithm fed by guess values, which actually masks a circular reference. The modeling of time-log residual variogram allows for the computation of the estimation variance for different regression conditions. Consequently, the initial time is defined as the time at which the TRT experimental data are not compatible with ILS theory hypothesis. The final time is simply identified, in advance and during the test, by the minimum time able to guarantee the required confidence for the estimation results.

The Part II of this series of articles is going to further investigate the calculation of underground thermal conductivity (λ_g), underground volumetric heat capacity (c_g) and borehole thermal resistance (R_b). Based on a geostatistical residual model in the time-logarithm, the drift analysis of temperature records allows for more precise λ_g estimation. Afterwards, based on λ_g , t_0 and t_f estimates, a new monivariate regression on the original data allows for the identification of the theoretical logarithmic relationship between c_g and R_b . Then, the methodology requires the user to propose a tentative monivariate Probability Distribution Function (PDF) for each variable. Once available, the joint Probability Distribution Function conditional to the $c_g - R_b$ relationship is found; finally, the conditional expectation allows for the identification of the correct and optimal couple of the $c_g - R_b$ estimated values.